

Development and Analysis of Transient Models for
the Biofiltration of Single and Mixed Volatile
Organic Compounds (VOCs)

by

Ansar Zaman

A Thesis Presented to the

FACULTY OF THE COLLEGE OF GRADUATE STUDIES

KING FAHD UNIVERSITY OF PETROLEUM & MINERALS

DHAHRAN, SAUDI ARABIA

In Partial Fulfillment of the
Requirements for the Degree of

MASTER OF SCIENCE

In

CHEMICAL ENGINEERING

May, 1996

INFORMATION TO USERS

This manuscript has been reproduced from the microfilm master. UMI films the text directly from the original or copy submitted. Thus, some thesis and dissertation copies are in typewriter face, while others may be from any type of computer printer.

The quality of this reproduction is dependent upon the quality of the copy submitted. Broken or indistinct print, colored or poor quality illustrations and photographs, print bleedthrough, substandard margins, and improper alignment can adversely affect reproduction.

In the unlikely event that the author did not send UMI a complete manuscript and there are missing pages, these will be noted. Also, if unauthorized copyright material had to be removed, a note will indicate the deletion.

Oversize materials (e.g., maps, drawings, charts) are reproduced by sectioning the original, beginning at the upper left-hand corner and continuing from left to right in equal sections with small overlaps. Each original is also photographed in one exposure and is included in reduced form at the back of the book.

Photographs included in the original manuscript have been reproduced xerographically in this copy. Higher quality 6" x 9" black and white photographic prints are available for any photographs or illustrations appearing in this copy for an additional charge. Contact UMI directly to order.

UMI

**A Bell & Howell Information Company
300 North Zeeb Road, Ann Arbor MI 48106-1346 USA
313/761-4700 800/521-0600**





**Development and Analysis of Transient
Models for the Biofiltration of Single and Mixed
Volatile Organic Compounds (VOCs)**

BY

Ansar Zaman

A Thesis Presented to the
FACULTY OF THE COLLEGE OF GRADUATE STUDIES
KING FAHD UNIVERSITY OF PETROLEUM & MINERALS
DHAHRAN, SAUDI ARABIA

In Partial Fulfillment of the
Requirements for the Degree of

MASTER OF SCIENCE
In
CHEMICAL ENGINEERING

May, 1996

UMI Number: 1379995

UMI Microform 1379995
Copyright 1996, by UMI Company. All rights reserved.
This microform edition is protected against unauthorized
copying under Title 17, United States Code.

UMI
300 North Zeeb Road
Ann Arbor, MI 48103

KING FAHD UNIVERSITY OF PETROLEUM & MINERALS

DHAHRAN, SAUDI ARABIA


This Thesis written by

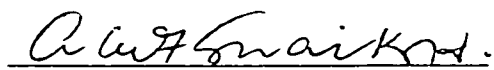
Ansar Zaman

*under the direction of his Thesis Advisor, and approved by his Thesis Committee,
has been presented to and accepted by the Dean, College of Graduate Studies, in
partial fulfillment of the requirements for the degree of*


MASTER OF SCIENCE IN CHEMICAL ENGINEERING

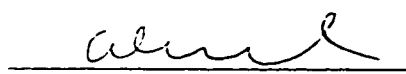
Thesis Committee


Chairman (Dr. S. M. Zarook)


Co-Chairman (Dr. A. A. Shaikh)


Member (Dr. A. H. Fatehi)


Dr. Dulaihan K. Al-Harbi
Department Chairman


Dr. Ala H. Rabeh
Dean, College of Graduate Studies

Date: 5.6.96



Dedicated
To
My Father and Mother

ACKNOWLEDGMENT

Praise and Gratitude be to Almighty Allah with whose gracious help it was possible to accomplish this work.

The present work involved extensive application of the computer facility especially the mainframe system. Long gruelling hours were spent in front of the computer screen. I gratefully thank our Department Chairman Dr. Al Harbi for allowing me access to the computer facilities in the Department.

It is hard to put into words the support provided by my thesis advisor Dr. Zarook. I used to constantly interrupt him in his office and pick his brains endlessly. He was always there to help when I was in trouble and my morale was down. Working with him was indeed a pleasant and learning experience.

My co-advisor Dr. Shaikh, despite his busy schedule, provided me with invaluable inspiration, encouragement and timely advises. I acknowledge my deepest gratitude for him.

I also gratefully acknowledge the suggestions and comments by my committee member Dr. Fatehi to improve the work.

Dr. Loughlin helped me a lot in the numerical solution of the problem and with his constructive suggestion on adsorption. I thank him for all his help.

I thank all my friends who lent me help during different stages of this work. I would like to make a special mention of my friend Salman Naqvi, without whose help this work would have been though completed, but God knows when. It was some sacrifice on his part to allocate time, usually at midnight, from his ever busy and confused schedule to help me during the initial crucial stages of this work.

Last, but by no means the least, I am obliged to offer my indebtedness and sincere appreciation to my parents, brother, sister and her family for all their love, moral support, prayers, encouragement, and understanding.

CONTENTS

	Page
LIST OF TABLES	VII
LIST OF FIGURES	VIII
NOTATION	XII
ABSTRACT (ENGLISH)	XVIII
ABSTRACT (ARABIC)	XIX
1 INTRODUCTION	1
1.1 Background	1
1.2 Biofiltration	3
2 LITERATURE REVIEW	6
2.1 Steady State Models	6
2.2 Transient Models	11
2.3 Analysis of Published work	13
3 MODEL DEVELOPMENT	14
3.1 Biofilm	15
3.2 Gas Phase	18
3.3 Solid Phase	21
3.4 Functional Expressions used in the Model	24
3.5 Solution of the Model Equations	27
4 BIOFILTRATION OF SINGLE VOCs	28
Approximate model and General model	
4.1 Approximate Model	29
4.2 General Model	33
4.3 Model Parameter Estimation	34
4.4 Numerical Solution of the Model equations	37
4.5 Results and Discussions	38

5	BIOFILTRATION OF VOC MIXTURES	58
	Approximate model and General model	
5.1	Approximate Model	60
5.2	General Model	64
5.3	Numerical Solution of the Model equations	66
5.4	Model Parameter Estimation	66
5.5	Results and Discussions	69
6	PERTURBATION STUDIES	92
6.1	Introduction	92
6.2	Administration of Shock loads in the model	95
6.3	Perturbation to the Inlet Concentrations	97
6.4	Perturbation to the Temperature	121
6.5	Perturbation to the pH of the system	127
6.6	Perturbation to the Inlet Gas Flowrate	132
7	ASYMPTOTIC STUDY OF THE GENERAL MODEL	137
8	CONCLUSIONS AND RECOMMENDATIONS	146
7.1	Conclusions	146
7.2	Recommendations	149
	REFERENCES	146
	APPENDICES	
Appendix A	Numerical discretization for Chapter 4	156
Appendix B	Numerical discretization for Chapter 5	160
Appendix C	Computer Program for solving the <i>Approximate</i> model for Single VOC	164
Appendix D	Computer Program for solving the <i>General</i> model for Single VOC	171
Appendix E	Computer Program for solving the <i>Approximate</i> model for Binary VOC mixtures	179
Appendix F	Computer Program for solving the <i>General</i> model for Binary VOC mixtures	186

LIST OF TABLES

Table	Description	Page
4.1	Parameter values used for solving the approximate and general model equations for single VOCs.	36
4.2	Comparison of biofilter models against experimental data of benzene (Zarook & Baltzis, 1994a) under steady state conditions.	40
4.3	Biofiltration of toluene vapor : Experimental data and comparison of model predictions. The units of C are g m^{-3} and those of R are $\text{gm}^{-3} \cdot \text{packing h}^{-1}$.	41
5.1	Parameter values used for solving the approximate and general model equations for mixtures.	67
5.2	Biofiltration of benzene-toluene mixtures: Experimental data and model predictions.	71

LIST OF FIGURES

Figure	Description	Page
3.1	Schematic representation for the model concepts used in the development of the model. (a) segment of the biofilter. (b) a solid support particle which is partially covered with biofilm (c) oxygen and VOC transported into the biofilm where diffusion and reaction take place	23
4.1	Equilibrium adsorption isotherm of benzene on a peat/perlite mixture. The curve represents a fitting of the data points to the Freundlich equation.	42
4.2	Model predicted toluene concentration profiles and experimental data for $C_{ti}=2.81 \text{ g m}^{-3}$ and $\tau = 6.3 \text{ min}$.	43
4.3	Concentration of toluene with time. Experimental data and predictions by different models.	44
4.4 a & b	Concentration of benzene with time. Experimental data and model (general) predictions.	45
4.5 a & b	Benzene concentration profiles along the bed. Experimental data and model predictions.	46
4.6	Concentration profiles of toluene and oxygen in the biofilm at different inlet concentrations.	49
4.7	Transient concentration profiles of oxygen and toluene for the given inlet conditions.	50
4.8	Effect of the inlet oxygen concentration on the exit toluene concentration.	51
4.9	Effect of Peclet number of toluene on the concentration profile in the biofilter.	54
4.10	Effect of Peclet number of oxygen on the concentration profile in the biofilter.	55
4.11	Effect of different non dimensional groups on the exit toluene concentration. Relative parameter value 1 refers to conditions of	56

	actual experiment.	
4.12	Effect of the various biofilm dimensionless groups on the exit toluene concentration.	57
5.1	Concentrations of benzene and toluene with time.	72
5.2	Concentration profiles of benzene and toluene in the biofilter. Experimental data and model predictions.	73
5.3	Concentrations of benzene and toluene with time.	74
5.4	Concentrations of benzene and toluene with time.	75
5.5 a & b	Experimental data and Model (general) predictions of the benzene and toluene concentration profiles along the column	76
5.6	Effect of the inlet oxygen concentration on the benzene and toluene exit concentrations.	78
5.7	Concentration profiles of benzene, toluene and oxygen in the biofilm at different inlet gas concentrations.	79
5.8	Effect of the biofilm parameters ϕ_1 and ϕ_2 on the exit benzene/toluene concentrations.	83
5.9	Effect of Biofilm parameters η_1 and η_2 on the exit benzene/toluene concentrations.	84
5.10	Effect of parameters ε_B , ε_T and ε_O on the exit benzene/toluene concentrations.	85
5.11	Effect of kinetic parameters γ , σ_1 and σ_2 on the exit benzene/toluene concentrations	86
5.12	Effect of dimensionless groups β_1 , β_2 and β_3 on the exit benzene / toluene concentrations.	89
5.13	Effect of Pe_B on the transient and column benzene / toluene concentration profiles.	90
5.14	Effect of Pe_T on the transient and column benzene / toluene concentration profiles.	91

6.1	Transient response to abrupt change in the inlet toluene concentration. Model prediction and Experimental data.	100
6.2	Transient response of the exit toluene concentration to shut down and restart of the biofilter.	101
6.3	Experimental data and model predictions for two consecutive experiments with toluene vapor. Conditions were : $C_{ii}=0.62 \text{ g m}^{-3}$, $\tau=2.7 \text{ min}$. Five days later, the conditions were changed to $C_{ii}=0.92 \text{ g m}^{-3}$, $\tau=4.2 \text{ min}$.	104
6.4 a. b. c	Transient response of the exit toluene concentration to triangular, sinusoidal and random perturbations in the inlet concentration for the two cases studied : Curve 1: $C_{ii}=2.7 \text{ g m}^{-3}$: $\tau = 0.62 \text{ min}$ Curve 2: $C_{ii}=1.65 \text{ g m}^{-3}$: $\tau = 7.7 \text{ min}$	105-107
6.5 a & b	Transient response of the exit concentrations to sinusoidal and random perturbations in the inlet toluene concentration.	110.111
6.6 a. b. c	Transient response of the exit concentrations to triangular, sinusoidal and random perturbations in the inlet toluene concentration.	112-114
6.7 a & b	Transient response of the exit concentrations to sinusoidal and random perturbations in the inlet gas concentration (mixture)	115.116
6.8 a. b. c	Transient response of the exit concentrations to triangular, sinusoidal and random perturbations in the inlet oxygen concentration	118-120
6.9 a & b	Transient response of the exit toluene concentration to triangular and random perturbations in the column temperature.	123.124
6.10 a & b	Transient response of the benzene and toluene exit toluene concentration to triangular and random perturbations in the column temperature.	125.126
6.11	Transient response of the exit toluene concentration to random changes in the pH of the system.	129
6.12 a & b	Transient response of the benzene and toluene exit toluene concentration to triangular and random changes in the pH of the system.	130.131

6.13	Transient response to abrupt change in the inlet gas flowrate. Model prediction and experimental data.	133
6.14 a. b. c	Transient response of the exit toluene concentration to triangular, sinusoidal and random changes in the inlet gas flowrate.	134-136
7.1	Asymptotic behavior of the General model	145

NOTATIONS

- a_j : Extended Langmuir isotherm parameter defined as $C_{jp,sat} b_j$ (m^3 / g - particle)
- A_s^* : total surface area available for biolayer formation and adsorption per unit volume of biofilter (m^{-1})
- A_{sj} : biolayer surface area per unit volume of reactor, for VOC j (m^{-1})
- b_j : Extended Langmuir isotherm parameter (m^3 / g)
- C_j : concentration of substance j in the air at a position h along the biofilter ($g m^{-3}$)
- C_j^* : equilibrium pollutant j concentration in the gas phase ($g m^{-3}$)
- $C_{j,0}$: value of C_j at $t = 0$ ($g m^{-3}$)
- C_{je} : value of C_j at $h = H$ ($g m^{-3}$)
- C_{ji} : value of C_j at $h = 0$ ($g m^{-3}$)
- $C_{ji,0}$: value of C_j at $h = 0$ and $t = 0$ ($g m^{-3}$)
- C_{jp} : concentration of substance j on the solid particle
(g of pollutant j -adsorbed/g particle)
- $C_{jp,0}$: value of C_{jp} at $t = 0$ (g of pollutant j -adsorbed/g particle)
- $C_{jp,Sat}$: value of C_{jp} at saturation (g of pollutant j -adsorbed/g particle)
- C_O : oxygen concentration in the air at a position h along the biofilter ($g m^{-3}$)
- $C_{O,0}$: value of C_O at $t = 0$ ($g m^{-3}$)
- C_{Oi} : oxygen concentration in the air at the inlet of the biofilter ($g m^{-3}$)
- $C_{Oi,0}$: oxygen concentration at $h = 0$ and $t = 0$ ($g m^{-3}$)
- \bar{C}_j : dimensionless concentration of pollutant j in the air defined as

$$\bar{C}_j = C_j / C_{ji}$$

- \bar{C}_j^* : dimensionless equilibrium concentration of pollutant j defined as $\bar{C}_j^* = C_j^*/C_{ji}$
- \bar{C}_{jp} : dimensionless concentration of substance j on the solid particle defined as $(1-\nu)\rho_p C_{jp}/\nu C_{ji}$
- \bar{C}_o : dimensionless concentration of oxygen in the air defined as $\bar{C}_o = C_o/C_{oi}$
- CT : cycle time used in sinusoidal shock loads
- D_{jw} : diffusion coefficient of substrates in water ($m^2 h^{-1}$)
- D_j : dispersion coefficient of substrates in air ($m^2 h^{-1}$)
- D_{jA} : diffusion coefficient of substrates in air ($m^2 h^{-1}$)
- e_j : effectiveness factor based on pollutant j, defined by equations (4.6)
- e_o : effectiveness factor based on oxygen, defined by equation (4.7)
- f : relative parameter value
- f_{pH} : fractional decrease in the conversion due the pH change.
- $f(X_V)$: ratio of diffusivity of a compound in the biofilm to that in water
- h : position in the column (m) ; h = 0 at the entrance, h = H at the exit
- ht : amplitude of the triangular forcing function
- H : total height of the biofilter bed (m)
- k_a : mass transfer coefficient between the gas and the solid particle ($m h^{-1}$)
- k_{dj} : Freundlich isotherm parameter for the organic substrate j.
- K_j : constant in the specific growth rate expression of a culture growing on compound j ($g m^{-3}$)
- K_{lj} : inhibition constant in the specific growth rate expression of a culture growing on compound j ($g m^{-3}$)
- K_o : constant in the specific growth rate expression of a culture, expressing the effect of oxygen ($g m^{-3}$)

- K_{BT}, K_{TB} : kinetic interaction parameter (g m^{-3})
- m_j : distribution coefficient for the substance j/water system
- m_O : distribution coefficient for the oxygen-in-air/water system
- n_j : Freundlich isotherm parameter for substrate j removal
- R_p : radius of the particle (m)
- R_{exp} : experimentally measured removal rate of compound j, based on the entire biofilter ($\text{g m}^{-3}\text{-packing h}^{-1}$)
- R_{model} : model predicted removal rate of compound j, based on the entire biofilter ($\text{g m}^{-3}\text{-packing h}^{-1}$)
- S_j : concentration of pollutant j at a position x in the biolayer at a point h along the column (g m^{-3})
- $S_{j,0}$: value of S_j at $t = 0$ (g m^{-3})
- S_j^* : dimensionless concentration of substance j at a point θ in the biolayer; defined as $S_j(\theta) / S_j(\theta = 0)$
- S_O : oxygen concentration at a position x in the biolayer, at a point h along the column (g m^{-3})
- $S_{O,0}$: value of S_O at $t = 0$ (g m^{-3})
- t : time (h)
- T : temperature in the biofilm, ($^{\circ}\text{C}$)
- u_g : superficial air velocity in the biofilter; (m h^{-1})
- V : dummy parameter used administering shock loads
- V_p : volume of the biofilter bed (m^3)
- X_v : biofilm density ($\text{g-dry cells m}^{-3}$)
- x : position in the biolayer (m)

- Y_j : yield coefficient of a culture on VOC j (g-biomass g⁻¹-compound j)
- Y_{O_j} : yield coefficient of a culture on oxygen (g-biomass g⁻¹-oxygen).
when VOC j is the carbon source
- Z : dimensionless position in the biofilter ($Z = h/H$)

Greek Symbols

- α : fraction of total surface area available for biofilm formation
- δ : effective biolayer thickness (m)
- δ^* : actual biolayer thickness (m)
- θ : dimensionless time defined as $u_g t/H$
- θ : dimensionless position in the biolayer defined as x/δ
- μ_j : specific growth rate (h^{-1}), given by equations (3.18, 3.19)
- μ_j^* : constant in the specific growth rate expression (h^{-1})
- ρ_p : density of the solid particles ($g\ m^{-3}$)
- τ : space-time (h)
- ν : porosity of the biofilter bed
- β_{1j} : dimensionless group defined as $e_j \alpha \delta A_s^* X_v H \mu_j^* / (Y_j u_g C_{ji} \nu)$
- β_{2j} : dimensionless group defined as $e_o \alpha \delta A_s^* X_v H \mu_j^* / (Y_{Oj} u_g C_{Oj} \nu)$
- β_{3j} : dimensionless group defined as $D_{jw} H \alpha A_s^* f(X_v) K_j / (\delta u_g C_{ji} \nu)$
- β_4 : dimensionless group defined as $D_{ow} H \alpha A_s^* f(X_v) K_o / (\delta u_g C_{Oj} \nu)$
- χ_j : dimensionless group defined as $k_j (1 - \alpha) A_s^* H / (u_g \nu)$
- ϕ_{1j} : dimensionless group defined as $D_{jw} H f(X_v) / (u_g \delta^2)$
- η_{1j} : dimensionless group defined as $H X_v \mu_j / (u_g Y_j K_j)$
- ϕ_2 : dimensionless group defined as $D_{ow} H f(X_v) / (u_g \delta^2)$
- η_{2j} : dimensionless group defined as $H X_v \mu_j / (u_g Y_{Oj} K_{Oj})$
- γ : inverse dimensionless inhibition constant defined as $\gamma = K_j / K_{Ij}$

- ε_j : dimensionless Henry's coefficient for j defined as $C_{ji} / (m_j K_j)$
- ε_O : dimensionless Henry's coefficient for oxygen defined as $C_{O_i} / (m_O K_O)$
- Pe_j : Peclet number of substrate j defined as $u_g H / D_j \nu$
- Pe_O : Peclet number of oxygen defined as $u_g H / D_O$
- Ψ_j : dimensionless group defined as $(1 / C_{ji}) \left[\nu C_{ji} / (1 - \nu) \rho_p k_{dj} \right]^{1/j}$
- λ_{-1j} : dimensionless group defined as $a_j \rho_p (1 - \nu) /$
- λ_{-2j} : dimensionless group defined as b_j / C_{ji}

Special subscript

$j = B, T$: compounds are benzene and toluene respectively.

$J = B, T, O$: compounds are benzene, toluene and oxygen respectively.

THESIS ABSTRACT

NAME OF STUDENT	Ansar Zaman
TITLE OF STUDY	Development and Analysis of Transient Models for the Biofiltration of Single and Mixed Volatile Organic Compounds (VOCs)
MAJOR FIELD	Chemical Engineering
DATE OF DEGREE	May, 1996

In this study, a general transient model is developed for the biofiltration of mixed volatile organic compounds. The model incorporates general mixing phenomena, oxygen limitation effects, adsorption phenomena and actual biodegradation reaction kinetics. Solutions are presented with and without the assumption of pseudo steady-state for the biofilm leading to *approximate* and *general* models, respectively. The models are solved and validated for the cases of single VOCs and binary VOC mixtures. Dynamic analysis of the model is performed and compared with experimental data from the literature. Significant improvement in the model prediction is observed in comparison to earlier simplified models. The *general* model is superior to the *approximate* model as it does not require any correlations and its predictions seem to be better than the *approximate* model. However, the *general* model is mathematically very complex and difficult to solve, contrary to the approximate model. A thorough sensitivity analysis shows that mixing in the gas phase is an important phenomenon which should not be neglected and that some parameters need to be accurately estimated. Theoretical analysis shows that the assumption of excess oxygen availability is not a good one, specially at high inlet VOC concentration levels. The performance of the biofilter was analyzed when subjected to perturbations of various operational parameters. Transient behavior during shut-down and restart-up are also well predicted by the model and the transient period does not seem to be very long. Model predictions show that the biofilter is able to withstand extreme practical conditions such as random variations in the inlet concentration and gas flow rate.

MASTER OF SCIENCE DEGREE

KING FAHD UNIVERSITY OF PETROLEUM & MINERALS
DHAHRAN, SAUDI ARABIA

خلاصة الرسالة

- اسم الطالب الكامل : أنصار زمان
عنوان الرسالة : تطوير وتحليل نماذج رياضية للتصفية الحيوية غير المستقرة زمنياً للمركبات العضوية المتطايرة الفردية والمركبة .
التخصص : الهندسة الكيميائية .
تاريخ الشهادة : ذو الحجة ، ١٤١٦ هـ .

طُور في هذه الدراسة نموذج رياضي عام لوصف الأداء الغير مستقر للتصفية الحيوية للمركبات العضوية المتطايرة . وبأخذ هذا النموذج في الإعتبار مدى الخلط ، وتأثير الأوكسجين ، وظواهر الإدماز باستخدام سرعة تفاعل واقعية .

تُقدم هذه الدراسة حلولاً رقمية شاملة وأخرى مبنية على فرضية شبه حالة مستقرة في الطبقة الحيوية مما يؤدي إلى ما تجوز تسميته نماذج عامة وأخرى تقريبية . ولقد تم التأكد من صحة هذه النماذج في حالات المركب الفردي والمركبات الثنائية . لقد لوحظ أن هناك تحسناً كبيراً في تنبؤات هذه النماذج مقارنةً بما نشر سابقاً من أبحاث ، كما أن النموذج العام يعطي نتائج أفضل من النموذج التقريبي .

لقد أجريت دراسات حساسية للنماذج خلال هذه الدراسة وبينت أن الخلط في الطور الغازي مهم ولا ينصح بإهماله ، وأن هناك عوامل لابد من تقديرها بدقة . أما بالنسبة لتأثير الأوكسجين والفرضية السابقة بوجوده بكثرة فقد أثبتت الدراسة الحالية عدم صلاحية هذه الفرضية وخاصة عند وجود تركيز عالي للمادة العضوية .

ختاماً أجريت في هذه الرسالة دراسة على تأثير الإضطراب في عوامل التشغيل على أداء تفاعلات التصفية الحيوية ، وبينت هذه الدراسة أن المفاعل قادر بشكل عام على الأداء المعقول حتى في وجود إضطرابات كبيرة في تركيز وسرعة جريان الغاز الداخل إلى المفاعل .

درجة الماجستير في العلوم

جامعة الملك فهد للبترول والمعادن

الظهران ، المملكة العربية السعودية

ذو الحجة ١٤١٦ هـ

INTRODUCTION

1.1 BACKGROUND

Volatile Organic Compounds (VOCs) emitted from industries pose potential human risks in addition to causing severe environmental problems. These VOCs are highly carcinogenic even at low concentrations. Hence the environmental protection agencies throughout the world have imposed stringent regulations on the concentration of the VOCs in the atmosphere. The sources of VOCs emissions are many, the major contributors being the chemical and process industries starting from oil refineries to petrochemical industries, fertilizer plants, food industries, alcohol distilleries, breweries, paper mills, bio-industries etc.

A number of Air Pollution Control (APC) methods are available for the control of these VOC emissions. In general the APC methods can be broadly classified into two categories: physico-chemical methods and biological methods. In the former category, the most common methods are adsorption, absorption, condensation, incineration (thermal and catalytic) and some combined methods. The biological methods include the use of bioscrubbers, biotrickling filters and biofilters.

The selection of a specific control system for the treatment of VOCs depends on a number of factors including concentration of target VOCs, physico chemical properties of target VOCs, gas flow rate, gas characteristics (moisture content, temperature, pH etc.), desired removal efficiencies and space limitations. As obvious, the physico-chemical methods are quite complex and require elaborate equipment and are highly energy intensive. Hence these methods can be used economically only in the case of concentrated emissions. Moreover a majority of these methods like adsorption, absorption and condensation involve only transfer of the pollutant from one media to another resulting in secondary streams which may include a contaminated adsorbent phase which requires regeneration or disposal, a contaminated liquid stream (condensation and absorption) which requires further treatment such as thermal oxidation in which case harmful NO_x gases can be formed. Thus, though most industrial effluent gas streams can be efficiently controlled using the physico-chemical methods, the cost of doing so may be high and secondary stream issues may arise.

The biological methods involve the removal and decomposition of contaminants present in the gaseous form into non-hazardous substances through the use of microorganisms. Unlike conventional technologies, gas-phase biological treatment may afford VOC emission control at a relatively low cost and without secondary stream issues. One such technology, biofiltration, has proven to meet these objectives for VOC emissions. Among the biological gas purification methods, biofiltration has attracted growing interest in recent years.

1.2 BIOFILTRATION

Biofiltration is a new promising air pollution control technology involving the passage of polluted air stream through a packed bed containing micro organisms immobilized on to the bed packing material, forming biofilm or biolayer. As the contaminated vapor stream passes through the filter bed, the pollutants are transferred from the vapor to the biolayer. Within the biofilm, the contaminants may be used as carbon and / or energy sources by the micro organisms. For aerobic degradation of VOCs, the end products are typically carbon dioxide, water and new cell mass. The 'uptake' of contaminants (substrate) by micro organisms creates a concentration gradient within the biofilm which promotes molecular diffusion of substrate from the gas-biofilm interface toward the biofilm-solid interface. Proper selection of the microbial culture and of the biofilter size results in a pollutant-free airstream exiting the reactor.

For odor control purposes, biofilters have been used for years in removing inorganic substances (e.g., hydrogen sulfide, carbon disulfide) from the air, but only recently have they attracted attention for purposes of volatile organic compound (VOC) emission control (Lesson and Winer, 1991). The study of biofilters for removal of VOCs originated in Europe (Ottengraf and Van Der Oever, 1983; Ottengraf, 1986). When compared to alternate control technologies, such as flaring, catalytic oxidation, incineration, and activated carbon adsorption, biofiltration has the following advantages: (i) it is capable of treating large volumes of off-gases containing low concentrations of easily biodegradable components, (ii) it is a process in which the pollutants undergo destruction, not just media transfer, (iii) it is an environmentally friendly process as it gives harmless final products, (iv) it is more

economical than any alternate pollution control technologies as the operation is carried out at ambient temperature and pressure.

Although a number of experimental studies have established biofiltration as an efficient and environmental friendly process for the treatment of VOCs, the knowledge-base associated with the fundamental mechanisms that affect the biofilter performance as well as optimal biofilter operating conditions, continues to lag far behind existing knowledge related to conventional control technologies. The design of a biofilter is still an exercise based on empirical correlations and experimental extrapolation rather than a consequence of theoretical analysis. And since experimentation on a biofilter is a very tedious and time consuming process, there is a need for a mathematical model which would predict the performance of a biofilter under different operating conditions. In order to understand the process better and develop it into an optimized technology, effective modeling of the process is required. Process modeling is fundamentally important as realistic models can lead to the development of reliable design equations, as well as reduce the time and cost of experimentation at the pilot scale.

As will be evident from the literature review (Chapter 2), very few studies have been reported on the mathematical modeling of a biofilter column, infact there are no models available for the biofiltration of VOC mixtures. No work has been reported on effects of axial dispersion in the column and the oxygen concentration on the biofiltration process. There has been no attempt to model the effects of shock loading on the biofiltration process. Hence this study has been initiated with the main objective to develop *an advanced model for the biofiltration of VOC mixtures*, which incorporates general mixing phenomena, oxygen

limitation aspects, adsorption and general reaction kinetics. To accomplish the above objective, the following specific objectives were set:

1. To improve an existing approximate transient model for the biofiltration of single component VOCs (Zarook and Baltzis, 1994b) by including axial dispersion effects.
2. To develop an approximate transient model for the biofiltration of binary VOC mixtures. This is done by making a quasi-steady-state approximation for the biolayer, and the use of effectiveness factors (Tong and Fan, 1988).
3. To develop more realistic general transient biofiltration models for single component VOC and binary VOC mixtures. This is done by rederiving the above two models without using the quasi-steady state approximation and the effectiveness factors.
4. To make a parametric sensitivity analysis of the model.
5. To study the effects of shock loading on the various operational parameters like the inlet gas concentrations, flowrate, temperature and pH.
6. To study the asymptotic behavior of the general model

It should be mentioned that though the model developed will represent the biofiltration of multi-component VOC mixtures, the model predictions will be validated with the experimental data taken from the work of Zarook (1994) for the cases of single and binary VOC mixtures.

LITERATURE REVIEW

An important step in the development of biofilter technology is to derive and experimentally validate mathematical models for the predictive and scale-up calculations. There are at least two reasons for this: one is that models are tools for process engineering design; the other is that models help us achieve a better understanding of phenomena. Modeling and experimentation are interdependent with each other providing input to and taking information from the other.

In the last few years, a number of experimental studies have been carried out which have established biofiltration as an efficient process for VOC treatment. But very limited work has been reported on the mathematical modeling of the process. The existing models can be broadly classified into two groups: steady state models and transient models.

2.1 STEADY STATE MODELS

The earliest and most widely used steady state biofiltration model was developed by Ottengraf and van den Oever (1983). Because of its simplicity, this model has been used by a number of other researchers (Van Lith, 1989; Dharmavaram, 1991; Leson and Winer, 1991; Ergas et al., 1993; Deshusses and Hamer, 1993). The model assumes plug flow behavior in

the gas phase and flat geometry of the biofilm. The gas and liquid phase concentrations of each pollutant are assumed to be always in equilibrium at the phase boundary and related by Henry's law. Nutrient transport in the biofilm is by diffusion and can be described by an effective diffusion coefficient. For the microkinetics of biodegradation occurring in the biofilm, the authors start with the Monod expression. Although the authors acknowledge that based on shake-flask experiments the biodegradation kinetics of single VOCs follow the Monod model, they only consider two limiting cases. At low concentrations, they consider first order kinetics and arrive at the following analytical expression for the exit concentration:

$$\frac{C_{je}}{C_{ji}} = \exp\left(\frac{-H a D_e}{m_l u_g \delta} \phi_l \tanh \phi_l\right) \quad (2.1)$$

where $\phi_l = \delta \sqrt{\frac{K}{D_e}}$, K is the first-order rate constant.

At high concentrations, the rate expression approaches zero-order kinetics in the substrate concentration, for which case, two situations are distinguished (Ottengraf, 1983; 1987);

(i) reaction limitation: where the biolayer is fully active and hence the conversion rate is only controlled by the reaction rate (ii) diffusion limitation: where the biolayer is not fully active or in other words, the depth of penetration in the biolayer is smaller than the biolayer thickness. The following expressions were derived for reaction limitation:

$$\frac{C_{je}}{C_{ji}} = 1 - \frac{K_o a \delta H}{u_g C_{ji}} \quad (2.2)$$

and for diffusion limitation:

$$\frac{C_{se}}{C_{st}} = \left(1 - \frac{Ha}{u_c} \sqrt{\frac{K_0 D_e}{2 m_i C_{st}}} \right)^2 \quad (2.3)$$

The authors conclude that total compound removal in the bed is achieved if

$$\frac{K_0 a \delta H}{u_c C_{st}} \geq 2 \quad (2.4)$$

where, K_0 is the zero-order rate constant.

For downward flow, the authors claim to use the same equations by substituting the depth of the sample port measured from the inlet (top) of the column for the height h . The above model equations are based on the assumption that oxygen in the column is present in excess and hence does not affect the degradation of the VOC and is limited to the case of a single VOC. In case of mixed VOCs, the authors propose to use the same model in additive sense. They assumed that biofiltration of each compound could be described independent of the presence of the other compounds in the mixture.

Based on the work of Ottengraf, described above for the case of zero-order kinetics, van Lith (1989, 1990) presented a design method for a biofilter column. The Ottengraf model is used as such without any improvements and the following expression for the effective biofilm thickness is derived :

$$\delta_{eff} \sqrt{\frac{K_0 m}{D_{jw} C_g}} = \sqrt{2} \quad (2.5)$$

where D_{jw} is the diffusion coefficient of the VOC in water.

Finally the authors arrive at the following expression for the limiting concentration at which the process goes from diffusion controlled to reaction rate controlled :

$$C_{gas\ limit} = \left(\frac{l}{A_f} \sqrt{\frac{mK_0}{2D_{jw}}} \right)^2 \quad (2.6)$$

where A_f is the specific surface area of the filter material.

Building on the work of Ottengraf and van den Oever (1983) for the case of first order kinetics, and that of Harremoes (1988), Ergas et al., (1993) arrived at the following analytical expressions for the exit concentration from a biofilter,

$$\frac{S_j H}{C_{je}} = Cosh \phi \cdot Sech \left(\frac{\phi x}{H} + \phi \right) \quad (2.7)$$

and

$$\ln \frac{C_{je}}{C_{ji}} = - \frac{K_l z A_s H \tanh \phi}{H u_g \phi} \quad (2.8)$$

$$\text{where } \phi = \sqrt{\frac{K H^2}{D_{jw}}}$$

As seen, the above researchers have used simple kinetic models (zero, first orders) for describing the biodegradation of the VOCs in the biofilm. However, this is not always the case. There are now enough experimental evidence (Zarook et al., 1993; Deshusses and Hamer, 1993; Chang et al., 1993; Zarook, 1994) suggesting that biodegradation kinetics for a compound are more complex than zero or first order type kinetics and are different when this compound is present alone or in a mixture with other organic compounds which are also biodegradable. This kinetic interference is bound to play a significant role in the biofiltration of VOC mixtures. Recent studies by Deshusses and Hamer (1993) have shown that biofiltration of mixtures containing vapors of methyl-ethyl-ketone and methyl-isobutyl-

ketone cannot be explained unless significant interactions between the respective elimination processes of each individual pollutant occur during simultaneous elimination.

By eliminating some of the major assumptions of the model developed by Ottengraf and van den Oever (1983), like the presence of excess oxygen in the column, and using actual kinetic expressions such as Andrew's inhibitory kinetics from shake-flask experiments, Zarook and Baltzis (1994a) arrived at an advanced steady state model wherein they have used expressions for the reaction rate which explicitly takes into account for the potential limiting effects of oxygen. They have shown that the presence of oxygen in the column plays a significant role in the biodegradation of VOCs especially in the case of hydrophilic compounds such as methanol (Zarook, 1994), where oxygen gets depleted faster in the biofilm and determines the effective biolayer thickness. Infact, for the case of methanol vapor removal, these authors have shown that the process is mass transfer-limited by oxygen and kinetic-limited by methanol. Their model is however limited to the case of plug flow of the gas phase. The authors improved their above model for the case of VOC mixtures (Zarook, 1994), where they have considered interactive kinetics for the VOCs and oxygen, inhibitive and Monod type kinetic expressions.

2.2 TRANSIENT MODELS

From a review of the literature, it is seen that to date, efforts to model the process have focused on steady state biofiltration. There are very few published studies on the transient performance and response of biofilters. However, in practical applications, and especially for cases of emissions, transient operation is expected to be the rule rather than the exception. This is due to the fact that the VOC emissions level in any plant is unlikely to be constant. Furthermore, biofiltration can be applied to batch processes and thus, even if the emission level is constant, biofilters may be operating in an intermittent mode (e.g., in painting booth facilities). Hence, questions such as how well can a biofilter respond to variations in volumetric flow rate, concentration, and composition are of paramount importance for commercial application of this technology. The fact that biofilters are most likely to operate under varying load conditions was recognized early by Ottengraf et al.(1983); the load is defined as the rate of VOC mass supply per unit volume of biofilter bed

Zarook and Baltzis (1994b) have developed a transient model for the biofiltration of a single VOC. This model is an improvement of their steady state model for a single component. A major feature of the model is that the authors have considered the adsorption of the VOC in the bare patches where there is no biofilm growth. To simplify the solution of the transient model, they have made a quasi-steady-state approximation for the biolayer, used the concept of "effectiveness factors" following the approach of Tong and Fan (1988). This model is again restricted to the case of plug flow in the gas phase.

Recently, Hodge and Devinny (1995) published an axial dispersion model for the transient biofiltration of single VOC. But the values of the air phase dispersion coefficient

are chosen arbitrarily. The model treats the porous medium as a two-phase system: the air phase and the water and solids phase. The authors treat the water and solids as a single phase, hence ignores some important phenomena, such as diffusion in the water/biofilm layer and details of adsorption processes at the water-solid interface. The model also describes the evolution of carbon dioxide by the microorganisms. The other major assumptions are the use of simple first-order kinetics for the degradation of the VOC (ethanol) and the presence of excess oxygen in the column.

Very recently Deshusses et al. (1995) have presented a model for the determination of both the transient and steady state behavior of biofilters degrading MEK and MIBK vapors. The major assumptions of this model are: negligible gas-phase interfacial resistance, planar geometry and plug flow in the gas phase. The biofilter height is divided into layers, and within each layer three main sections exist: the gas phase, the biofilm and a liquid sorption volume. The sorption volume consists of water content dispersed within the carrier and is assumed to be equal to the water content of the support material minus the biofilm volume, and no biological reaction takes place within the sorption volume. Uniform biofilm thickness throughout the column is assumed. The authors assume that the VOC diffuses through the entire thickness of the biofilm and then diffuses into the sorption volume, and the mass transfer coefficient between the biofilm and sorption volume assumed to be the same as within the biofilm. Oxygen limitation is neglected through some experimental studies. However, the authors agree that additional mass balances for oxygen could be incorporated if necessary. For the kinetics of biodegradation, Michaelis-Menten (Monod) type kinetics with competition between substrates is assumed.

2.3 ANALYSIS OF PUBLISHED WORK

A thorough review of the literature leads to the following conclusions:

1. Very few theoretical studies have been undertaken to predict the performance of biofilter columns.
2. Available theoretical models have been solved for simple cases by employing a number of simplifying assumptions.
3. Very limited attempts have been made to model the transient operation of a biofilter for VOC removal. In fact, there is no mathematical model available for the transient removal of VOC mixtures.
4. Very limited attempts have been made to study the dispersion effects in a biofilter model.
5. Very few experimental studies and no mathematical modeling have been reported on the performance of a biofilter when subjected to perturbations in environmental and process parameters such as, temperature, pH, feed concentrations, flowrate etc. These parameters largely govern the effectiveness of a biofilter column.

MODEL DEVELOPMENT

A mathematical model is a set of equations which, subject to certain assumptions, represent one or more aspects of a physical system. While the model itself obviously lacks the detailed reality of the system, the behavior of a valid model duplicates the actual responses of the system. Future responses may therefore be predicted by the operation of the model and manipulation of the results in the process termed *simulation*.

When deriving a theoretical model describing the behavior of a biofilter bed, one starts from a concept that is very customary in cases where the packing material serves as a support for microorganisms. A biofilter consists of three regions or phases :

1. A liquid biolayer where the substrates are transported and degraded (Figure 3.1c).
2. A gas phase which carries the substrate and oxygen.
3. A solid surface where the substrate gets adsorbed (Figure 3.1d).

3.1 THE BIOFILM

A biofilm is a collection of microorganisms and extra cellular products of microorganisms bound to a solid (living or inanimate) surface termed as substratum. Essentially any interface that exhibits biological activity can be conceptually termed a biofilm.

In a biofilter, when air flows around the biofilm, there is a continuous mass transfer between the gas phase and the biolayer. The volatile pollutants present in the gas phase, as well as oxygen, are partially dissolved in the liquid phase of the biolayer and are degraded or consumed by the microorganisms. In this way a concentration gradient is created in the biolayer which maintains a continuous flow of the component from the gas phase to the wet biolayer. The transportation within the biofilm is by molecular diffusion.

As the microorganisms multiply, the thickness of the biolayer increases. At some thickness, the diffusing oxygen is consumed by reaction before it penetrates through the entire biolayer. As a result, bacteria near the solid surface are in anaerobic environment. In addition, most of the substrate is consumed before reaching the solid surface of the packing material so that anaerobic bacteria adjacent to the surface enter the endogenous phase of growth. These bacteria become carbon sources for the bacteria at the outer layers.

Most of the biological conversion occurs in the aerobic portion of the film, called the effective or active biolayer, the depth of which depends on the rate of reaction, diffusivity of oxygen and VOCs. Concentration gradient of both oxygen and substrate exists in the biofilm. Under steady-state conditions, the mass fluxes of substrate and oxygen across the gas-biofilm interface equal the corresponding rates of substrate and oxygen consumption by reaction in the biolayer.

During start-up of a biofilter unit, the formation of the biolayer around the solid particles is not fully completed. As the biolayer is still in formation, its thickness varies with time. This phenomena associated with process start-up cannot be easily described and is out of the scope of the present study. Hence, the transient model proposed here is really applicable only for the transition from one set of operating conditions to another, after the biolayer has been fully developed.

In developing a theoretical model describing the elimination of carbon sources in the biofilm, the following assumptions are made:

- The biolayer is formed on the exterior surface of the particles. Biomass does not grow in the pores of the particles because the pore diameter is small enough to prevent microbial penetration (Deshusses et al, 1995). Therefore no biological reaction is assumed to take place in the solid.
- The biofilm geometry is considered to be flat, as assumption that holds if the thickness of the biofilm is less than 1 % of the radius of curvature of the support media (Rittman & Mc Carty, 1978)
- The extent of the biofilm patch is much larger than its depth. Hence, the VOC and oxygen transported into the biolayer through the side surfaces of the biofilm patch can be neglected, and diffusion/reaction in the biofilm can be considered in a single direction only.
- The VOC and/or oxygen are depleted in a fraction of the actual biolayer. This fraction is called the effective biolayer (see Figure 3.1c).

- Diffusivities of the VOC and oxygen are equal to the diffusivities of the same compounds in water, corrected by a factor depending on the biofilm density according to the expression of Fan et al. (1990).
- The biofilm density, defined as the amount of dry biomass per unit volume of biolayer, is constant i.e., the rate of biomass production is equal to the biomass decay.
- There is no accumulation of biomass in the filter bed and thus, the specific biolayer surface area is constant.

Mass Balance on the Biofilm

(a) Organic Substrate ($j = 1, 2, \dots, n$)

$$\frac{\partial S_j}{\partial t} = f(X_V) D_{jw} \frac{\partial S_j^2}{\partial x^2} - \frac{X_V}{Y_j} \mu_j(S_j, S_O) \quad (3.1)$$

(b) Oxygen

$$\frac{\partial S_O}{\partial t} = f(X_V) D_{Ow} \frac{\partial S_O^2}{\partial x^2} - \sum_{j=1}^n \frac{X_V}{Y_{Oj}} \mu_j(S_1, \dots, S_n, S_O) \quad (3.2)$$

where, n is the total number of organic substrates. The initial and boundary conditions are as follows,

$$t = 0 \quad h = 0, x = 0 \quad S_j = \frac{C_{j0}}{m_j} \quad (3.3)$$

$$t = 0 \quad 0 < h \leq H ; x = 0 \quad S_j = \frac{C_{j,0}(h)}{m_j} \quad (3.4)$$

$$t = 0 \quad 0 < x \leq \delta \quad S_j = S_{j,0}(x) \quad (3.5)$$

$$x = 0 \quad 0 < t < \tau ; h > u_g t \quad S_j = \frac{C_{j,0}(h)}{m_j} \quad (3.6)$$

$$x = 0 \quad 0 < t < \tau ; h < u_g t \quad S_j = \frac{C_j(h)}{m_j} \quad (3.7)$$

$$x = 0 \quad t > \tau ; h > 0 \quad S_j = \frac{C_j(h)}{m_j} \quad (3.8)$$

$$x = \delta \quad h > 0 ; t > 0 \quad \frac{\partial S_j}{\partial x} = 0 \quad (3.9)$$

Usually, transients of the biofiltration process last very long (even days), while the space time (τ) is in the order of minutes. For this reason, and without any loss of accuracy, one can omit boundary conditions (3.6) and (3.7), and use the condition (3.8) for any $t > 0$ rather than for $t > \tau$ only.

3.2 GAS PHASE

In deriving the mass balance equations for the gas phase, the following assumptions are made

- Due to a small particle diameter (order of several millimeters) usually applied in biofilter beds and a generally low solubility of the compounds to be transferred, the mass transfer resistance in the gas phase is ignored. This is proved by calculating the number of mass

transfer units in the gas phase defined as $N_o = \frac{k_g a H}{u_g}$ (Perry and Chilton, 1973) for each

of the components. k_g is the mass transfer coefficient given by the following semi-empirical relation (Ottengraf, 1986): $Sh_j = 1.0 Re_j^{1/2} Sc_j^{1/2}$ where Sh_j , Re_j and Sc_j are

the Sherwood-, Reynolds- and the Schmidt numbers respectively of the component J.

They are defined as follows :

$$Sh_J = \frac{v}{(1-v)} \frac{k_{rJ} d_p}{D_{JA}} \quad Re_J = \frac{\rho_{rJ} u_g d_p}{(1-v) \mu_{rJ}} \quad Sc_J = \frac{\mu_{rJ}}{\rho_{rJ} D_{JA}}$$

and a is the specific area for a fixed bed packed by a regular configuration of spherical

particles and is given as, $a = \frac{6(1-v)}{d_p}$.

The values obtained for N_O and the corresponding height of a transfer unit (H.T.U) calculated according to : $HTU = H / N_O$ for the flow rate range studied are as follows:

Compound	N_O	H.T.U (m)
Benzene	600 - 2355	$1.05 \times 10^{-3} - 2.67 \times 10^{-4}$
Toluene	566 - 2220	$1.11 \times 10^{-3} - 2.8 \times 10^{-4}$
Oxygen	1430 - 5610	$1.12 \times 10^{-4} - 4.4 \times 10^{-4}$

As can be seen, the HTU for a biofilter bed is of the same order of magnitude as the particle size and the number of mass transfer units is very much higher than the number of reaction units, which for biological reactions are found to be generally less than 10 (Ottengraf et al. 1983). The authors concluded that the compound concentrations in the wet biolayer at the interface are continuously in equilibrium with the respective concentrations in the bulk of the gas phase. However, this point still needs to be verified.

- The VOC and oxygen at the biolayer / air interface are assumed to be in equilibrium as dictated by Henry's law. The distribution coefficients are the same as if the biolayer was made of water only.

Mass Balance on the Gas Phase

(a) Organic Substrate

$$v \frac{\partial C_j}{\partial t} = D_j v \frac{\partial^2 C_j}{\partial h^2} - u_g \frac{\partial C_j}{\partial h} + f(X_v) D_{jw} \alpha A_s \left(\frac{\partial S_T}{\partial x} \right)_{x=0} - (1-\alpha) A_s k_j (C_j - C_j^*) \quad (3.10)$$

(b) Oxygen

$$v \frac{\partial C_o}{\partial t} = D_o v \frac{\partial^2 C_o}{\partial h^2} - u_g \frac{\partial C_o}{\partial h} + f(X_v) D_{ow} \alpha A_s \left(\frac{\partial S_o}{\partial x} \right)_{x=0} \quad (3.11)$$

with the following initial and boundary conditions:

$$t = 0 \quad h = 0 \quad C_j = C_{j,0} \quad (3.12)$$

$$t = 0 \quad 0 < h \leq H \quad C_j = C_{j,0}(h) \quad (3.13)$$

$$h = 0 \quad t > 0 \quad D_j \frac{\partial C_j}{\partial h} = -u_g (C_j|_{0^-} - C_j|_{0^+}) \quad (3.14)$$

$$h = H \quad t > 0 \quad \frac{\partial C_j}{\partial h} = 0 \quad (3.15)$$

Conditions (3.14) and (3.15) are the well known Dankwerts' boundary conditions which account for axial dispersion effects at the inlet and exit condition of the biofilter.

3.3 SOLID PHASE

It has been reported by Zarook and Baltzis (1994b) that the biofilm is not necessarily formed uniformly over the entire particle surface. In actuality, there are patches of biofilm on the solids, as shown in Figure 3.1, leaving the bare surface of the solids in direct contact with the air stream. In these bare surfaces, the VOC gets adsorbed. It has been demonstrated by Hodge and Devanny (1995) that during start-up conditions of a biofilter, adsorption is the controlling removal mechanism. In the later stages of operation, when the filter material is saturated with the contaminant, the removal is dominated by biodegradation. In deriving the mass balance equations on the solid, the following assumptions are made :

- Adsorption is a reversible process and its equilibrium characteristics are described through the use of adsorption isotherms. In this model, the term adsorption is used loosely and it refers to both actual adsorption on the solid as well as absorption of VOCs in the water retained in the pores of the solid. It actually represents the VOC retaining capacity of the solid.
- Adsorption of the pollutant occurs only through the direct bare solid / air interface. It does not occur in the biofilm (see Figure 3.1d)
- There is no series adsorption of the substrate onto the solid through the biofilm. This is due to the low concentrations of the VOCs generally encountered in biofiltration. The biofilm thickness is sufficiently large enough that the entire substrate diffusing into the biofilm is depleted in the effective biolayer.
- There is no back diffusion of the substrate from the solid into the biofilm. This can be explained as follows: (a) the adsorptive capacity of the packing material considered (peat)

is very low ($K_{DJ} = 2.25 \times 10^{-5}$ g /g-particle for toluene and 8.68×10^{-6} g / g-particle for benzene). (b) the fractional surface area covered by the biofilm (30 %) is much less than the bare surface (70 %). So there is more probability of the substrate diffusing through the bare surface, which is accounted for by the isotherm.

- Oxygen does not get adsorbed on the solid particles.

Mass Balance on the Solid Phase

$$(1 - v) \rho_p \frac{\partial C_{jP}}{\partial t} = k_j (1 - \alpha) A_s^* (C_j - C_j^*) \quad (3.16)$$

$$t = 0 \qquad h \geq 0 \qquad C_{jP} = C_{jP,0}(h) \quad (3.17)$$

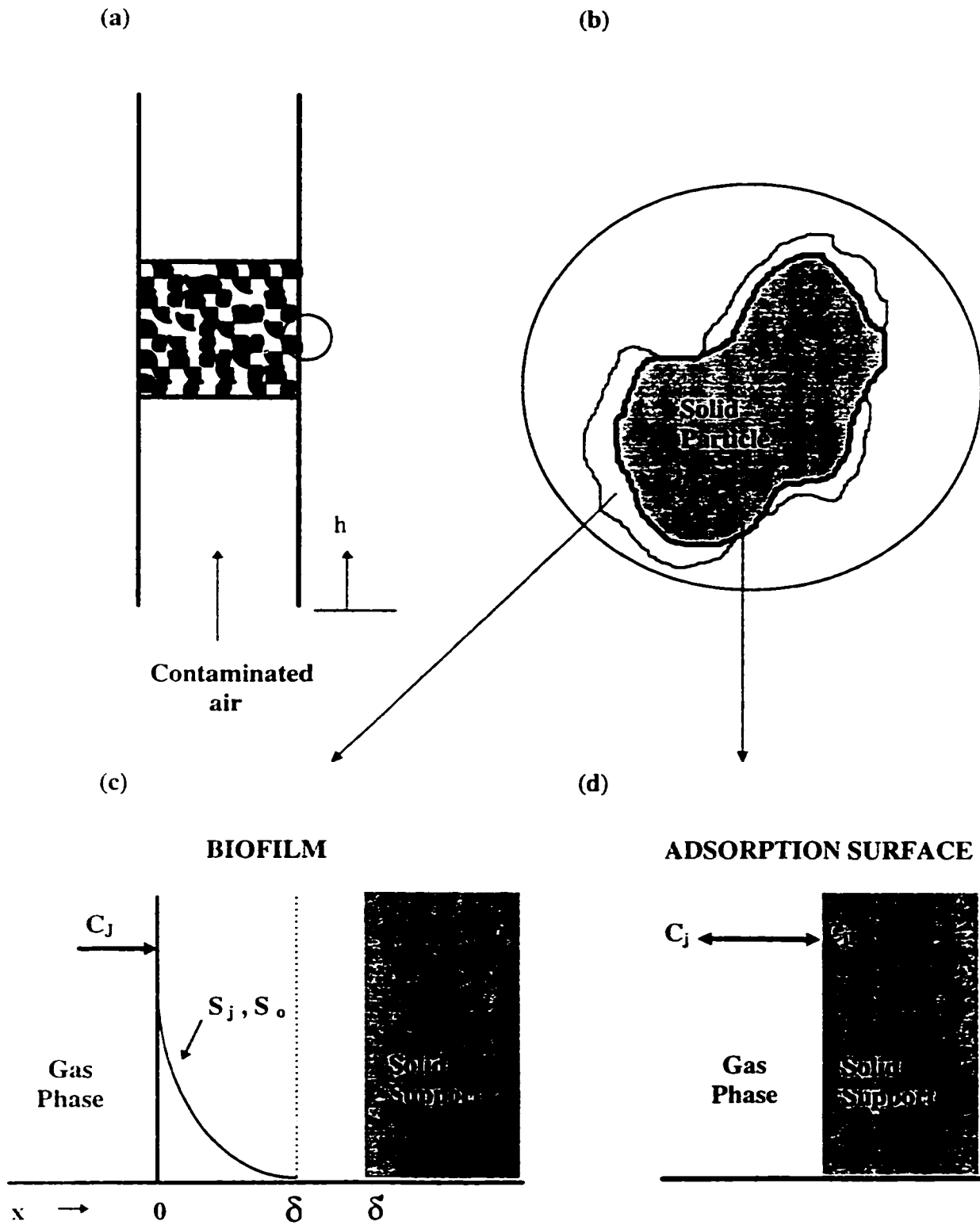


Figure 3.1 : Schematic Diagram of the Processes in a Biofilter

3.4 FUNCTIONAL EXPRESSIONS USED IN THE MODEL

(i) Degradation Kinetics

Solution of the model requires knowledge of the kinetic expressions and adsorption isotherms. This model is compared, as will be discussed in the later sections, with the transient biofiltration data of two hydrophobic solvents, and more specifically benzene and toluene. Both substances are classified as primary pollutants by the US EPA. They are present in gasolines (Potter, 1992), and they are also widely used as industrial solvents, as well as feedstocks for synthesis (Reisch, 1992).

The specific growth rates of the biomass on benzene and toluene were determined through shake flask experiments by Oh et al (1993) and Zarook and Baltzis (1993) as follows:

Andrews (or Haldane) kinetics for toluene

$$\mu_j(S_j) = \frac{\mu_j^* S_j}{\left(K_j + S_j + \frac{S_j^2}{K_{Ij}}\right)} g(S_o) \quad (3.18)$$

Monod kinetics for benzene

$$\mu_j(S_j) = \frac{\mu_j^* S_j}{(K_j + S_j)} g(S_o) \quad (3.19)$$

where $g(S_o)$ is the functional dependence of the specific growth rate oxygen given by

$$g(S_o) = \frac{S_o}{(K_o + S_o)} \quad (3.20)$$

The biodegradation kinetics for a compound are different when this compound is present alone or in a mixture with other organic compounds which are also biodegradable. It has

been proved that there will be some kinetic interaction between the two compounds. This kinetic interference is bound to play a significant role in the biofiltration of VOC mixtures. The kinetic expressions for the removal of benzene and toluene in a mixture of the same are given by the following expressions (Zarook and Baltzis, 1994c)

$$\mu_B(S_B, S_T, S_O) = \frac{\mu_B^* S_B S_O}{(K_B + S_B + K_{BT} S_T)(K_{OB} + S_O)} \quad (3.21)$$

$$\mu_T(S_B, S_T, S_O) = \frac{\mu_T^* S_T S_O}{(K_T + S_T + \frac{S_T^2}{K_{TT}} + K_{TB} S_B)(K_{OT} + S_O)} \quad (3.22)$$

The above expressions imply that in the absence of toluene, and when oxygen is present at high, non-changing levels, benzene is removed according to a Monod expression (Monod, 1942). In the absence of benzene, and when oxygen does not affect the kinetics, toluene is removed according to the Andrews inhibitory expression (Andrews, 1968). Parameters K_{BT} and K_{TB} indicate the interactions of toluene and benzene, respectively, with the kinetics of benzene and toluene removal, respectively.

(ii) Temperature

The reaction rate constants in the above kinetic expressions are functions of temperature and pH. The relationship can be written as follows (Metcalf and Eddy, 1990)

$$\mu = \mu_0 \exp\{0.098(T - 15)\} \text{ at a pH of 7.2} \quad (3.23)$$

where

$$\mu_0 = \mu_{max} \text{ at } 15^\circ \text{C}$$

(iii) pH

The fractional decrease in growth rate due to deviations from the optimum pH is represented by a Gaussian curve (de Beer et al., 1992)

$$f_{pH} = e^{-\left(\frac{pH-7.02}{0.5}\right)^2} \quad (3.24)$$

(iv) Adsorption isotherm

The adsorption of toluene on the solid packing is described by the Freundlich isotherm as given by Zarook and Baltzis (1994b). The same experimental method was used in the present work to determine the equilibrium adsorption isotherm of the benzene-peat system. An amount of packing material was prepared and a quantity of sterile medium was added to the packing. Equal amounts (10 g) of packing material were placed in several serum bottles (158 ml). The bottles were closed with Teflon-faced silicon septa and aluminium crimp caps. Using a 10 μ l liquid syringe, precise volumes of toluene were added to the bottles, and the solvent was allowed to evaporate and reach equilibrium within the enclosed space. Headspace samples were taken with a gas-tight 0.5 ml pressure-LOK syringe, and were subjected to GC analysis. Samples were taken on a daily basis, until the concentration in the air reached a constant value. Unchanging concentrations indicated that equilibrium had been reached, and these equilibrium toluene concentrations were used in deriving the adsorption isotherm of Freundlich which explain the data very well (see Figure 4.1)

$$C_{j,p} = k_{jd} (C_j^*)^{n_j} \quad (3.25)$$

If mixtures of two compounds are considered, then the isotherm for mixtures needs to be used. However, the experimental measurement of multicomponent adsorption isotherms is time consuming because of the large number of variable involved, and the problem of predicting binary and multicomponent equilibria from single component adsorption data has therefore attracted much attention. The experimental data for the adsorption of benzene and toluene have been fitted to the Extended Langmuir Model (Ruthven, 1994) as shown below and the constants b_T and b_B are determined. a_T and a_B are defined as the ratios of the particle concentrations to the corresponding saturation concentrations.

$$C_{TP} = \frac{a_T C_T^*}{1 + b_T C_T^* + b_B C_B^*} \quad (3.26)$$

$$C_{BP} = \frac{a_B C_B^*}{1 + b_T C_T^* + b_B C_B^*} \quad (3.27)$$

3.5 SOLUTION OF THE MODEL EQUATIONS

The transient model, described by equations (3.1-3.17) constitutes a problem of coupled partial differential equations in three dimensions ; time, biolayer and bed height. The above equations form a system of highly non-linear complex set of equations. This system is solved by two approaches. In the first approach, the number of equations is reduced to three by making an assumption of quasi steady-state used by Zarook and Baltzis (1993). Hence the resulting final equations are labeled as an *approximate model*. In the second approach the model equations are solved as such without any assumptions and hence the resulting final model equations are labeled as the *general model*.

BIOFILTRATION OF SINGLE VOCS

Approximate model and the General Model

In the present chapter modeling the biofiltration of single VOCs is considered. The model equations can be obtained by setting $j=1$ in the equations 3.1 - 3.5, 3.10-3.11 and 3.16. As discussed in Chapter 4, the resulting set of five equations describing the transient biofiltration of single VOCs are solved using the two approaches. In the first approach, for the approximate model, the number of equations is reduced to five by making an assumption of quasi steady state in the biofilm. For the general model, the actual set of five equations are solved as such. The models are also valid for any binary mixture provided the kinetic and adsorption expressions are replaced.

The following are the final model equations obtained by putting $j=1$ in equations 3.1-3.5.

$$\frac{\partial S_j}{\partial t} = f(X_V) D_{jw} \frac{\partial S_j^2}{\partial x^2} - \frac{X_V}{Y_j} \mu_j(S_j, S_O) \quad (4.1)$$

$$\frac{\partial S_O}{\partial t} = f(X_V) D_{Ow} \frac{\partial S_O^2}{\partial x^2} - \frac{X_V}{Y_{Oj}} \mu_j(S_j, S_O) \quad (4.2)$$

$$v \frac{\partial C_j}{\partial t} = D_j v \frac{\partial^2 C_j}{\partial h^2} - u_s \frac{\partial C_j}{\partial h} + f(X_V) D_{jw} \alpha A_s^* \left(\frac{\partial S_T}{\partial x} \right)_{x=0} - (1-\alpha) A_s^* k_j (C_j - C_j^*) \quad (4.3)$$

$$v \frac{\partial C_o}{\partial t} = D_o v \frac{\partial^2 C_o}{\partial h^2} - u_s \frac{\partial C_o}{\partial h} + f(X_v) D_{ow} \alpha A_s^* \left(\frac{\partial S_o}{\partial x} \right)_{x=0} \quad (4.4)$$

$$(1-v) \rho_p \frac{\partial C_{jP}}{\partial t} = k_j (1-\alpha) A_s^* (C_j - C_j^*) \quad (4.5)$$

The initial and boundary conditions are the same as those given in chapter 3.

4.1 APPROXIMATE MODEL

In this approach, to simplify the solution of the transient model, a quasi steady-state approximation was made for the biolayer. This assumption can be justified as follows. A measure of the time scale of events in the biolayer is given by $\delta^2 / (f(X_v) D_{jW})$, (Karel et al., 1985). Of the compounds diffusing into the biofilm, toluene and oxygen, toluene has the lowest diffusivity. Based on the values of $f(X_v)$, D_{TW} and δ , it has been shown by Zarook and Baltzis (1994b) that the time scale of events in the biolayer is about 6 sec, a value which is two orders of magnitude less than residence times used in the experiments (see Tables 4.2 and 4.3). Since τ can be taken as an indication of the time scale of events in the gas phase, one can conclude that the biolayer can be viewed as being always under steady-state conditions. Effectiveness factors are introduced following the approach of Tong and Fan (1988). These factors are defined as follows :

$$e_j = \frac{f(X_v) D_{jW} \left(\frac{\partial S_j}{\partial x} \right)_{x=0}}{\delta \frac{X_v}{Y_j} [\mu_i(S_j, S_o)]_{x=0}} \quad (4.6)$$

$$e_o = - \frac{f(X_v) D_{ow} \left(\frac{\partial S_o}{\partial x} \right)_{x=0}}{\delta \frac{X_v}{Y_o} [\mu_o(S_T, S_o)]_{x=0}} \quad (4.7)$$

The use of effectiveness factors in conjunction with the quasi-steady-state approximation, permits the omission of equations (4.1) and (4.2) for the biofilm. The following are the non-dimensional groups derived for this model:

$$\begin{aligned} \bar{C}_j &= \frac{C_j}{C_{j1}} & \bar{C}_o &= \frac{C_o}{C_{o1}} & \bar{C}_{jP} &= \frac{C_{jP} (1-\nu) \rho_P}{u_g \nu} \\ Z &= \frac{h}{H} & \theta &= \frac{x}{\delta} & \epsilon_j &= \frac{C_{ji}}{K_j m_j} & \epsilon_o &= \frac{C_{oi}}{K_o m_o} \\ \xi &= \frac{u_g t}{H} & Pe_j &= \frac{u_g H}{\nu D_j} & Pe_o &= \frac{u_g H}{\nu D_o} & \gamma &= \frac{K_j}{K_{lj}} \\ \beta_{1j} &= \frac{e_j H \alpha A_s^* \delta X_v}{\nu u_g C_{ji} Y_j} & \beta_{2j} &= \frac{e_o H \alpha A_s^* \delta X_v}{\nu u_g C_{oi} Y_{oj}} \\ \chi_j &= \frac{(1-\alpha) H A_s^* k_{Mj}}{\nu u_g} & \psi_j &= \frac{1}{C_{ji}} \left[\frac{\nu C_{ji}}{(1-\nu) \rho_P k_{dj}} \right]^{1/n_j} \end{aligned}$$

Introducing the above dimensionless groups, the model equations are reduced to the following system of three differential equations along with the initial and boundary conditions.

Mass Balance in the Gas Phase

$$\frac{\partial \bar{C}_j}{\partial \xi} = \frac{1}{Pe_j} \frac{\partial^2 \bar{C}_j}{\partial Z^2} - \frac{\partial \bar{C}_j}{\partial Z} - \beta_{1j} g_1(\bar{C}_j, \bar{C}_o) - \chi_j (\bar{C}_j - \bar{C}_j^*) \quad (4.8)$$

$$\frac{\partial \bar{C}_o}{\partial \xi} = \frac{1}{Pe_o} \frac{\partial^2 \bar{C}_o}{\partial Z^2} - \frac{\partial \bar{C}_o}{\partial Z} - \beta_{2j} g_1(\bar{C}_j, \bar{C}_o) \quad (4.9)$$

Mass Balance in the Solid Phase

$$\frac{\partial \bar{C}_{jP}}{\partial \xi} = \chi_j (\bar{C}_j - \bar{C}_j^*) \quad (4.10)$$

where $g_1(\bar{C}_j, \bar{C}_o)$ is given by Andrews (or Haldane) Kinetics as

$$g_1(\bar{C}_j, \bar{C}_o) = \frac{\bar{C}_j \bar{C}_o \varepsilon_j \varepsilon_o}{(1 + \bar{C}_j \varepsilon_j + \bar{C}_j^2 \varepsilon_j^2 \gamma)(1 + \bar{C}_o \varepsilon_o)} \quad (4.11)$$

and for Monod Kinetics

$$g_1(\bar{C}_j, \bar{C}_o) = \frac{\bar{C}_j \bar{C}_o \varepsilon_j \varepsilon_o}{(1 + \bar{C}_j \varepsilon_j)(1 + \bar{C}_o \varepsilon_o)} \quad (4.12)$$

$$\bar{C}_j^* = \psi_j (\bar{C}_{jP})^{\frac{1}{n}} \quad (4.13)$$

Initial conditions :

$$\xi = 0 \quad Z = 0 \quad \bar{C}_j = 1 \quad \bar{C}_{jP} = \bar{C}_{jP,0}(0) \quad (4.14)$$

$$\xi = 0 \quad 0 \leq Z \leq 1 \quad \bar{C}_j = \bar{C}_{j,0}(Z) \quad \bar{C}_{jP} = \bar{C}_{jP,0}(Z) \quad (4.15)$$

Boundary Conditions :

$$Z = 0 \quad \xi > 0 \quad \frac{\partial \bar{C}_J}{\partial Z} = -Pe_J (\bar{C}_J|_{Z=0^-} - \bar{C}_J|_{Z=0^+}) \quad (4.16)$$

$$Z = 1 \quad \frac{\partial \bar{C}_J}{\partial Z} = 0 \quad (4.17)$$

Solution of the approximate model requires correlations for film thickness and effectiveness factors (e_j , e_0). The correlations used in the work of Zarook and Baltzis (1994b) were obtained by fitting film thickness and effectiveness factors to the solution of the model under quasi-steady state approximation in the biofilm. Thus, this procedure even though simplifies the mathematical complexity, requires elaborate calculations prior to the solution of the model. Furthermore, the correlations are not general and they are dependent on the VOC under study. Hence, general model, without any simplifications is solved as described in the next section.

4.2 GENERAL MODEL

The following are the additional non dimensional groups derived for the general model,

$$\begin{aligned} \bar{S}_T &= \frac{S_T}{K_T} & \bar{S}_O &= \frac{S_O}{K_O} \\ \beta_{3j} &= \frac{D_{jW} H \alpha A_S^* f(X_V) K_j}{v u_g C_{ji} \delta} & \beta_4 &= \frac{D_{OW} H \alpha A_S^* f(X_V) K_O}{v u_g C_{O1} \delta} \\ \phi_{1j} &= \frac{D_{jW} H f(X_V)}{u_g \delta^2} & \phi_2 &= \frac{D_{OW} H f(X_V)}{u_g \delta^2} \\ \eta_{ij} &= \frac{H \mu_j^* X_V}{Y_{Oj} K_{Oj} u_g} & \eta_{2j} &= \frac{H \mu_j^* X_V}{Y_j K_j u_g} \end{aligned}$$

Introducing the dimensionless parameters, the model can be reduced to the following system of five differential equations.

Mass Balance in the Biofilm

$$\frac{\partial \bar{S}_j}{\partial \xi} = \phi_{1j} \frac{\partial^2 \bar{S}_j}{\partial \theta^2} - \eta_{1j} (\bar{S}_j, \bar{S}_O) \quad (4.18)$$

$$\frac{\partial \bar{S}_O}{\partial \xi} = \phi_2 \frac{\partial^2 \bar{S}_O}{\partial \theta^2} - \eta_{2j} (\bar{S}_j, \bar{S}_O) \quad (4.19)$$

with initial and boundary conditions,

$$\xi = 0 \quad Z = 0, \theta = 0 \quad \bar{S}_j = \varepsilon_j \quad (4.20)$$

$$\xi = 0 \quad 0 < Z \leq 1; \theta = 0 \quad \bar{S}_j = \varepsilon_j \bar{C}_{j,0}(Z) \quad (4.21)$$

$$\xi = 0 \quad 0 < \theta \leq 1 \quad \bar{S}_j = \bar{S}_{j,0}(\theta) \quad (4.22)$$

$$\theta = 0 \quad Z > 0 \quad \bar{S}_j = \epsilon_j \bar{C}_j(Z) \quad (4.23)$$

$$\theta = 1 \quad Z > 0 ; \xi > 0 \quad \frac{\partial \bar{S}_j}{\partial x} = 0 \quad (4.24)$$

Mass Balance in the Gas Phase

$$\frac{\partial \bar{C}_j}{\partial \xi} = \frac{1}{Pe_j} \frac{\partial^2 \bar{C}_j}{\partial Z^2} - \frac{1}{v} \frac{\partial \bar{C}_j}{\partial Z} - \beta_{sj} \left(\frac{\partial \bar{S}_j}{\partial \theta} \right)_{\theta=0} - \chi_j (\bar{C}_j - \bar{C}_j^*) \quad (4.25)$$

$$\frac{\partial \bar{C}_o}{\partial \xi} = \frac{1}{Pe_o} \frac{\partial^2 \bar{C}_o}{\partial Z^2} - \frac{1}{v} \frac{\partial \bar{C}_o}{\partial Z} - \beta_s \left(\frac{\partial \bar{S}_o}{\partial \theta} \right)_{\theta=0} \quad (4.26)$$

Mass balance in the solid phase (equation 4.10) and initial and boundary conditions (equations 4.14 through 4.16) required for solving the mass balance equations in the gas and solid phases are the same for both approximate and general models.

4.3 MODEL PARAMETER ESTIMATION

Solution of these two models requires parameter values. Most of the parameters needed to solve the models can be obtained from the previous works (Zarook, 1994; Zarook and Baltzis 1994a & 1994b). As stated previously, the adsorption parameters for benzene have been experimentally found, in this work, by using the same procedure described by Zarook and Baltzis (1994b). The mass transfer coefficient of benzene from gas to solid phase is assumed to be the same as that for toluene. The film thickness and effectiveness factor correlations obtained from the same study were used to solve the approximate model. Thus,

the correlations used were $\delta_j = 1.5C_j + 33.4$ and $e_k = 0.03C_k + 0.2$ for film thickness and effectiveness factors, respectively. In the case of the general model, a value of the film thickness is not necessary as the model itself determines the value when either VOC or oxygen gets completely consumed. This procedure of estimating the effective film thickness is discussed in more detail by Zarook et al. (1993). The values for the gas phase dispersion coefficients for the compounds benzene, toluene and oxygen were estimated using the following correlation which is, in general, valid for flow through porous packed-beds (Ruthven, 1984).

$$D_j = \gamma_1 D_{jA} + \gamma_2 2R_p u_g / v \quad (4.27)$$

where γ_1 and γ_2 are constants which normally have values of about 0.7 and 0.5, respectively. Considering the bed as an assemblage of randomly oriented cylindrical pores suggests $\gamma_1 = 1/\sqrt{2}$, which is close to the experimental values derived from dispersion measurements for gases at low Reynolds number (Ruthven, 1984). A typical biofilter operates at a low Reynolds number of about 0.2 to 0.5 (Hodge and Devinny, 1995). The bed tortuosity is related to voidage as $\gamma_2 = 0.45 + 0.55v$. Once an average radius of particle (R_p), γ_1 and γ_2 are known, one can estimate the dispersion coefficient D_j from equation (4.27). All the other parameters used in solving the model equations are listed in Table 4.1. The value of the effective diffusivity was calculated by Zarook (1994) using the following empirical equation developed by Fan et al. (1990).

$$f(X_v) = \frac{D_{j, film}}{D_{j, w}} = 1 - \frac{0.43 X_v^{0.92}}{11.19 + 0.27 X_v^{0.99}} \quad (4.28)$$

Table 4.1 : Parameter values used for solving the approximate and general model equations.

PARAMETER	VALUE	UNITS	REF.
A_{ST}	40.0	m^{-1}	1
A_{SB}	23.3	m^{-1}	1
C_{O_i}	275.0	$g\ m^{-3}$	1
D_{BA}	0.0895	$cm^2\ s^{-1}$	3
D_{TA}	0.0792	$cm^2\ s^{-1}$	3
D_{OA}	0.2132	$cm^2\ s^{-1}$	3
D_{BW}	1.04×10^{-9}	$m^2\ s^{-1}$	1
D_{TW}	1.03×10^{-9}	$m^2\ s^{-1}$	1
D_{OW}	2.41×10^{-9}	$m^2\ s^{-1}$	1
$f(X_V)$	0.195	-	1
k_B, k_T	6.04×10^{-3}	$m\ h^{-1}$	2
k_{dB}	8.68×10^{-6}	$g / g\text{-particle}$	present study
k_{dT}	2.25×10^{-5}	$g / g\text{-particle}$	2
K_{TT}	78.94	$g\ m^{-3}$	1
K_O	0.26	$g\ m^{-3}$	1
K_B	12.22	$g\ m^{-3}$	1
K_T	11.03	$g\ m^{-3}$	1
m_B	0.23	-	1
m_O	34.4	-	1
m_T	0.27	-	1
n (toluene)	1.04	-	2
n (benzene)	0.93	-	present study
X_V	100.0	$kg\ m^{-3}$	1
Y_B	0.708	-	1
Y_{OB}	0.336	-	1
Y_{OT}	0.341	-	1
Y_T	0.708	-	1
α	0.3	-	2
μ_T^*	1.50	h^{-1}	1
μ_B^*	0.68	h^{-1}	1
u	0.3	-	2
ρ_P	4.28×10^5	$g\ m^{-3}$	2

¹Zarook & Baltzis, (1994 a); ²Zarook & Baltzis. (1994 b); ³Hsieh et al., (1993)

4.4 NUMERICAL METHOD

In simulation problems related to such type of mathematical formulations, the numerical solution scheme of orthogonal collocation has been found to be quite effective. In essence, the orthogonal collocation replaces the spatial derivatives by the so-called collocation matrices and hence the set of partial differential equations is reduced to a set of simultaneous ordinary differential equations which can then be solved by a variety of standard numerical schemes available for the solution of ordinary differential equations. The resulting partial differential equations for the approximate model equations (4.8-4.10) and the general model (4.17-4.18, 4.24-4.25 and 4.10) are reduced to ordinary differential equations by orthogonal collocation (Appendix A). Ten collocation points were used for discretizing the column height Z (from $Z=0$ to $Z=1$) for both models. In the case of the general model, six points were used to discretize θ , the biofilm depth (from $\theta = 0$ to 1), in addition to ten collocation points for the column height Z . The resulting set of simultaneous ordinary differential equations, 30 for the *approximate* model and 150 for the *general* model, were then solved using the subroutine DIVPRK of the International Mathematical Subroutine Library (IMSL).

5.5 RESULTS AND DISCUSSIONS

Validation of the Models

For validating the models, the experimental data of Zarook and Baltzis (1994a, 1994b), and Tang et al. (1995) are used. Figure 4.2 shows the experimental and model predicted concentration values for toluene along the column, comparing the *approximate* and the *general* model. As can be seen, there is not much difference in the predictions of the two models. Figure 4.3 shows comparisons between the predicted concentration profiles of three models, namely the plug flow model of Zarook and Baltzis (1994b), *approximate* and *general* models of this work against the toluene transient biofiltration data. At one third height indicated by the group (a), it is clear that both the *general* and *approximate* models predict better than the plug flow model. However, the predictions by the general model are better. At the exit of the column indicated by the group (b), data are scattered, thus it is difficult to give any conclusion from this graph. However, all model predictions are not widely different. Both experimentally evaluated (Zarook and Baltzis, 1994a) steady-state removal rate, which is defined as the mass of VOC consumed per volume of packing per time, was also compared. In almost all cases, the approximate and general model predict better than the plug flow model, and the general model predictions being closer to the experimental values. Hence, results from only the general model are used in the analysis of subsequent sections. In the case of toluene as discussed, the improvement is not significant as can be seen from Table 4.3. However this is not the case with benzene. Table 4.2 shows the space time, measured inlet and exit concentration of benzene at steady-state conditions. The predicted exit

concentration profile by the *general* model is improved significantly as compared to the previous model of Zarook and Baltzis(1994a).

Figures 4.4a and 4.4b again show the experimental and model (general) predicted transient concentration profiles for benzene in the column for two different operating conditions. As can be seen, the general model predictions are in good agreement with the experimental results. However, Figure 4.4a shows that the initial period of four days is not well described by the general model. Experimental data reported in Figure 4.4a were obtained prior to those of Figure 4.4b, thus the initial adsorption process as well as the process of formation of biofilm in the initial period may be the reasons for this long transient period. Hence, the general model developed in this study, may not give reasonable predictions of the *initial* start-up period, however, it can be used for predicting the transient performance from one set of operating conditions to the other.

Figures 4.5a and 4.5b, show the general model predictions of the steady state concentration profile of benzene along the biofilter column for two different operating conditions. As can be seen, the model predictions are in close agreement with the experimental results.

Table 4.2 : Comparison of biofilter models against experimental data of benzene (Zarook & Baltzis, 1994a) under steady state conditions

τ (min)	C_{inlet} g/m^3	C_{out} (exp) g/m^3	C_{out} (model) ¹ g/m^3	Error %	C_{out} (model) ² g/m^3	Error %
4.1	0.28	0.19	0.16	-15.8	0.18	-5.3
4.5	0.43	0.23	0.25	8.7	0.24	4.3
4.7	0.56	0.21	0.31	47.6	0.29	38.1
2.7	0.13	0.09	0.09	0.0	0.09	0.0
2.7	0.12	0.08	0.09	-11.1	0.08	0.0
4.1	0.07	0.04	0.04	0.0	0.04	0.0

¹ Plug flow model of Zarook and Baltzis (1994 a)

² General Model

Table 4.3: Biofiltration of Toluene vapor: Experimental data and comparison of model predictions.
The units of C are g m^{-3} and those of R are $\text{g m}^{-3} \cdot \text{h}^{-1}$.

t (min)	C_{inlet}	C_{out} (exp)	R_{exp}	R_{model}¹	Error %	R_{model}²	Error %	R_{model}³	Error %
6.3	2.81	0.20	24.8	21.5	-13.3	21.6	-12.9	22.3	-10.0
2.7	0.62	0.21	9.4	7.4	-21.3	7.8	-17.02	7.8	-17.02
4.2	0.92	0.19	10.4	9.0	-13.5	9.8	-5.8	9.57	-7.9
8.6	0.68	0.00	4.8	4.4	-8.3	4.32	-10.0	4.3	-10.4
7.7	1.65	0.07	12.2	11.3	-7.4	11.31	-7.3	11.3	-7.3

¹ Zarook and Baltzis (1994 b);

² Approximate Model;

³ General Model

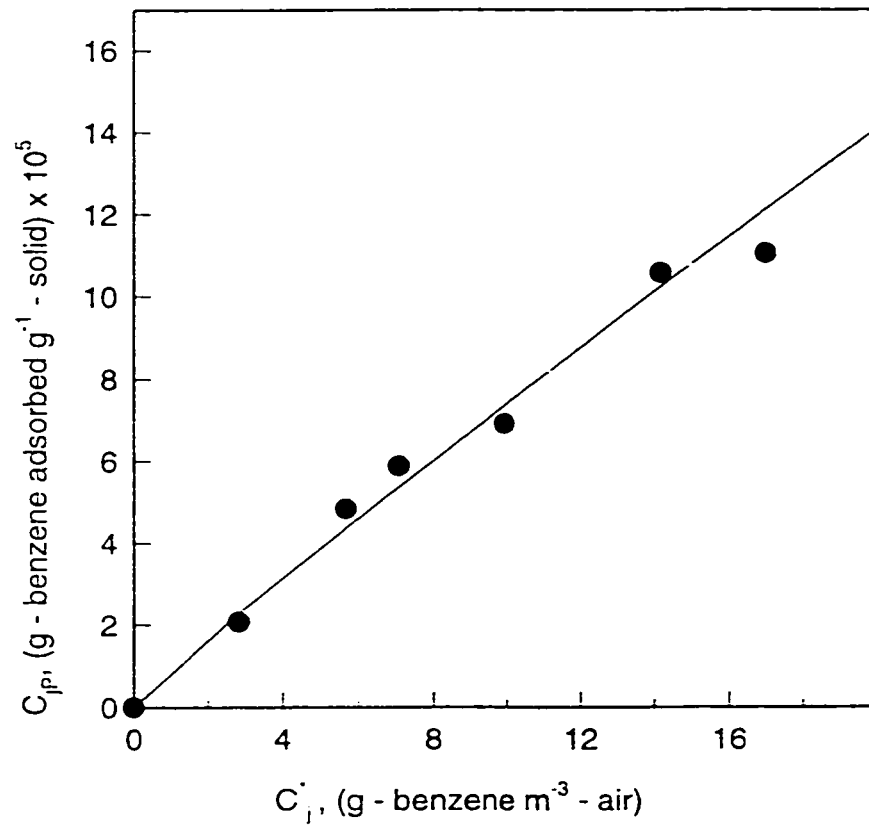


Figure 4.1: Equilibrium adsorption isotherm of benzene on a peat/perlite mixture. The curve represents a fitting of the data points to the Freundlich equation.

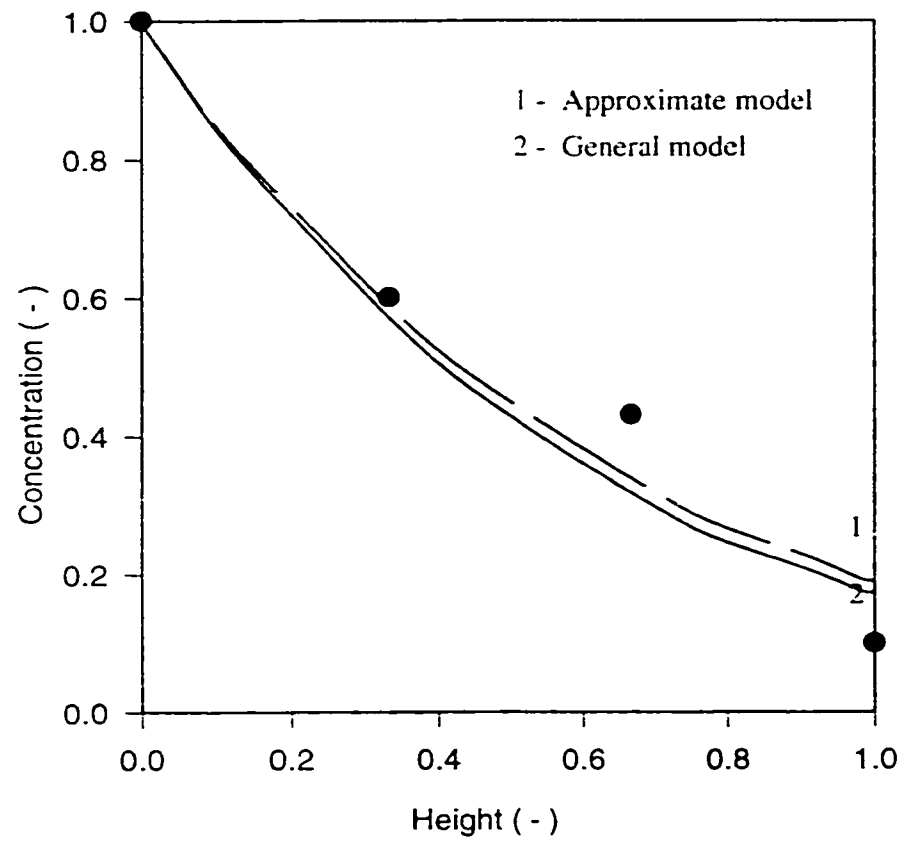


Figure 4.2: Model predicted toluene concentration profiles and experimental data for $C_{ii}=2.81 \text{ g m}^{-3}$ and $\tau = 6.3 \text{ min}$.

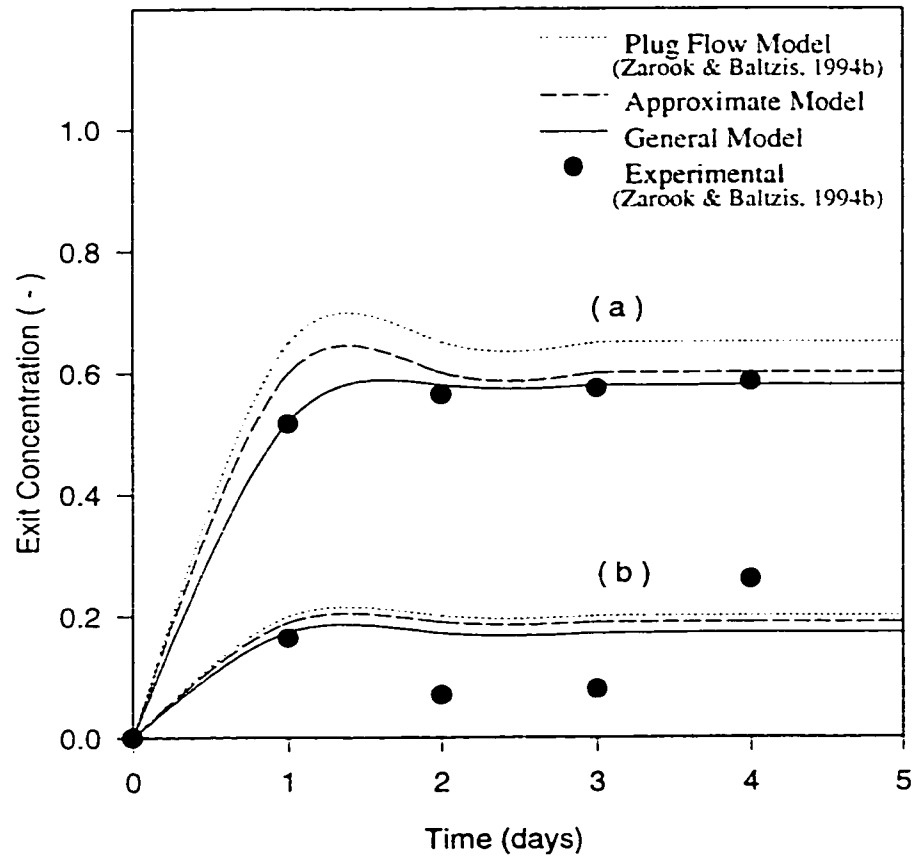


Figure 4.3: Concentration of toluene with time. Experimental data and predictions by different models.

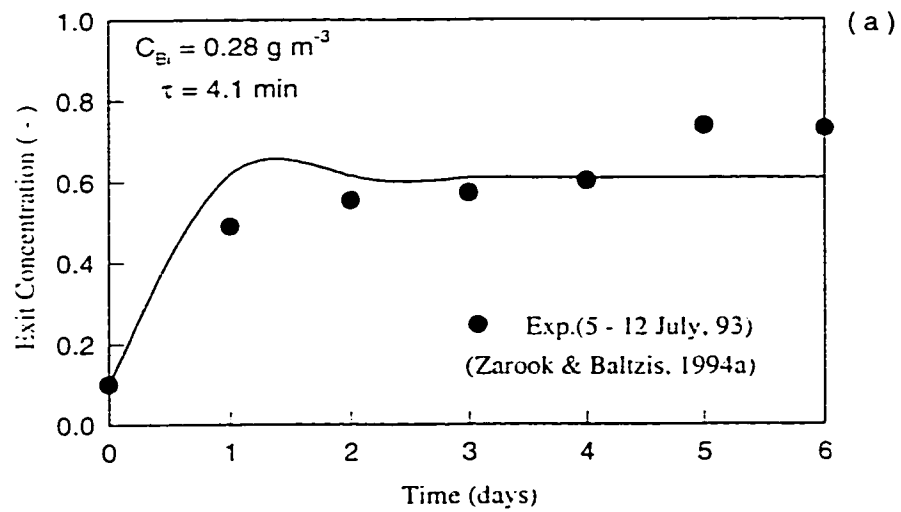
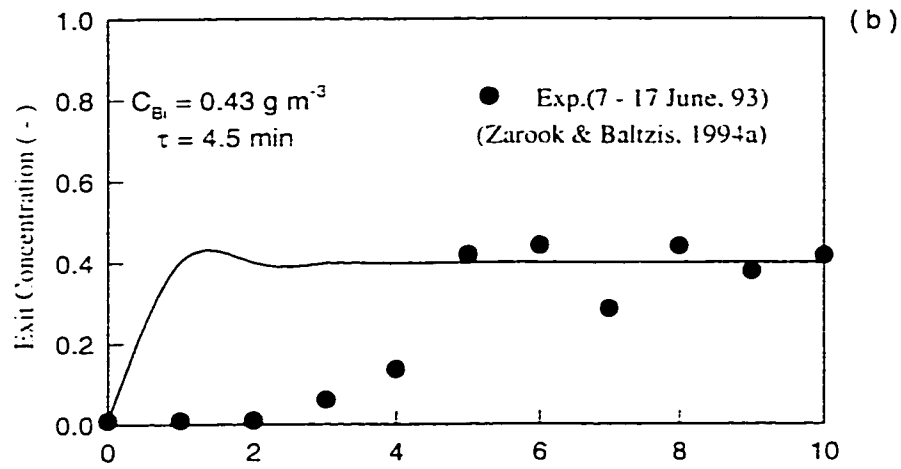


Figure 4.4a & 4.4b: Concentration of benzene with time. Experimental data and model (general) predictions.

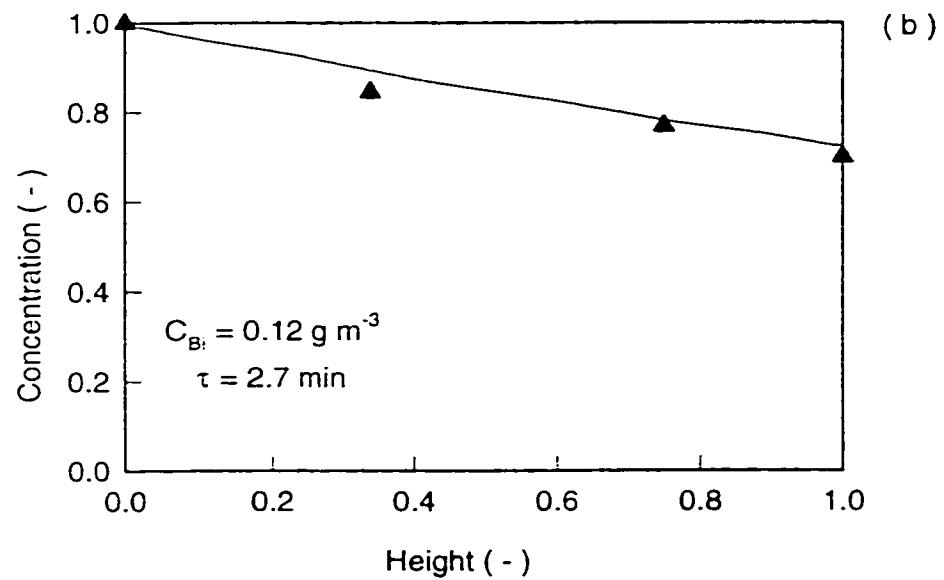
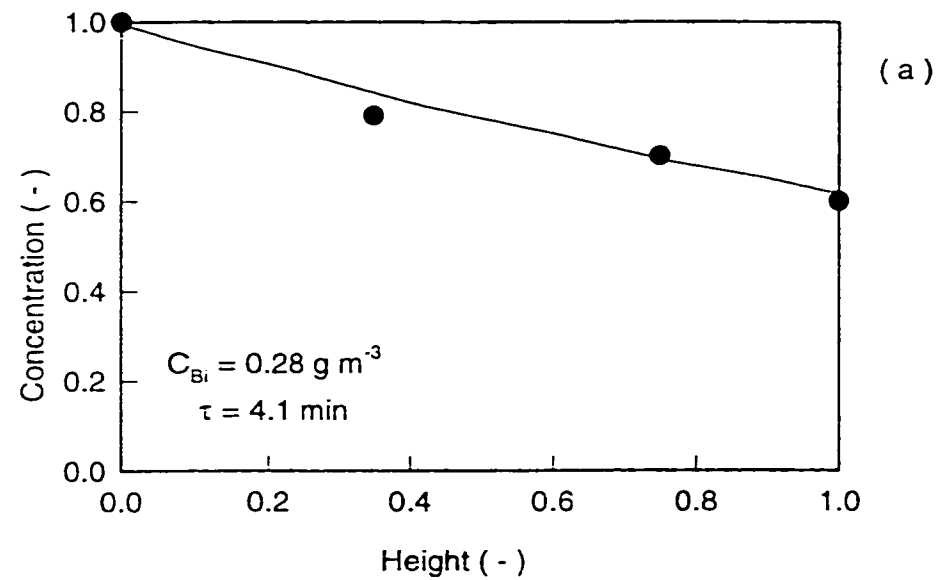


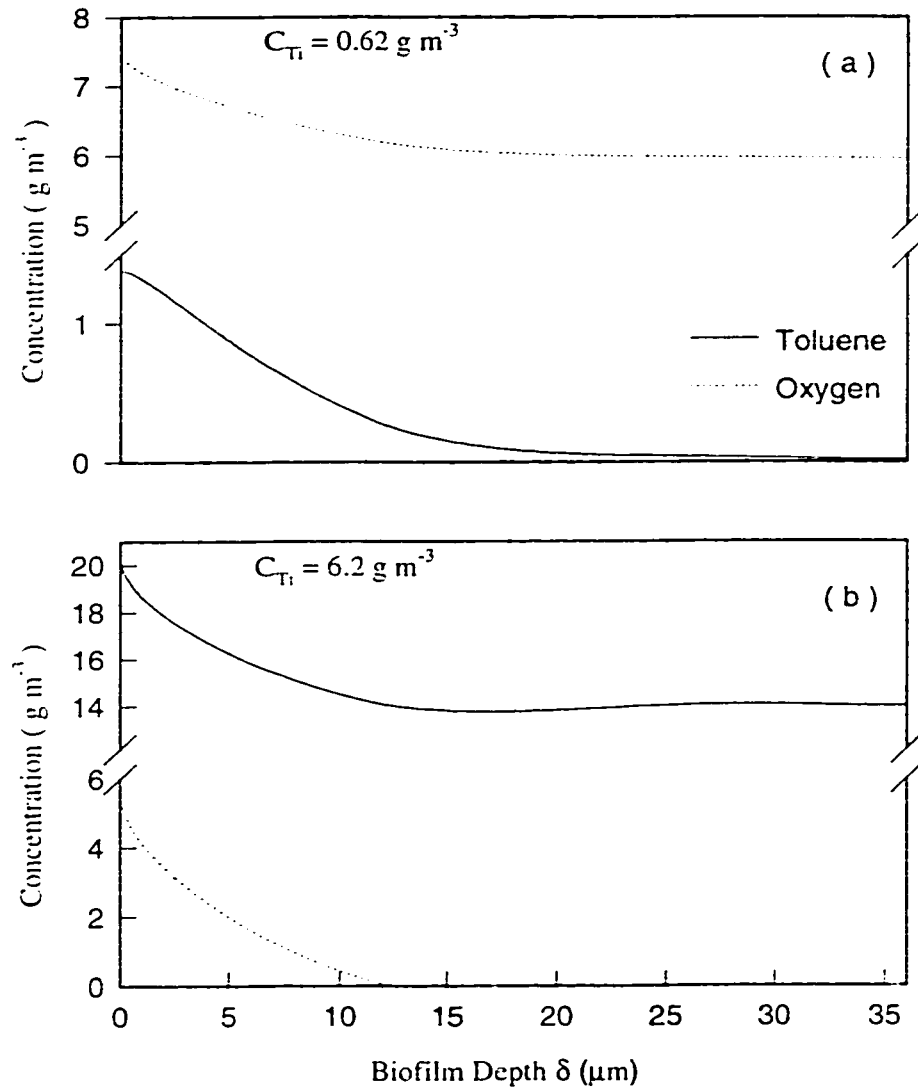
Figure 4.5a & 4.5b: Benzene concentration profiles along the bed. Experimental data and model predictions.

Oxygen Limitations

Figures 4.6a and 4.6b show the concentration profiles of toluene and oxygen in the biofilm at a column height of 0.25 m and at different inlet concentrations. It can be seen that at an inlet concentration of 0.62 g/m^3 , toluene gets depleted at a biofilm depth of around $35 \text{ }\mu\text{m}$ (Figure 4.6a). But interestingly, as the inlet concentration is increased to 6.2 g/m^3 , oxygen gets depleted at a depth of around $12 \text{ }\mu\text{m}$ indicating oxygen limitation at higher substrate concentrations. This confirms the findings by Zarook and Baltzis (1993) that for hydrophilic solvents oxygen limits the process even at low inlet VOC concentrations.

Numerical results also show that at moderately high inlet toluene concentrations and large residence times, the exit oxygen concentration was low, indicating greater consumption of oxygen in the biofilter. Figure 4.7 shows predictions of the exit concentration profile along the biofilter column by the *general* model for inlet toluene concentration of 2.81 g m^{-3} and residence time of 6.3 minutes. As can be seen, the exit oxygen dimensionless concentration falls sharply and remains constant at a value of about 0.6. Thus, oxygen level drops from 21% to 13% in the polluted air. The transient model of Dehusses et al. (1995) is limited to conditions where oxygen limitation does not occur, as in the case of biofiltration of methyl ethyl ketone (MEK) and methyl isobutyl ketone (MIBK). Even for this system, at high inlet concentrations oxygen limitation may occur. Furthermore, it is the depletion of oxygen or VOC that determines the active biofilm thickness. All of these results imply that oxygen needs to be explicitly taken into account in the modeling of biofiltration process under steady- state or transient conditions.

Figure 4.8 shows the effect of the inlet oxygen concentration on the exit toluene concentration. As can be seen, the oxygen concentration plays an important role in the biofiltration process. It affects the conversion very drastically especially for low relative values, less than 1 ($C_{O_2} < 275 \text{ g m}^{-3}$, atmospheric condition). For higher concentrations the effect is marginal. This implies that oxygen plays a very crucial role and has potential limiting effects in the biofiltration process especially as the process is aerobic.



Figures 4.6a & 4.6b: Concentration profiles of toluene and oxygen in the biofilm at different inlet concentrations.

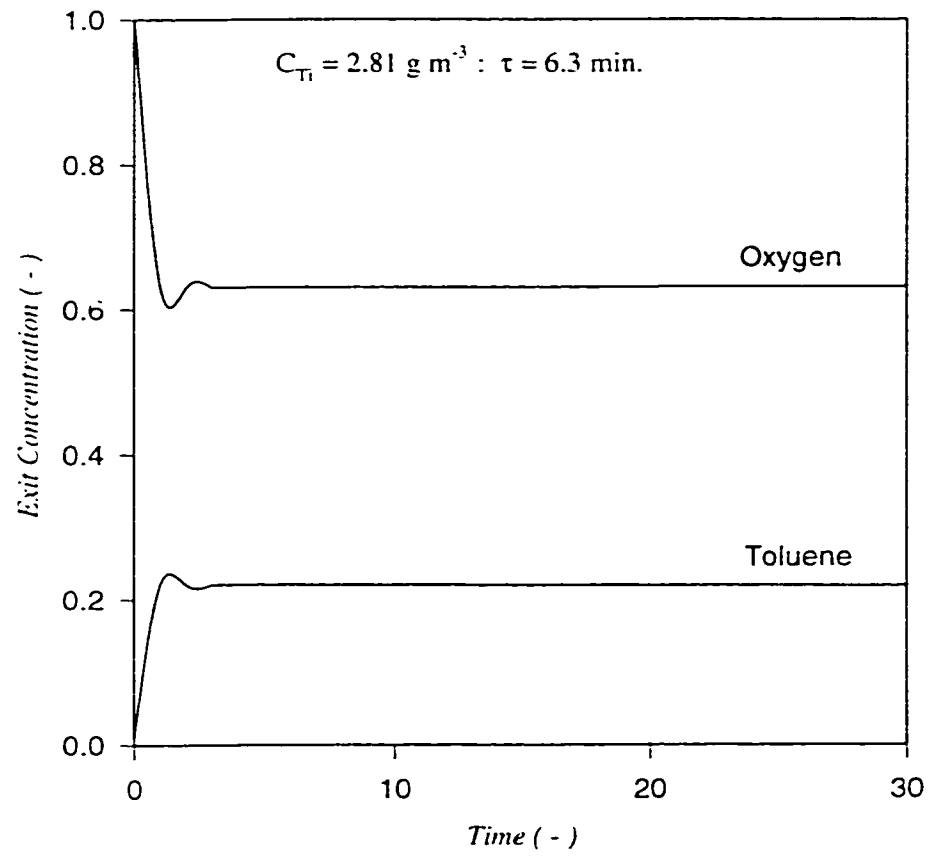


Figure 4.7: Transient concentration profiles of oxygen and toluene for the given inlet conditions.

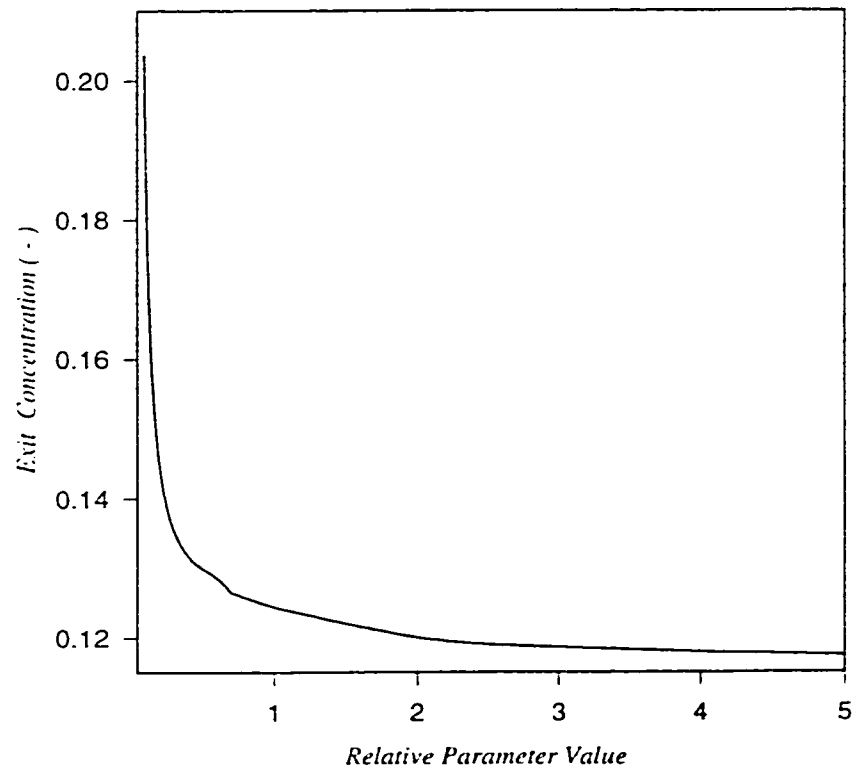


Figure 4.8: Effect of the inlet oxygen concentration on the exit toluene concentration.

Sensitivity Studies

Figure 4.9 show that the effect of Pe_T on the toluene concentration profile in the column. The symbol f is the relative parameter value of Pe_T i.e., large value of f implies higher Peclet number as compared to the predicted values calculated using the parameters given in Table 4.1. A high value for Pe_T denotes plug flow and low value indicates well mixed flow in the biofilter. It can be seen that as the value of f decreases, the concentration profile flattens, indicating a transition from plug flow behavior to mixed flow. A decrease in Pe_T implies better mixing in the gas phase leading to higher rates of mass transfer and better conversions. These conditions prevail more at the inlet of the column where the concentration levels are maximum. Similarly, the *general* model seems to be very sensitive to the value of Pe_O . It can be seen in Figure 4.10 that as the value of Pe_O is reduced by a factor of 10, the concentration profile along the column is flat with a higher exit toluene concentration. These results indicate that prior knowledge of the mixing pattern is very important in model predictions. Thus, the plug flow assumption of previous works (Ottengraf and van den Oever, 1993; Zarook et al., 1993; Zarook and Baltzis, 1994b; Deshusses et al., 1995) is questionable and mixing pattern in the gas phase still needs to be experimentally verified through residence time distribution (RTD) studies.

Figure 4.11 shows the effects of dimensionless parameters β_{1j} , β_{2j} , ϵ_j and ϵ_O on the exit toluene concentration. As can be seen, the model is very sensitive to these parameters for low relative values, less than one, after which the effect is not significant. The parameter β_{1j} can be interpreted as the ratio of the amount of substrate diffused into

the biofilm to the degree of convection in the gas phase. Larger values of β_{1j} or β_{2j} imply greater mass transport into the biofilm resulting in higher conversions. Large values of ε_j imply lower volatility of the compound; i.e., the lower the volatility of the compound, the greater the diffusion and reaction in the biofilm. The figure also shows the effect of ε_o on the exit concentration. As ε_o increases the exit concentration falls sharply. This happens at very low relative parameter values. This is expected as ε_o is proportional to the inlet oxygen concentration which has a drastic effect on the conversion.

Figure 4.12 shows the effect of the biofilm parameters ϕ_{1j} , ϕ_2 and η_{1j} on the exit concentration of toluene. As can be seen, the model is very sensitive to all these parameters. The exit concentration increases with increase in ϕ_{1j} . A large value of ϕ_{1j} indicates higher diffusion of toluene into the biofilm. This leads to reaction limitation in the biofilm resulting from substrate inhibition due to large toluene concentration and less availability of oxygen. Large values of η_{1j} , on the other hand, imply greater reaction in the biofilm and less convection in the gas phase. This result could be easily expected due to high rate of reaction and large residence time. Greater diffusion of oxygen in the biofilm results in greater conversion and this explains the behavior of the exit concentration for the parameter ϕ_2 . These results indicate that except for the parameter ϕ_{1j} all other parameters, at high relative parameter values (>1), are not sensitive, thus accurate determination of parameter ϕ_{1j} is more important than the others. However at low relative values (<1), the model is sensitive to all of these parameters.

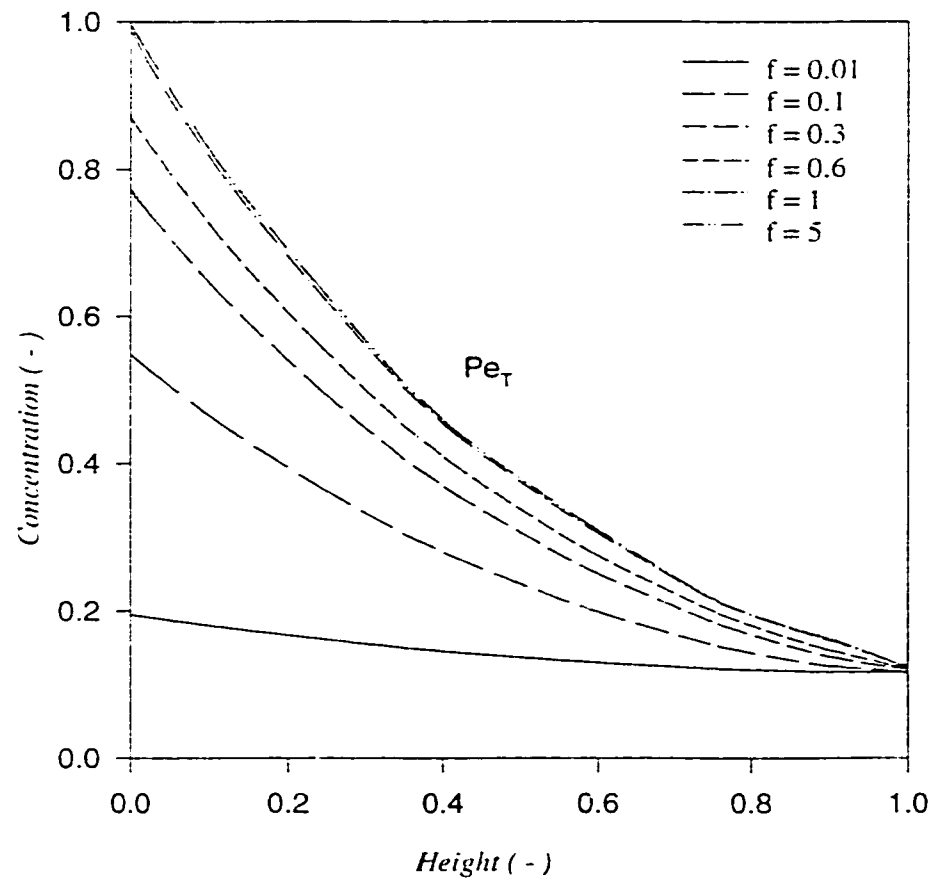


Figure 4.9: Effect of Peclet number of toluene on the concentration profile in the biofilter.

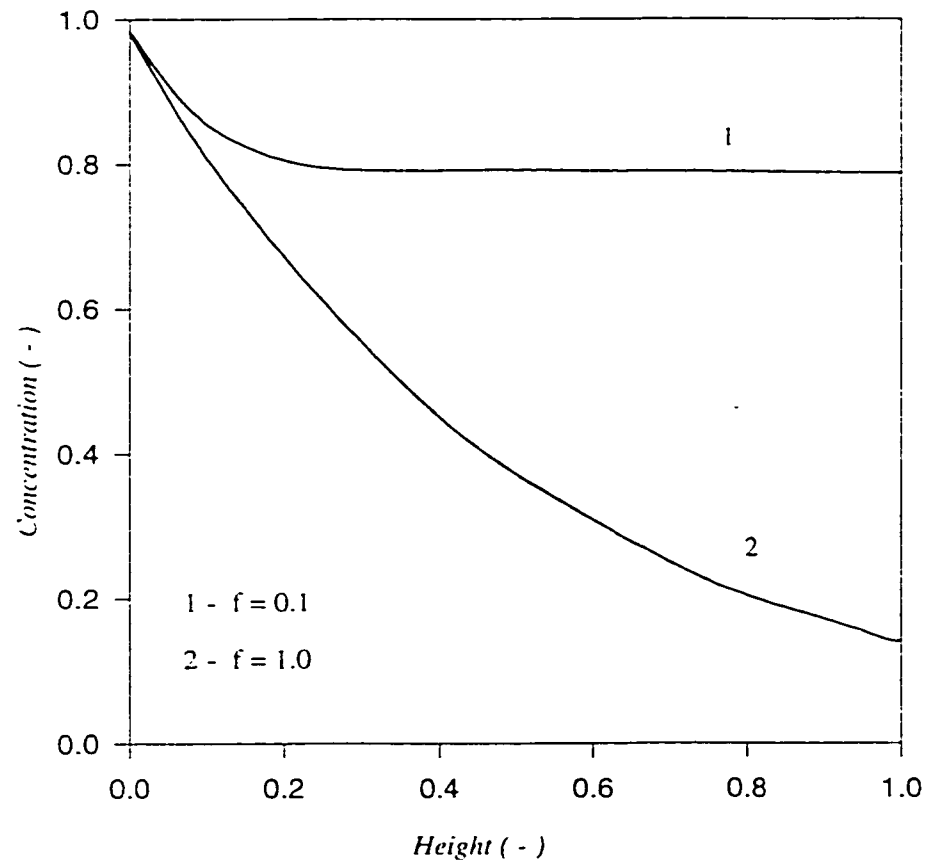


Figure 4.10: Effect of Peclet number of oxygen on the concentration profile in the biofilter.

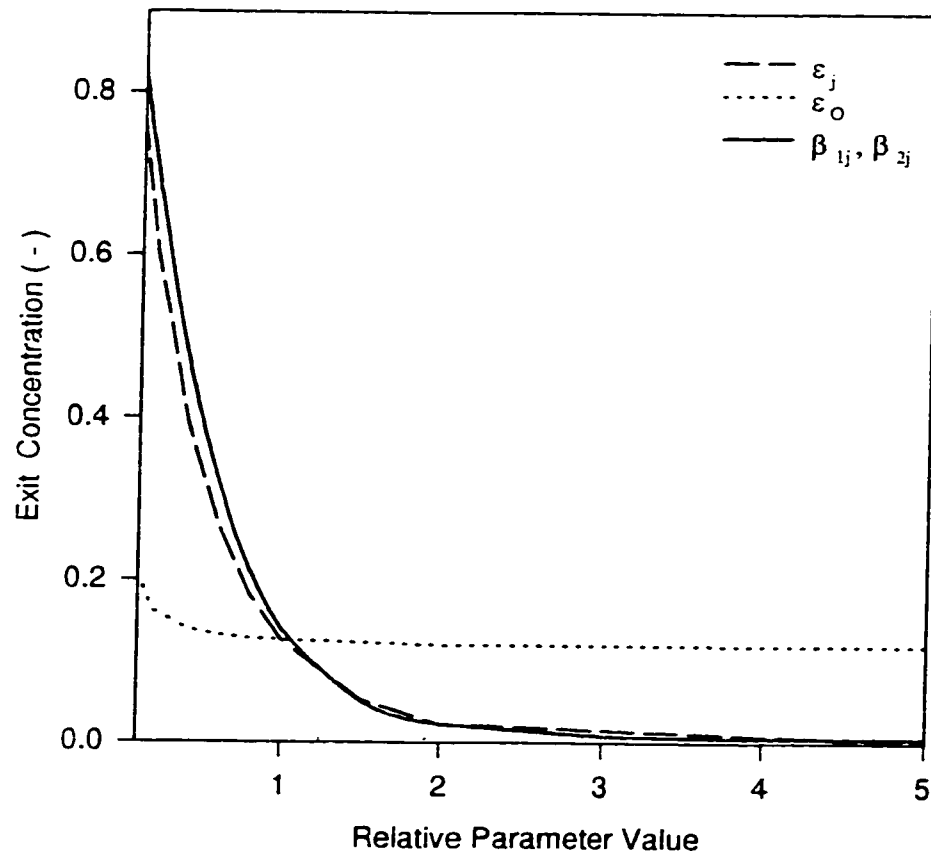


Figure 4.11: Effect of different non dimensional groups on the exit toluene concentration. Relative parameter value 1 refers to conditions of actual experiment.

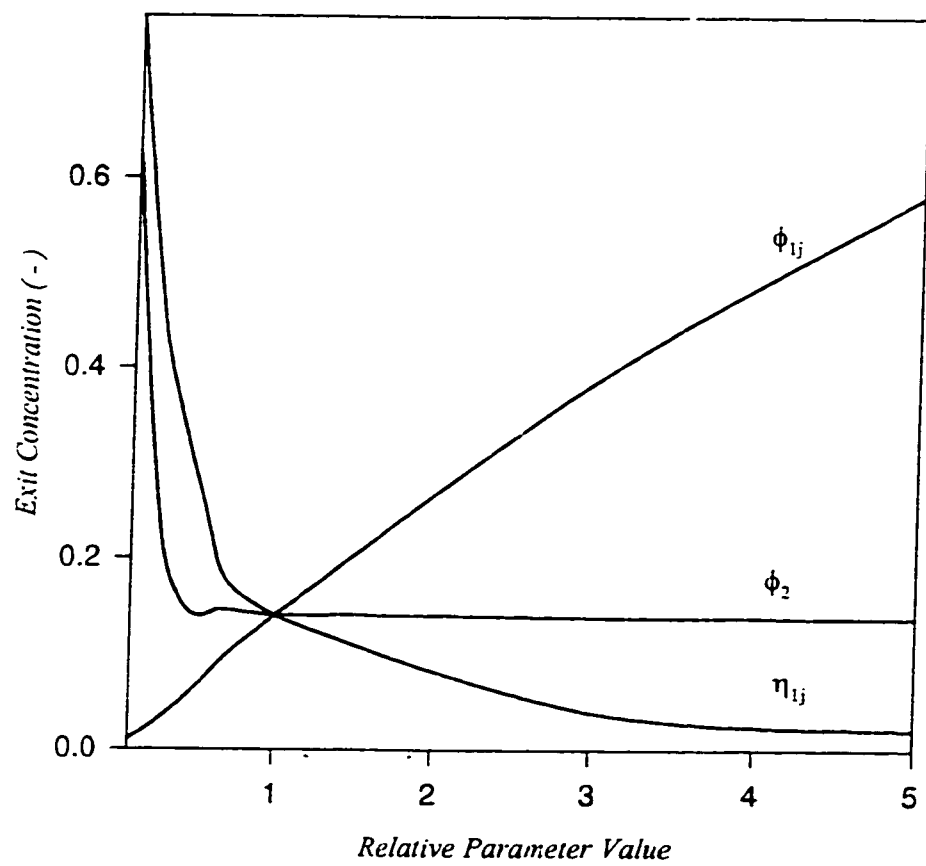


Figure 4.12: Effect of the various biofilm dimensionless groups on the exit toluene concentration.

BIOFILTRATION OF VOC MIXTURES

Approximate model and General Model

Since most practical applications involve mixed VOC emissions, understanding the biofiltration of mixtures is very important. There are actually very few studies on the biofiltration of mixtures. In the present chapter modeling the biofiltration of VOC mixtures is considered. The model equations for the biofiltration of VOC mixtures can be obtained by setting $j=2$ in the equations 3.1 - 3.5, 3.10-3.11 and 3.16 where, for the present study, compound 1 is taken as toluene and 2, for benzene. The resulting set of eight partial differential equations are shown below. As done for the case of single VOCs, the resulting set of eight equations describing the transient biofiltration of binary VOC mixtures are solved using the two approaches. In the first approach, for the approximate model, the number of equations is reduced to five by making an assumption of quasi steady state in the biofilm. For the general model, the actual set of eight equations are solved as such. The models are also valid for any binary mixture provided the kinetic and adsorption expressions are replaced.

The final model equations obtained for the biofiltration of VOC mixtures are as

follows:

$$\frac{\partial S_T}{\partial t} = f(X_V) D_{TW} \frac{\partial^2 S_T}{\partial x^2} - \frac{X_V}{Y_T} \mu_T(S_B, S_T, S_O) \quad (5.1)$$

$$\frac{\partial S_B}{\partial t} = f(X_V) D_{BW} \frac{\partial^2 S_B}{\partial x^2} - \frac{X_V}{Y_B} \mu_B(S_B, S_T, S_O) \quad (5.2)$$

$$\frac{\partial S_O}{\partial t} = f(X_V) D_{OW} \frac{\partial^2 S_O}{\partial x^2} - \frac{X_V}{Y_{OT}} \mu_T(S_B, S_T, S_O) - \frac{X_V}{Y_{OB}} \mu_B(S_B, S_T, S_O) \quad (5.3)$$

$$\begin{aligned} v \frac{\partial C_T}{\partial t} = D_T v \frac{\partial^2 C_T}{\partial h^2} - u_s \frac{\partial C_T}{\partial h} + f(X_V) D_{TW} \alpha A_S^* \left(\frac{\partial S_T}{\partial x} \right)_{x=0} \\ - (1 - \alpha) A_S^* k_T (C_T - C_T^*) \end{aligned} \quad (5.4)$$

$$\begin{aligned} v \frac{\partial C_B}{\partial t} = D_B v \frac{\partial^2 C_B}{\partial h^2} - u_s \frac{\partial C_B}{\partial h} + f(X_V) D_{BW} \alpha A_S^* \left(\frac{\partial S_B}{\partial x} \right)_{x=0} \\ - (1 - \alpha) A_S^* k_B (C_B - C_B^*) \end{aligned} \quad (5.5)$$

$$v \frac{\partial C_O}{\partial t} = D_O v \frac{\partial^2 C_O}{\partial h^2} - u_s \frac{\partial C_O}{\partial h} + f(X_V) D_{OW} \alpha A_S^* \left(\frac{\partial S_O}{\partial x} \right)_{x=0} \quad (5.6)$$

$$(1 - v) \rho_p \frac{\partial C_{BP}}{\partial t} = k_B (1 - \alpha) A_S^* (C_B - C_B^*) \quad (5.7)$$

$$(1 - v) \rho_p \frac{\partial C_{TP}}{\partial t} = k_T (1 - \alpha) A_S^* (C_T - C_T^*) \quad (5.8)$$

The initial and boundary conditions are the same as described in chapter 3.

5.1 APPROXIMATE MODEL

The effectiveness factors are defined as follows :

$$e_B = - \frac{f(X_V) D_{BW} \left(\frac{\partial S_B}{\partial X} \right)_{X=0}}{\delta \frac{X_V}{Y_B} [\mu_B(S_B, S_T, S_O)]_{X=0}} \quad (5.9)$$

$$e_T = - \frac{f(X_V) D_{TW} \left(\frac{\partial S_T}{\partial X} \right)_{X=0}}{\delta \frac{X_V}{Y_T} [\mu_T(S_B, S_T, S_O)]_{X=0}} \quad (5.10)$$

$$e_O = - \frac{f(X_V) D_{OW} \left(\frac{\partial S_O}{\partial X} \right)_{X=0}}{\delta \frac{X_V}{Y_{Oj}} \sum_{j=1}^n [\mu_j(S_B, S_T, S_O)]_{X=0}} \quad (5.11)$$

The use of effectiveness factors in conjunction with the quasi-steady-state approximation, permits the omission of equations (5.1),(5.2) and (5.3) in the biofilm.

The following are the non dimensional groups and variables derived for this model,

$$\begin{aligned} \bar{C}_T &= \frac{C_T}{C_{T_i}} & \bar{C}_B &= \frac{C_B}{C_{B_i}} & \bar{C}_O &= \frac{C_O}{C_{O_i}} \\ \bar{C}_{TP} &= \frac{C_{TP} (1-\nu) \rho_p}{u_x \nu} & \bar{C}_{BP} &= \frac{C_{BP} (1-\nu) \rho_p}{u_x \nu} \\ Z &= \frac{h}{H} & \theta &= \frac{x}{\delta} & \xi &= \frac{u_c t}{H} \\ \varepsilon_T &= \frac{C_{T_i}}{K_T m_T} & \varepsilon_B &= \frac{C_{B_i}}{K_B m_B} & \varepsilon_O &= \frac{C_{O_i}}{K_O m_O} \end{aligned}$$

$$\gamma = \frac{K_i}{K_{T,i}}$$

$$\sigma_1 = \frac{K_T K_{BT}}{K_B}$$

$$\sigma_2 = \frac{K_B K_{TB}}{K_T}$$

$$Pe_T = \frac{u_x H}{\nu D_T}$$

$$Pe_B = \frac{u_x H}{\nu D_B}$$

$$Pe_O = \frac{u_x H}{\nu D_O}$$

$$\beta_{IT} = \frac{e_T H \alpha A_S^* \delta X_V}{\nu u_g C_{Ti} Y_T}$$

$$\beta_{IB} = \frac{e_B H \alpha A_S^* \delta X_V}{\nu u_g C_{Bi} Y_B}$$

$$\beta_{OT} = \frac{e_O H \alpha A_S^* \delta X_V}{\nu u_g C_{Oi} Y_{OT}}$$

$$\beta_{OB} = \frac{e_O H \alpha A_S^* \delta X_V}{\nu u_g C_{Oi} Y_{OB}}$$

$$\chi_T = \frac{(1-\alpha) H A_S^* k_{MT}}{\nu u_c}$$

$$\chi_B = \frac{(1-\alpha) H A_S^* k_{MB}}{\nu u_c}$$

$$\psi_T = \frac{l}{C_{Ti}} \left[\frac{\nu C_{Ti}}{(1-\nu) \rho_P k_{dT}} \right]^{\frac{1}{n_T}}$$

$$\psi_B = \frac{l}{C_{Bi}} \left[\frac{\nu C_{Bi}}{(1-\nu) \rho_P k_{dB}} \right]^{\frac{1}{n_B}}$$

$$\lambda_{IT} = \frac{a_T \rho_P (1-\nu)}{\nu}$$

$$\lambda_{IB} = \frac{a_B \rho_P (1-\nu)}{\nu}$$

$$\lambda_{OT} = b_T C_{Ti}$$

$$\lambda_{OB} = b_B C_{Bi}$$

Introducing the above dimensionless groups, the model can be reduced to the following system of five differential equations.

Mass Balance in the Gas Phase

$$\frac{\partial \bar{C}_T}{\partial \xi} = \frac{l}{Pe_T} \frac{\partial^2 \bar{C}_T}{\partial Z^2} - \frac{l}{\nu} \frac{\partial \bar{C}_T}{\partial Z} - \beta_{IT} g_T(\bar{C}_B, \bar{C}_T, \bar{C}_O) - \chi_T (\bar{C}_T - \bar{C}_T^*) \quad (5.12)$$

$$\frac{\partial \bar{C}_B}{\partial \xi} = \frac{l}{Pe_B} \frac{\partial^2 \bar{C}_B}{\partial Z^2} - \frac{l}{\nu} \frac{\partial \bar{C}_B}{\partial Z} - \beta_{IB} g_B(\bar{C}_B, \bar{C}_T, \bar{C}_O) - \chi_B (\bar{C}_B - \bar{C}_B^*) \quad (5.13)$$

$$\frac{\partial \bar{C}_O}{\partial \xi} = \frac{1}{Pe_O} \frac{\partial^2 \bar{C}_O}{\partial Z^2} - \frac{1}{v} \frac{\partial \bar{C}_O}{\partial Z} - \beta_{2T} g_B(\bar{C}_B, \bar{C}_T, \bar{C}_O) - \beta_{2B} g_T(\bar{C}_B, \bar{C}_T, \bar{C}_O) \quad (5.14)$$

Mass Balance in the Solid Phase

$$\frac{\partial \bar{C}_{TP}}{\partial \xi} = \chi_T (\bar{C}_T - \bar{C}_T^*) \quad (5.15)$$

$$\frac{\partial \bar{C}_{BP}}{\partial \xi} = \chi_B (\bar{C}_B - \bar{C}_B^*) \quad (5.16)$$

where

$$g_T(\bar{C}_B, \bar{C}_T, \bar{C}_O) = \frac{\bar{C}_T \bar{C}_O \varepsilon_T \varepsilon_O}{(1 + \bar{C}_T \varepsilon_T + \bar{C}_T^2 \varepsilon_T^2 \gamma + \bar{C}_B \varepsilon_B \sigma_2)(1 + \bar{C}_O \varepsilon_O)} \quad (5.17)$$

$$g_B(\bar{C}_B, \bar{C}_T, \bar{C}_O) = \frac{\bar{C}_B \bar{C}_O \varepsilon_B \varepsilon_O}{(1 + \bar{C}_B \varepsilon_B + \bar{C}_T \varepsilon_T \sigma_1)(1 + \bar{C}_O \varepsilon_O)} \quad (5.18)$$

$$\bar{C}_T^* = \frac{\bar{C}_{TP}(1 - \lambda_3 \bar{C}_B^*)}{(\lambda_1 - \lambda_2 \bar{C}_{TP})} \quad (5.19)$$

$$\bar{C}_B^* = \frac{\bar{C}_{BP}(1 - \lambda_2 \bar{C}_T^*)}{(\lambda_4 - \lambda_3 \bar{C}_{BP})} \quad (5.20)$$

Initial conditions :

$$\xi = 0 \quad Z = 0 \quad \bar{C}_j = 1 \quad \bar{C}_{jP} = \bar{C}_{jP,0}(0) \quad (5.21)$$

$$\xi = 0 \quad 0 \leq Z \leq 1 \quad \bar{C}_j = \bar{C}_{j,0}(Z) \quad \bar{C}_{jP} = \bar{C}_{jP,0}(Z) \quad (5.22)$$

Boundary Conditions :

$$Z = 0 \quad \xi > 0 \quad \frac{\partial \bar{C}_j}{\partial Z} = -Pe_j (\bar{C}_j|_{Z=0^-} - \bar{C}_j|_{Z=0^+}) \quad (5.23)$$

$$Z = 1 \quad \frac{\partial \bar{C}_j}{\partial Z} = 0 \quad (5.24)$$

Solution of the *approximate* model requires correlations for film thickness and effectiveness factors (e_j , e_0). The same correlations used for the single component VOCs in chapter 5 are used in the present case for both the VOCs. These correlations were obtained by Zarook and Baltzis (1994b) by fitting the film thickness and effectiveness factors to the solution of the model under quasi-steady state approximation in the biofilm.

5.2 GENERAL MODEL

The following are the non dimensional and variables groups for the general model,

$$\begin{aligned}\bar{S}_T &= \frac{S_T}{K_T} & \bar{S}_B &= \frac{S_B}{K_B} & \bar{S}_O &= \frac{S_O}{K_O} \\ \beta_{3T} &= \frac{D_{TW} H \alpha A_S^* f(X_V) K_T}{\nu u_g C_{Ti} \delta} & \beta_{3B} &= \frac{D_{BW} H \alpha A_S^* f(X_V) K_B}{\nu u_g C_{Bi} \delta} \\ \beta_4 &= \frac{D_{OW} H \alpha A_S^* f(X_V) K_O}{\nu u_g C_{Oi} \delta} & \phi_{1T} &= \frac{D_{TW} H f(X_V)}{u_g \delta^2} \\ \phi_{1B} &= \frac{D_{BW} H f(X_V)}{u_g \delta^2} & \phi_2 &= \frac{D_{OW} H f(X_V)}{u_g \delta^2} \\ \eta_{1T} &= \frac{H \mu_T^* X_V}{Y_T K_T u_g} & \eta_{1B} &= \frac{H \mu_B^* X_V}{Y_B K_B u_g} \\ \eta_{2T} &= \frac{H \mu_T^* X_V}{Y_{OT} K_O u_g} & \eta_{2B} &= \frac{H \mu_B^* X_V}{Y_{OB} K_O u_g}\end{aligned}$$

Introducing the dimensionless parameters, the model can be reduced to the following system of five differential equations.

Mass Balance in the Biofilm

$$\frac{\partial \bar{S}_T}{\partial \xi} = \phi_{1T} \frac{\partial^2 \bar{S}_T}{\partial \theta^2} - \eta_{1T} g_3(\bar{S}_T, \bar{S}_B, \bar{S}_O) \quad (5.25)$$

$$\frac{\partial \bar{S}_B}{\partial \xi} = \phi_{1B} \frac{\partial^2 \bar{S}_B}{\partial \theta^2} - \eta_{1B} g_4(\bar{S}_T, \bar{S}_B, \bar{S}_O) \quad (5.26)$$

$$\frac{\partial \bar{S}_O}{\partial \xi} = \phi_2 \frac{\partial^2 \bar{S}_O}{\partial \theta^2} - \eta_{2T} g_3(\bar{S}_T, \bar{S}_B, \bar{S}_O) - \eta_{2B} g_4(\bar{S}_T, \bar{S}_B, \bar{S}_O) \quad (5.27)$$

The initial and boundary conditions are as follows:

$$\xi = 0 \quad Z = 0, \theta = 0 \quad \bar{S}_J = \varepsilon_J \quad (5.28)$$

$$\xi = 0 \quad 0 < Z \leq 1; \theta = 0 \quad \bar{S}_J = \varepsilon_J \bar{C}_{J,0}(Z) \quad (5.29)$$

$$\xi = 0 \quad 0 < \theta \leq 1 \quad \bar{S}_J = \bar{S}_{J,0}(\theta) \quad (5.30)$$

$$\theta = 0 \quad Z > 0 \quad \bar{S}_J = \varepsilon_J \bar{C}_J(Z) \quad (5.31)$$

$$\theta = 1 \quad Z > 0; \xi > 0 \quad \frac{\partial \bar{S}_J}{\partial x} = 0 \quad (5.32)$$

Mass Balances in the Gas Phase

$$\frac{\partial \bar{C}_T}{\partial \xi} = \frac{l}{Pe_T} \frac{\partial^2 \bar{C}_T}{\partial Z^2} - \frac{l}{v} \frac{\partial \bar{C}_T}{\partial Z} - \beta_{JT} \left(\frac{\partial \bar{S}_T}{\partial \theta} \right)_{\theta=0} - \chi_T (\bar{C}_T - \bar{C}_T^*) \quad (5.33)$$

$$\frac{\partial \bar{C}_B}{\partial \xi} = \frac{l}{Pe_B} \frac{\partial^2 \bar{C}_B}{\partial Z^2} - \frac{l}{v} \frac{\partial \bar{C}_B}{\partial Z} - \beta_{JB} \left(\frac{\partial \bar{S}_B}{\partial \theta} \right)_{\theta=0} - \chi_B (\bar{C}_B - \bar{C}_B^*) \quad (5.34)$$

$$\frac{\partial \bar{C}_O}{\partial \xi} = \frac{l}{Pe_O} \frac{\partial^2 \bar{C}_O}{\partial Z^2} - \frac{l}{v} \frac{\partial \bar{C}_O}{\partial Z} - \beta_{JO} \left(\frac{\partial \bar{S}_O}{\partial \theta} \right)_{\theta=0} \quad (5.35)$$

where

$$g_3 = \frac{\bar{S}_T \bar{S}_O}{(1 + \bar{S}_T + \bar{S}_T^* \gamma + \sigma_2 \bar{S}_B)(1 + \bar{S}_O)} \quad (5.36)$$

$$g_4 = \frac{\bar{S}_B \bar{S}_O}{(1 + \bar{S}_B + \sigma_1 \bar{S}_T)(1 + \bar{S}_O)} \quad (5.37)$$

Note that the mass balance in the solid phase (equations 5.15-5.16) and initial and boundary conditions (equations 5.21 through 5.24) required for solving the mass balance equations in the gas and solid phases are the same for both approximate and general models.

5.3 NUMERICAL SOLUTION OF THE MODEL EQUATIONS

As discussed before, applying the method of orthogonal collocation, the resulting partial differential equations for the *approximate model* and the *general model* are reduced to ordinary differential equations by orthogonal collocation (Appendix B). Ten collocation points were used for discretizing the column height Z (from $Z=0$ to $Z=1$) for the models. For the case of general model, six points were used to discretize θ , the biofilm depth (from $\theta = 0$ to l .) in addition to ten collocation points for the column height Z . The resulting set of simultaneous ordinary differential equations, 50 for the approximate model and 230 for the general model are solved using numerical schemes available in the International Mathematics Subroutine Library (IMSL).

5.4 MODEL PARAMETER ESTIMATION

Most of the parameters needed to solve the models are obtained from the previous works of Baltzis and Zarook (1994). The adsorption parameters for Benzene - Toluene mixture are calculated as discussed in Chapter 3. The film thickness and effectiveness factor correlations used for the approximate model are the same as used for single component in Chapter 4. For the general model, the value of the effective film thickness is found by the model itself as the value when any one of the substrates gets completely consumed. The parameter used in solving the model equations are listed in Table 5.1.

Table 5.1 : Parameter values used for solving the approximate and general model equations.

PARAMETER	VALUE	UNITS	REF.
A_{ST}	40.0	m^{-1}	1
A_{SB}	23.3	m^{-1}	1
C_{O_i}	275.0	$g\ m^{-3}$	1
D_{B_A}	0.0895	$cm^2\ s^{-1}$	3
D_{T_A}	0.0792	$cm^2\ s^{-1}$	3
D_{O_A}	0.2132	$cm^2\ s^{-1}$	3
D_{B_W}	1.04×10^{-9}	$m^2\ s^{-1}$	1
D_{T_W}	1.03×10^{-9}	$m^2\ s^{-1}$	1
D_{O_W}	2.41×10^{-9}	$m^2\ s^{-1}$	1
$f(X_V)$	0.195	-	1
m_B	0.23	-	1
m_O	34.4	-	1
m_T	0.27	-	1
X_V	100.0	$kg\ m^{-3}$	1
α	0.3	-	2
ν	0.3	-	2
ρ_P	4.28×10^5	$g\ m^{-3}$	2
k_B, k_T	6.04×10^{-3}	$m\ h^{-1}$	2
K_{PT}	78.94	$g\ m^{-3}$	1
K_O	0.26	$g\ m^{-3}$	1
K_B	12.22	$g\ m^{-3}$	1
K_T	11.03	$g\ m^{-3}$	1
K_{BT}	4.50	-	4
K_{TB}	0.20	-	4
Y_B	0.708	-	1
Y_{OB}	0.336	-	1
Y_{OT}	0.341	-	1
Y_T	0.708	-	1
μ_T^*	1.50	h^{-1}	1
μ_B^*	0.68	h^{-1}	1

Table 5.1: (Contd.)

a_T	2.34×10^{-5}	$m^3 / g\text{-particle}$	Present Study
a_B	8.38×10^{-6}	$m^3 / g\text{-particle}$	Present Study
b_T	0.02	m^3 / g	Present Study
b_B	0.01356	m^3 / g	Present Study

¹Zarook & Baltzis. (1994 a)

²Zarook & Baltzis. (1994 b)

³Hsieh et al., (1993)

⁴Baltzis and Zarook. (1994 c)

5.5 RESULTS AND DISCUSSIONS

Validation of the models

For validating the models, the experimental data of Zarook and Baltzis (1994a, 1994b) are used. Biofiltration experiments of a mixture of compounds benzene and toluene were carried out at various residence times and inlet concentrations. The results from the approximate model and the general model are given in Table 5.2. Table 5.2 shows the space time, the measured inlet concentrations of toluene on the airstream and compares the experimental removal rate with those predicted by the previous model of Zarook and Baltzis (1994b, 1994a), and the two models (approximate and general) of the present work. The removal rate is defined as $(C_{Ti} - C_{Te}) / \tau$ and its model predicted value at steady state is based on the predicted value for C_{Te} i.e., $C_T (h = H)$.

Figure 5.1 shows the comparison between the predicted concentration profiles of the *approximate* models and the *general* against the transient biofiltration data of benzene and toluene. Since the data are scattered, and both models predict closely, it is difficult to give any conclusion from this graph. The initial transient aspects of the process are not well described by the model. This is due to the start-up conditions of the experiment (Zarook, 1994), when the biofilm is in the formation state. However from Figure 5.2, which compares the predictions of the two models along the biofilter height, it can be seen that the *general* model predictions are better than that of the *approximate* model. Hence, from figure 5.2 and Table 5.2, it can be concluded that the *general* model predicts closer to the experimental results than the *approximate* model.

Figures 5.3 and 5.4 again show the experimental and model (general) predicted transient concentration profiles of benzene and toluene for two different operating conditions. As can be seen, the model predictions are in good agreement with the experimental results. As also seen in the previous chapter (Figure 4.4), the model does not adequately predict (Figure 5.1) the adsorption process during the initial period of operation or start-up of the biofilter. However, the model is able to predict the steady state values of the exit concentrations quite accurately. Figure 5.5 shows the experimental and model (*general*) predicted concentration profiles for benzene and toluene along the column at steady state for another two different sets of operating conditions. As can be seen, the model predictions are in very good agreement with the experimental results.

Table 5.2: Biofiltration of benzene-toluene mixtures: Experimental data and model predictions.

τ	Compound	C_{inlet} g/m ³	C_{out} (exp) g/m ³	C_{out} (model) ¹ g/m ³	Error %	C_{out} (model) ² g/m ³	Error %	C_{out} (model) ³ g/m ³	Error %
0.9'	Benzene	0.162	0.146	0.136	-6.8	0.147	0.6	0.139	-4.8
	Toluene	0.515	0.300	0.399	33.0	0.387	29.0	0.388	22.6
1.0	Benzene	0.130	0.108	0.105	-2.8	0.113	4.6	0.108	0.0
	Toluene	0.212	0.169	0.157	-7.1	0.151	-10.6	0.161	-4.7
1.3	Benzene	0.205	0.164	0.160	-2.4	0.176	7.3	0.162	-1.2
	Toluene	0.403	0.267	0.283	6.0	0.265	0.75	0.272	1.8
1.4	Benzene	0.165	0.130	0.125	-3.8	0.138	6.1	0.127	-2.3
	Toluene	0.382	0.239	0.258	7.9	0.241	0.84	0.255	6.7
1.5	Benzene	0.194	0.149	0.143	-4.0	0.157	5.3	0.148	-0.6
	Toluene	0.272	0.186	0.177	-4.8	0.165	-11.3	0.180	-3.2
2.0	Benzene	0.150	0.119	0.099	-16.8	0.115	-3.3	0.107	-10.0
	Toluene	0.298	0.158	0.167	5.7	0.153	-0.3	0.165	4.4
3.1	Benzene	0.367	0.186	0.194	4.3	0.242	30.1	0.186	0.0
	Toluene	0.225	0.102	0.092	-9.8	0.081	-20.5	0.095	-6.8

¹ Baltzis and Zarook, (1994 c); ² Approximate model; ³ General model

The volume of the packing used $V_p = 15291 \text{ cm}^3$

⁴ $V_p = 5097 \text{ cm}^3$

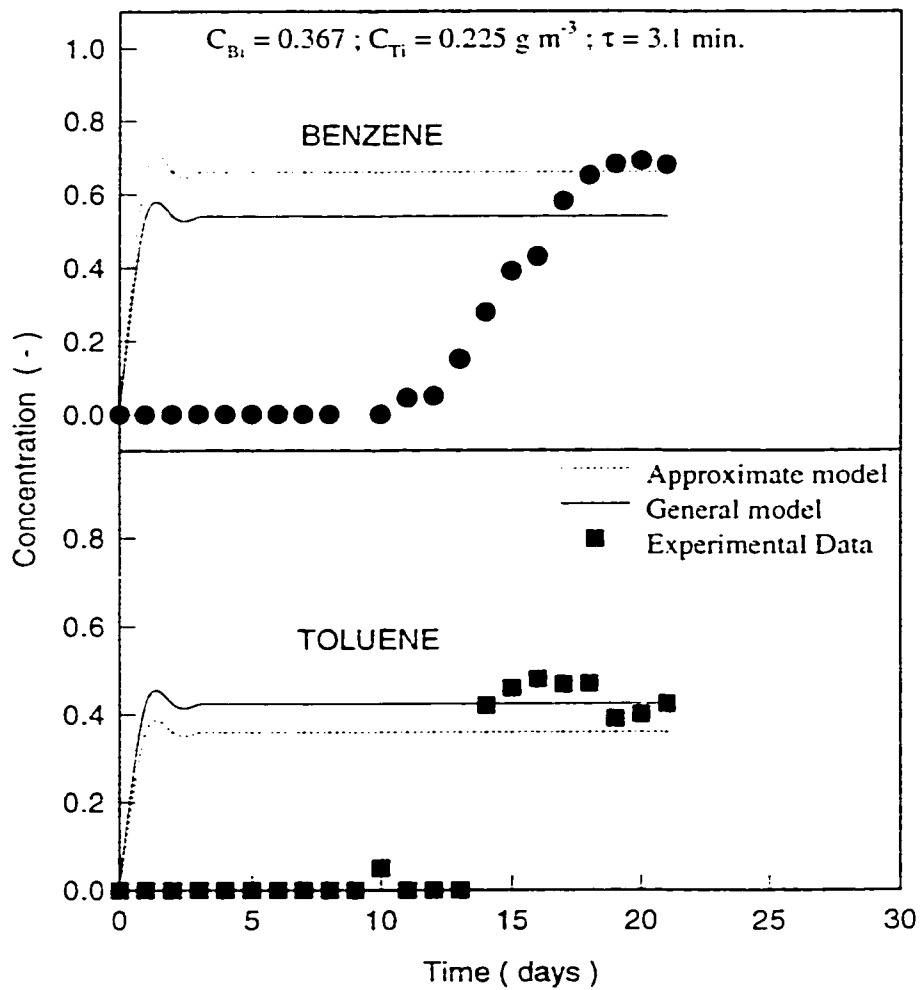


Figure 5.1 : Concentrations of benzene and toluene with time.

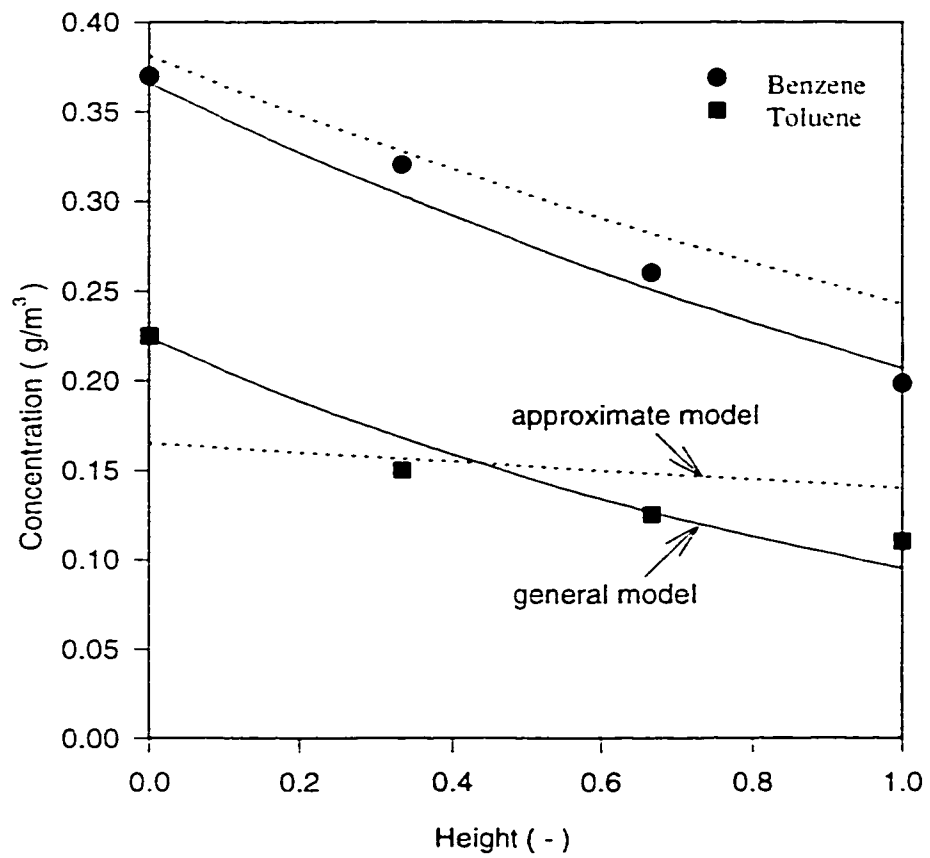


Figure 5.2 : Concentration profiles of benzene (1) and toluene (2) in the biofilter. Experimental data and model predictions.

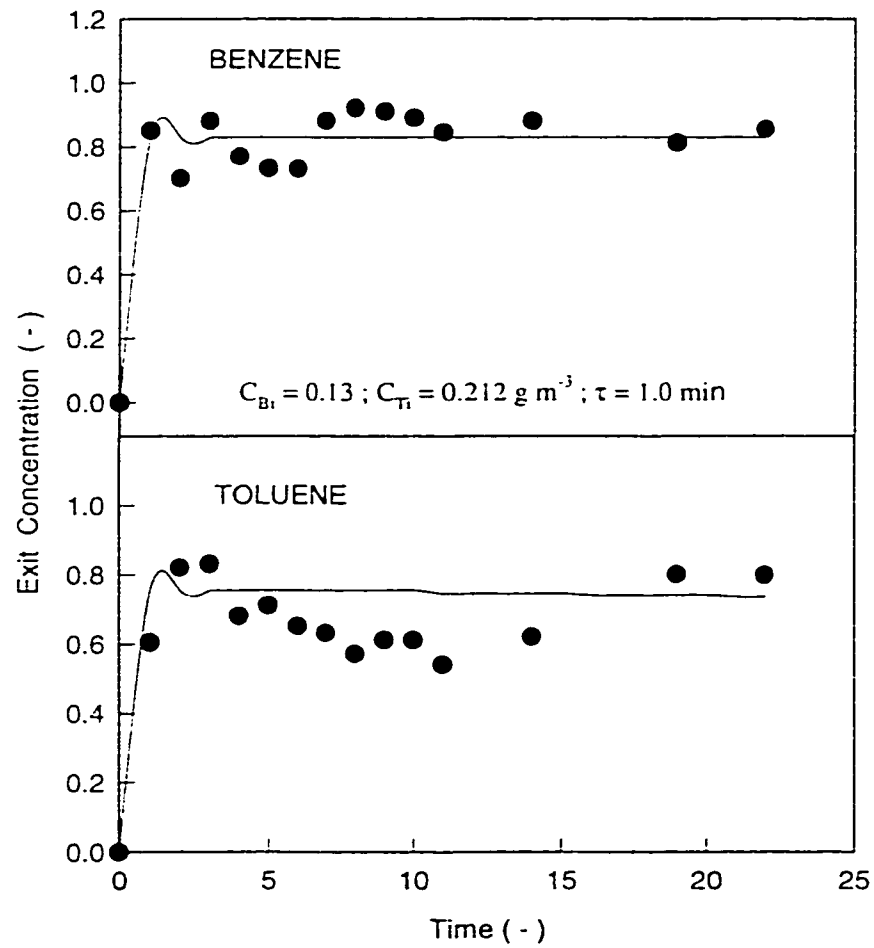


Figure 5.3 : Concentrations of benzene and toluene with time.

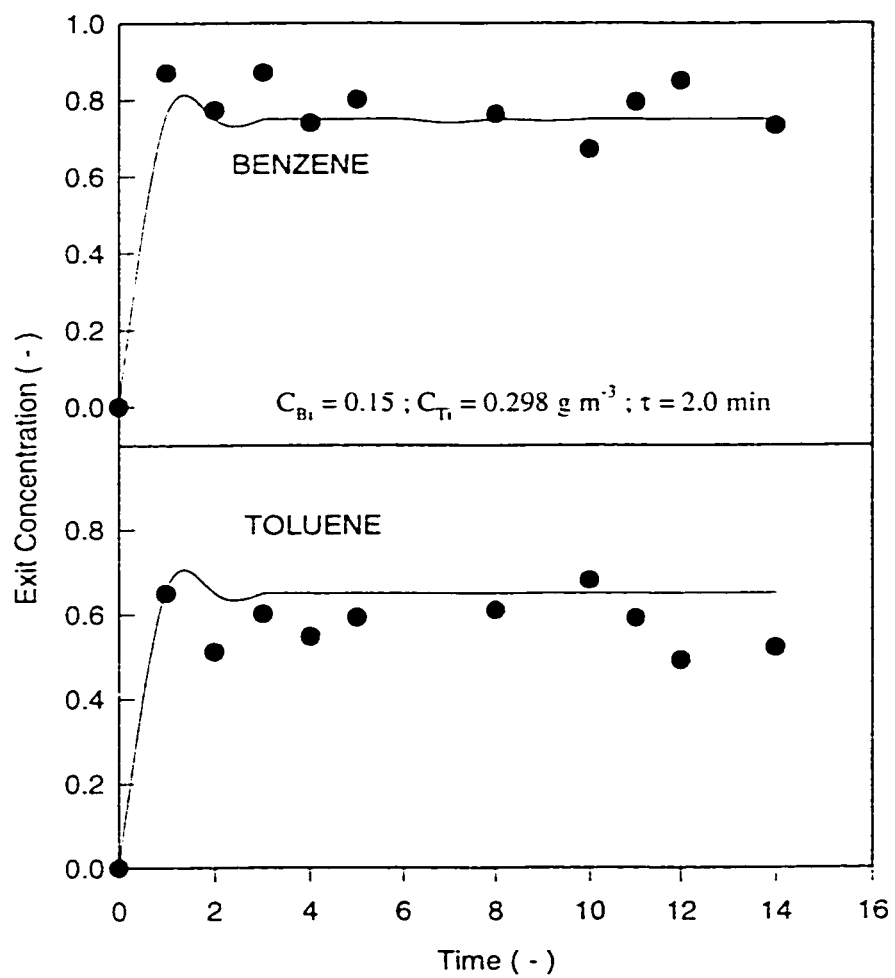


Figure 5.4: Concentrations of benzene and toluene with time.

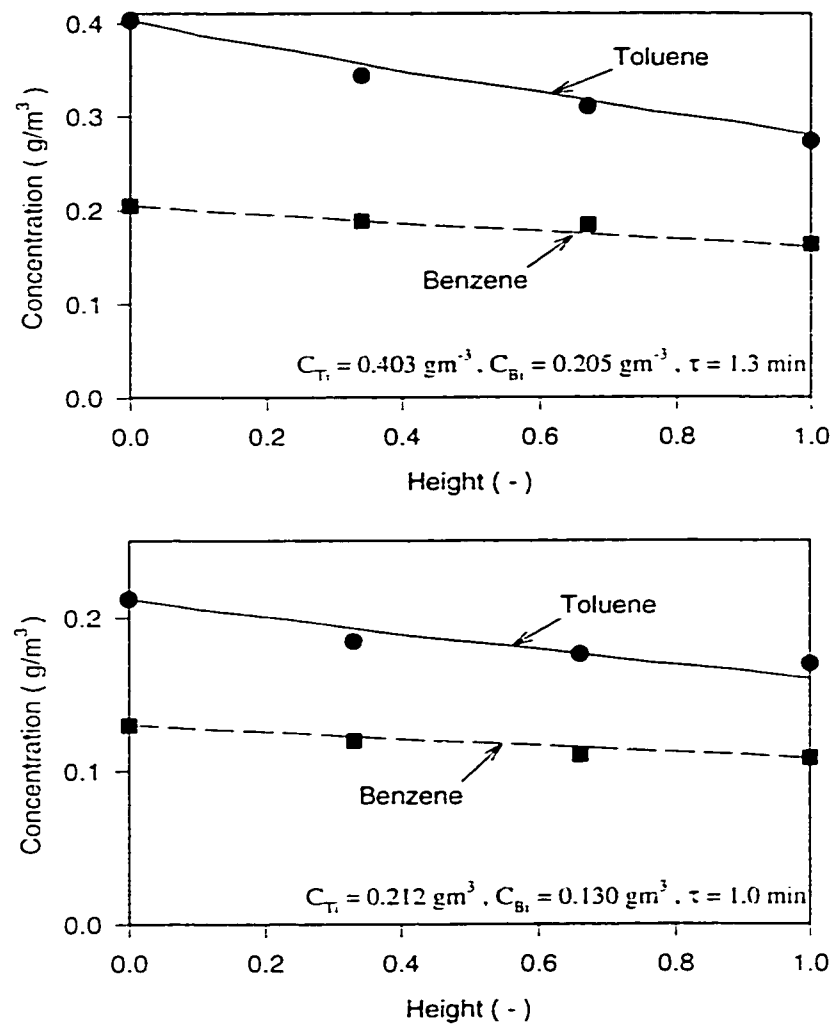


Figure 5.5 : Experimental data and Model (general) predictions of the benzene and toluene concentration profiles along the column.

Inlet oxygen concentration

Figure 5.6 shows the effect of the inlet oxygen concentration on the exit benzene and toluene concentrations. As can be seen, the oxygen plays an important role in the biofiltration of VOCs. It affects the conversion very drastically especially for low relative values, less than two. For higher concentrations, the effect is marginal. This implies that oxygen plays a very crucial role and has potential limiting effects in the biofiltration process especially as the process is aerobic. Thus in a practical biofiltration operation, the inlet air should contain an optimum quantity of oxygen. Operations at lower oxygen concentrations will result in poor conversions and hence low efficiencies.

Figures 5.7a and 5.7b show the concentration profiles of benzene, toluene and oxygen in the biofilm in the middle of the column. It is seen that at a relatively low inlet gas concentrations, toluene gets depleted at a biofilm depth of around 20 μ m as shown in figure 5.7a. But Figure 5.7b shows that as the inlet concentration is increased to a larger value, it is the oxygen that gets depleted first at a biofilm depth of around 15 μ m. This indicates that at lower substrate concentrations, oxygen is available in plenty and may even be ignored in the model and the effective thickness of the biofilm is governed by the faster depleting substrate. But as the concentration of the pollutant in the inlet gas increases, oxygen is consumed fast and dictates the effective biofilm thickness. Hence, oxygen has to be accounted for in the model equations.

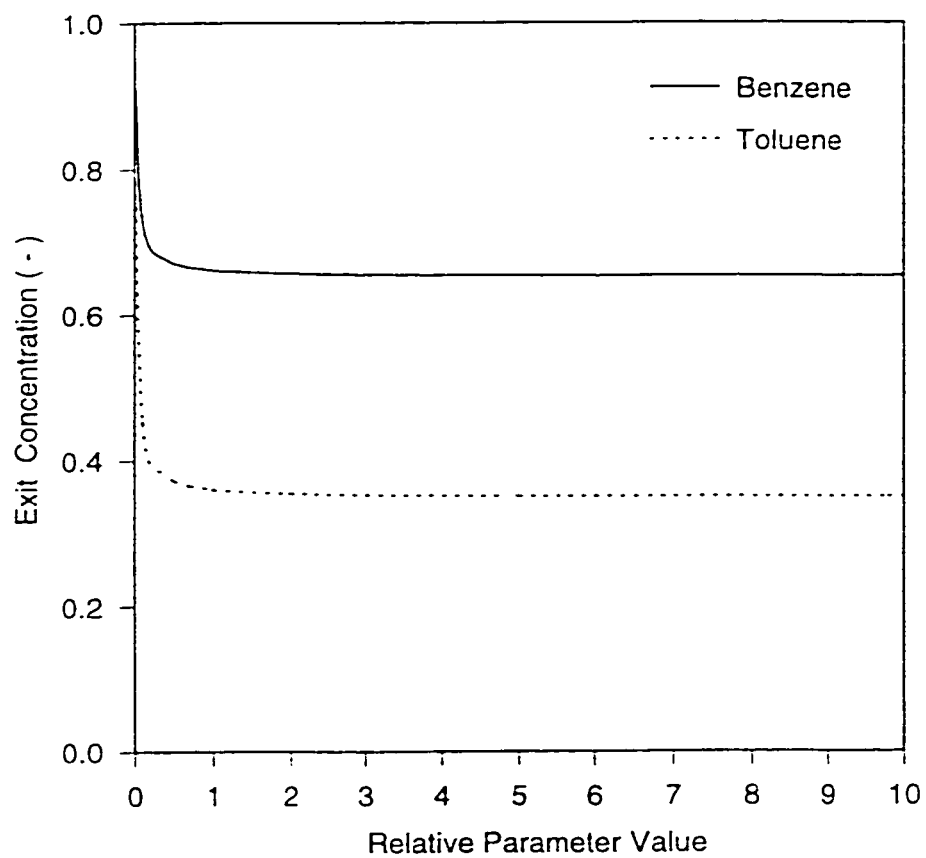


Figure 5.6: Effect of the inlet oxygen concentration on the benzene and toluene exit concentrations.

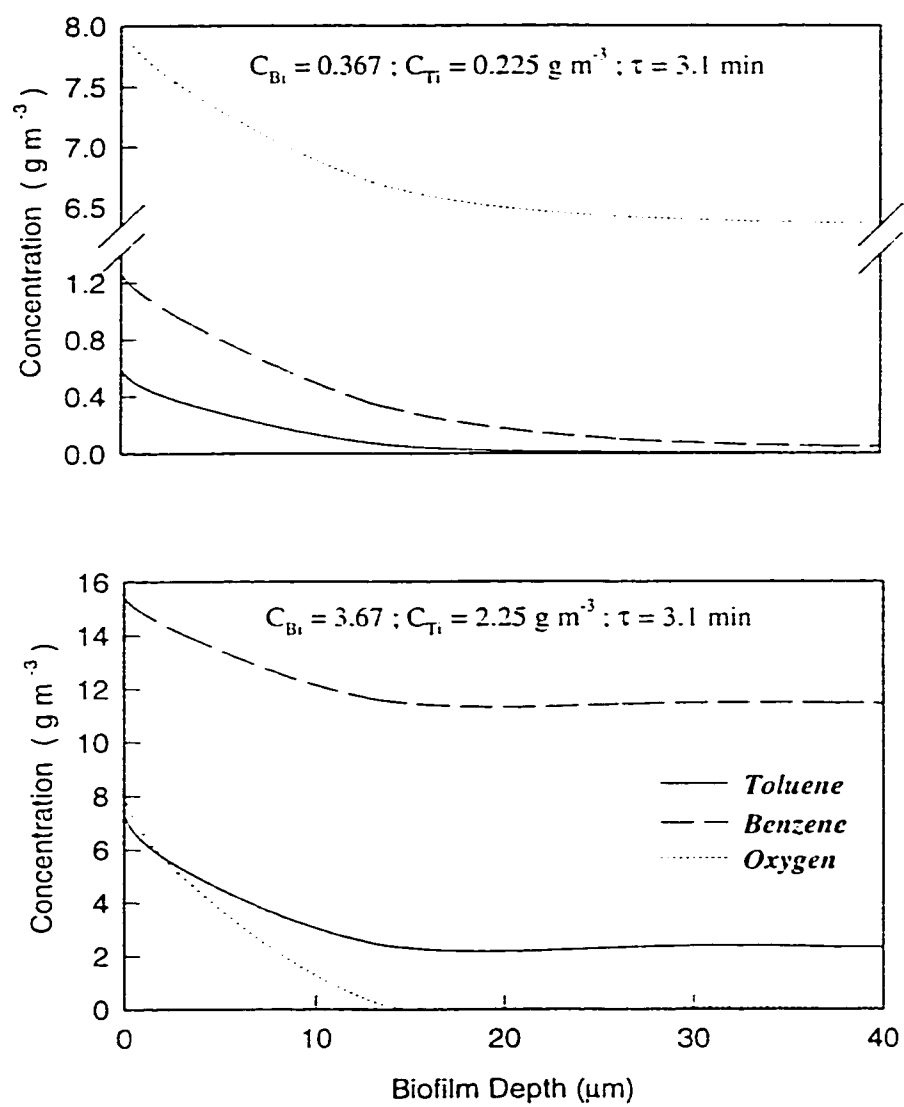


Figure 5.7: Concentration profiles of benzene, toluene and oxygen in the biofilm at different inlet gas concentrations.

Sensitivity studies

A thorough investigation of the models' sensitivity to their parameters was performed. The results are shown in Figures 5.8-5.13.

Biofilm parameters

Figure 5.8 show the effect of the biofilm parameters ϕ_{1T} and ϕ_{1B} on the exit concentrations of toluene and benzene, respectively. As can be seen, the model is very sensitive to these parameters. An increase in the value of ϕ_{1T} results in lower toluene conversions and hence higher exit toluene concentrations and vice versa. The reason for this can be explained as follows. Large value of ϕ_{1T} indicates large diffusion coefficient of toluene into the biofilm which results in reaction limitation in the biofilm and also possible substrate inhibition due to large toluene concentration and less availability of oxygen. However, there is no observable effect on the exit concentration of benzene. Similar effect can be seen on benzene conversions due to changes in the value of ϕ_{1B} . As the value of ϕ_{1B} increases, the exit benzene concentration increases. The explanation is the same as for ϕ_{1T} . As could be expected, a change in the values of these parameters for one component has very little or no effect on the other.

Figure 5.9 show the effects of parameters η_{1T} and η_{1B} on the exit concentrations of benzene and toluene from the biofilter. As can be seen, the model is very sensitive to these parameters. An increase in the value of η_{1T} or η_{1B} leads to a tremendous decrease in the exit concentrations of toluene and benzene respectively. Large values of η_{1T} implies greater reaction of toluene in the biofilm and less convection in the gas phase. The result could be easily expected as it is. The rate of increase in conversion decreases

as η_{1T} increases beyond a relative parameter value of three. This could be a result of diffusion limitation in the biofilm. Similarly increase in η_{1B} implies greater reaction of benzene in the biofilm resulting in lower exit benzene concentration.

Kinetic parameters

The effect of parameters ϵ_T , ϵ_B and ϵ_O can be seen in figure 5.10. As can be seen, the model is extremely sensitive to the parameters ϵ_T and ϵ_B . The dimensionless exit concentration varies from nearly zero ($\approx 100\%$ conversion) to nearly one ($\approx 0\%$ conversion) for high and low values respectively of ϵ_T and ϵ_B . Large value of ϵ_T implies low values of the Henry's constant i.e., lower volatility of any VOC. This could result in lower mass transfer resistance in the gas phase causing greater diffusion of a VOC in the biofilm, thus resulting in lower exit concentration. However, there is no observable effect of ϵ_T on benzene. Similar explanation can be given for the effect of ϵ_B on the exit concentrations.

As can be seen, the parameter ϵ_O has very little effect on the conversion of both benzene and toluene. It can be seen that ϵ_O affects the exit concentrations of both compounds at lower values. As the value of ϵ_O increases from zero, there is an observable decrease in the exit concentrations of both benzene and toluene. But after a relative parameter value of one, there is no effect at all. This behaviour could be attributed to the inlet oxygen concentration. As seen in figure 5.6, the inlet oxygen

concentration has potential limiting effects on the biofiltration process especially as the process is aerobic.

Figure 5.11 shows the effects of groups σ_1 and σ_2 on the exit benzene and toluene concentrations in the column. From the definition of parameter σ_1 , it is very clear that as the value of σ_1 increases, the conversion of benzene should decrease. Increase in σ_1 implies greater interference of toluene in the degradation kinetics of benzene and also a lower value of K_B . So naturally as σ_1 increases, the exit concentration of benzene increases. Similarly as σ_2 increases, the interference of benzene in the degradation kinetics of toluene increases resulting in lower toluene conversions i.e., higher exit toluene concentrations.

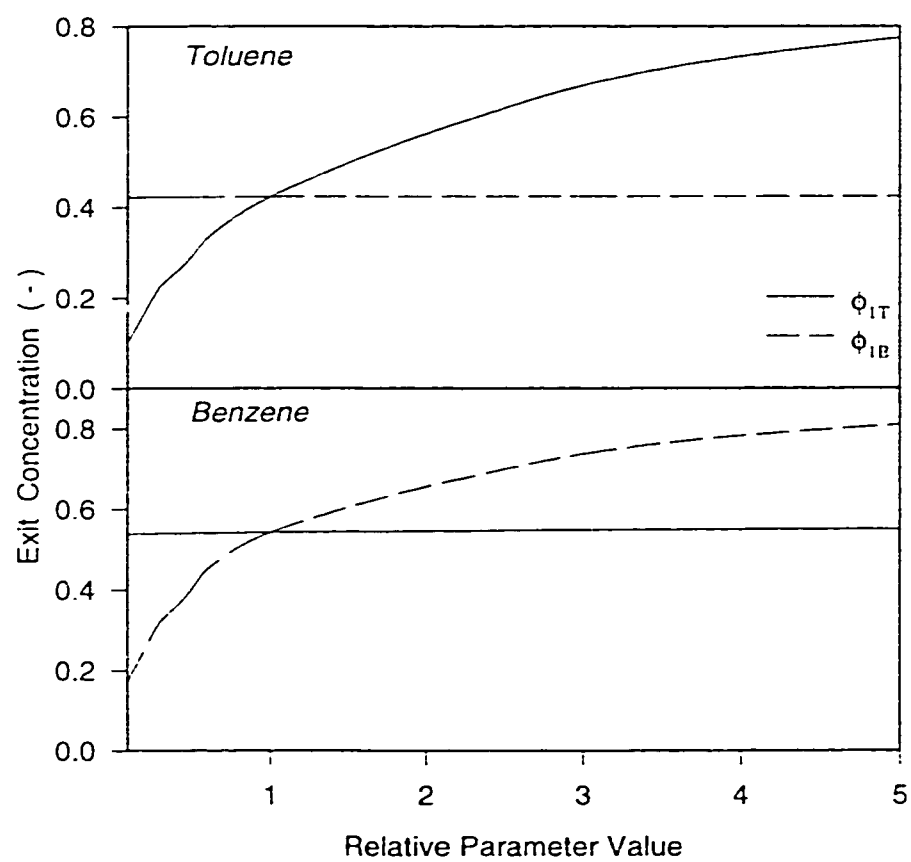


Figure 5.8: Effect of the biofilm parameters ϕ_1 and ϕ_2 on the exit benzene/toluene concentrations.

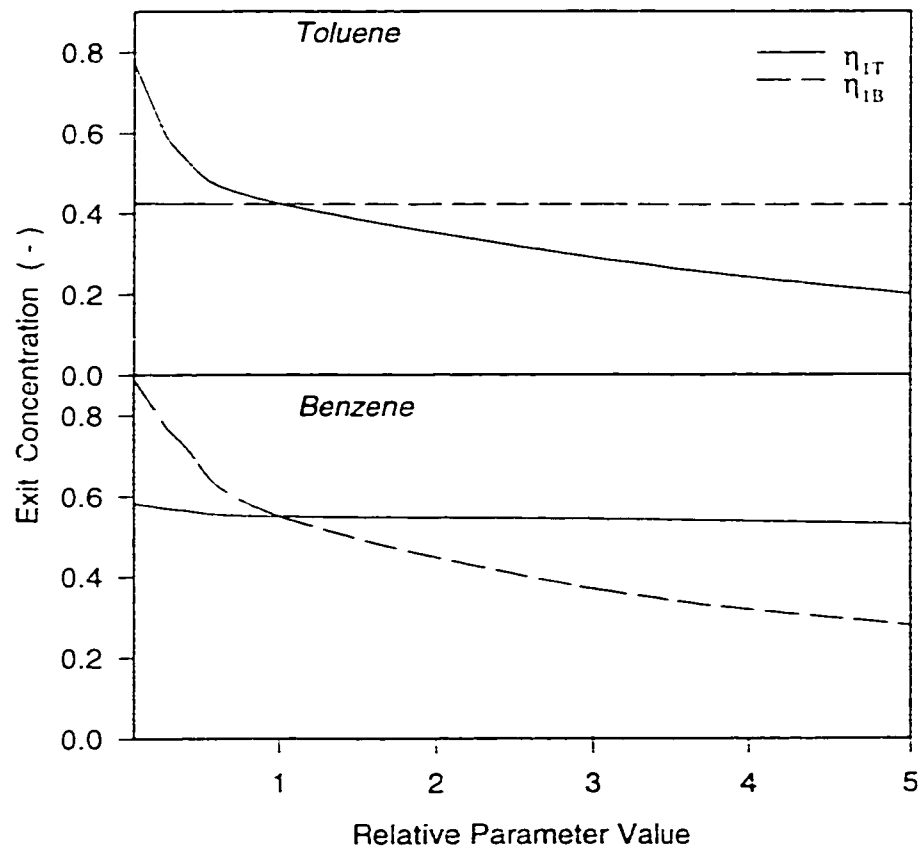


Figure 5.9: Effect of Biofilm parameters η_1 and η_2 on the exit benzene/toluene concentrations.

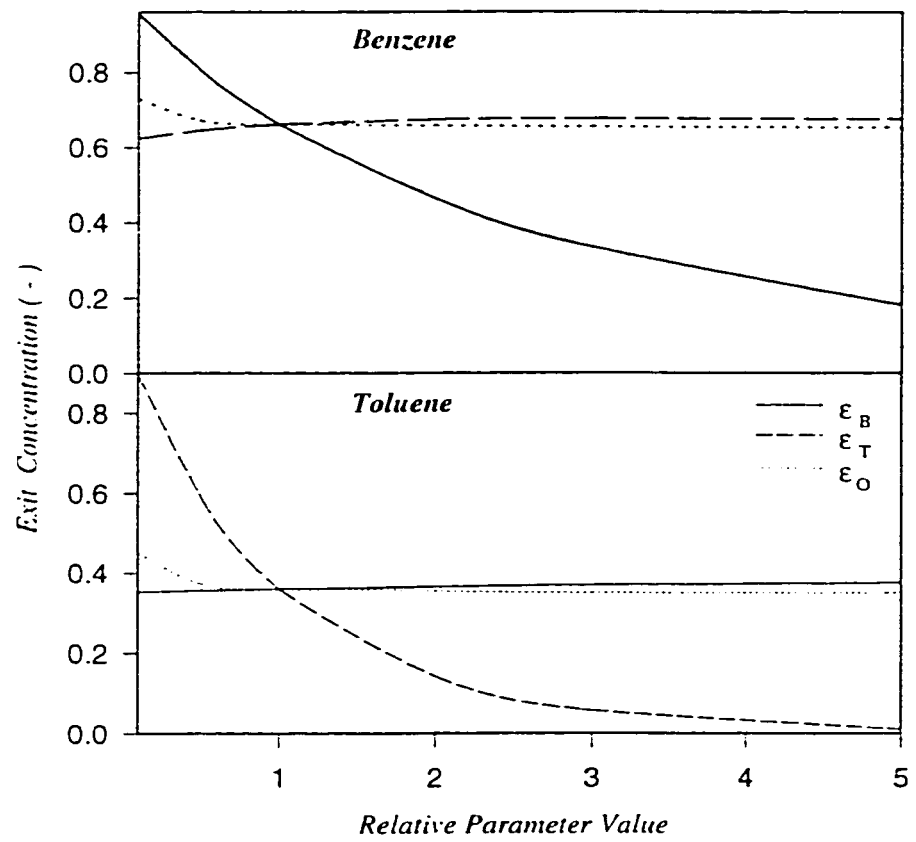


Figure 5.10: Effect of parameters ϵ_B , ϵ_T and ϵ_O on the exit benzene/toluene concentrations.

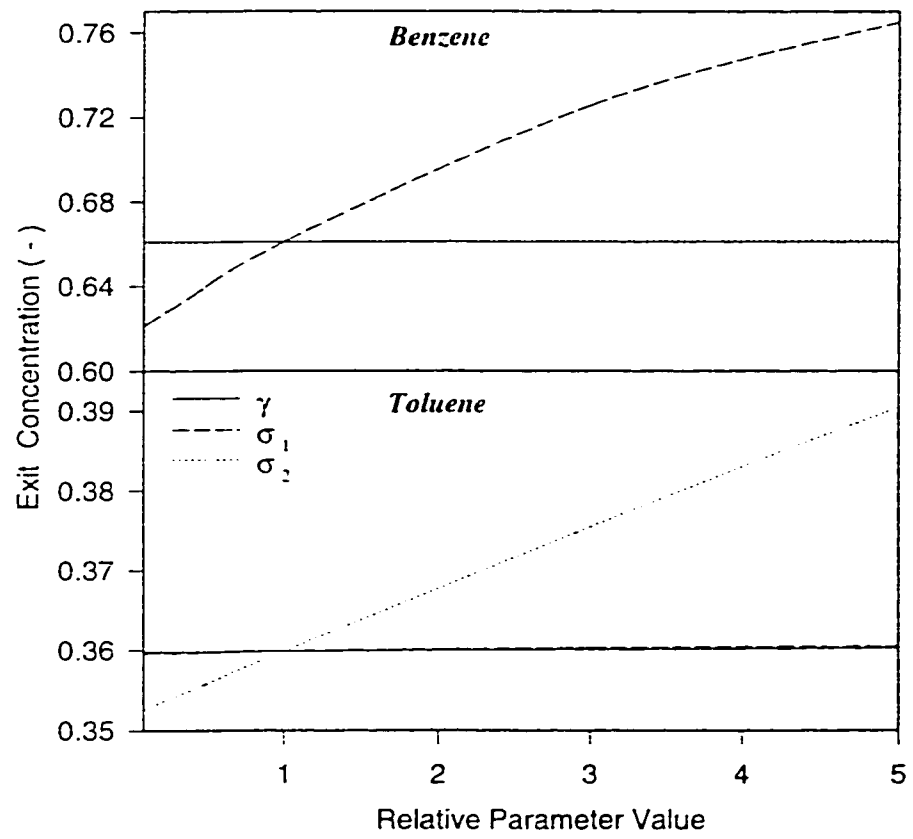


Figure 5.11: Effect of kinetic parameters γ , σ_1 and σ_2 on the exit benzene/toluene concentrations.

Gas phase parameters

Figures 5.12 show the effect of parameters β_{1T} , β_{1B} , β_{2T} and β_{2B} on the exit concentrations of benzene and toluene. As can be seen, the model is very sensitive to the parameters β_{1T} and β_{1B} and insensitive to β_{2T} and β_{2B} . The parameters β_{1T} and β_{1B} can be interpreted as the ratio of consumption in the biofilm of substrates toluene and benzene respectively to convection in the gas phase. Hence, an increase in the values of β_{1T} and β_{1B} leads to greater consumption or degradation in the biofilm and due to less convection in the gas phase, there is low mass transfer resistance in the gas phase, resulting in greater conversion in the biofilm. So, as expected, the exit concentration decreases with increase in the relative parameter values. There is no effect of the parameters β_{2T} and β_{2B} on the conversion.

It has been found that the parameters χ_T and χ_B have little effect on the performance on the biofilter column. This could be attributed to the low value of the mass transfer coefficients for toluene and benzene in the gas phase and extremely low adsorptive capacity of the packing material used in the study (peat/perlite) resulting in poor adsorption in the solid. Also it should be noted that the present model is valid for the case when the biofilter column is in operation, i.e., when the biofilm is fully developed. It has been reported by Hodge and Devlinny, (1995) that adsorption plays a significant role in the biofiltration process only during the start up stage after which biodegradation plays the dominating role. Hence, in the present case, the parameters χ_T and χ_B do not have much effect on

the model predictions. However, we expect these parameters to be significant in the cases of better adsorbents like activated carbon and during the start-up stages.

Figures 5.13 and 5.14 a and b show the effect of Peclet numbers of benzene and toluene on the benzene/toluene concentration profiles in the column and with time. Large relative parameter value implies higher Peclet number and vice versa. A relative parameter value of 1 represents the value of the Peclet number calculated from experimental conditions. High value for Peclet number denotes plug flow and low value mixed flow in the column. It is very clear that the Peclet number of one compound does not really affect the conversion of the other compound in the mixture. A change in the value of the Peclet number of benzene does not affect the concentration of toluene and vice versa. However, the Peclet number of a compound affects the conversion of that compound quite drastically. It can be seen from figures 5.13a and 5.14a that as the value of Peclet number decreases, the concentration profile becomes flatter, indicating a transition from plug flow behaviour to mixed flow. A decrease in the Peclet number implies better mixing in the gas phase leading to higher rates of mass transfer and better conversions. These conditions prevail more at the inlet of the column where the concentration levels are maximum. Figures 5.13b and 5.14b indicate that although a change in the Peclet number affects the exit concentration of the corresponding compound, the time required to attain steady state is almost unaffected.

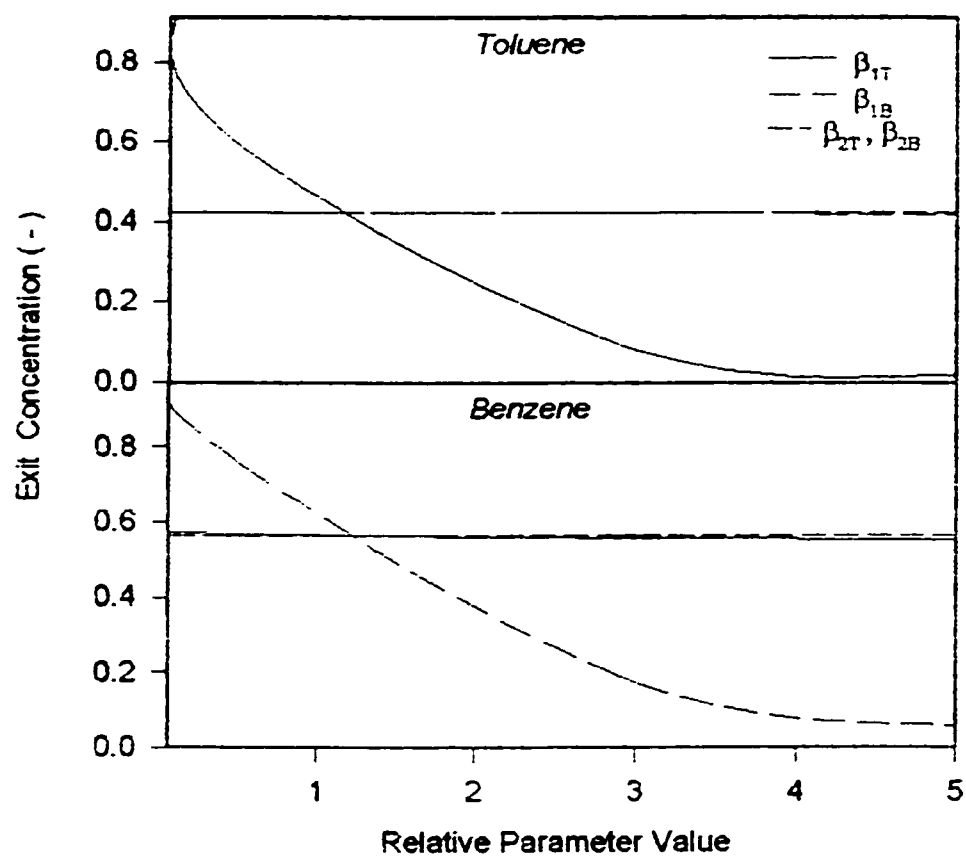


Figure 5.12: Effect of dimensionless groups β_{1j} and β_{2j} on the exit benzene / toluene concentrations.

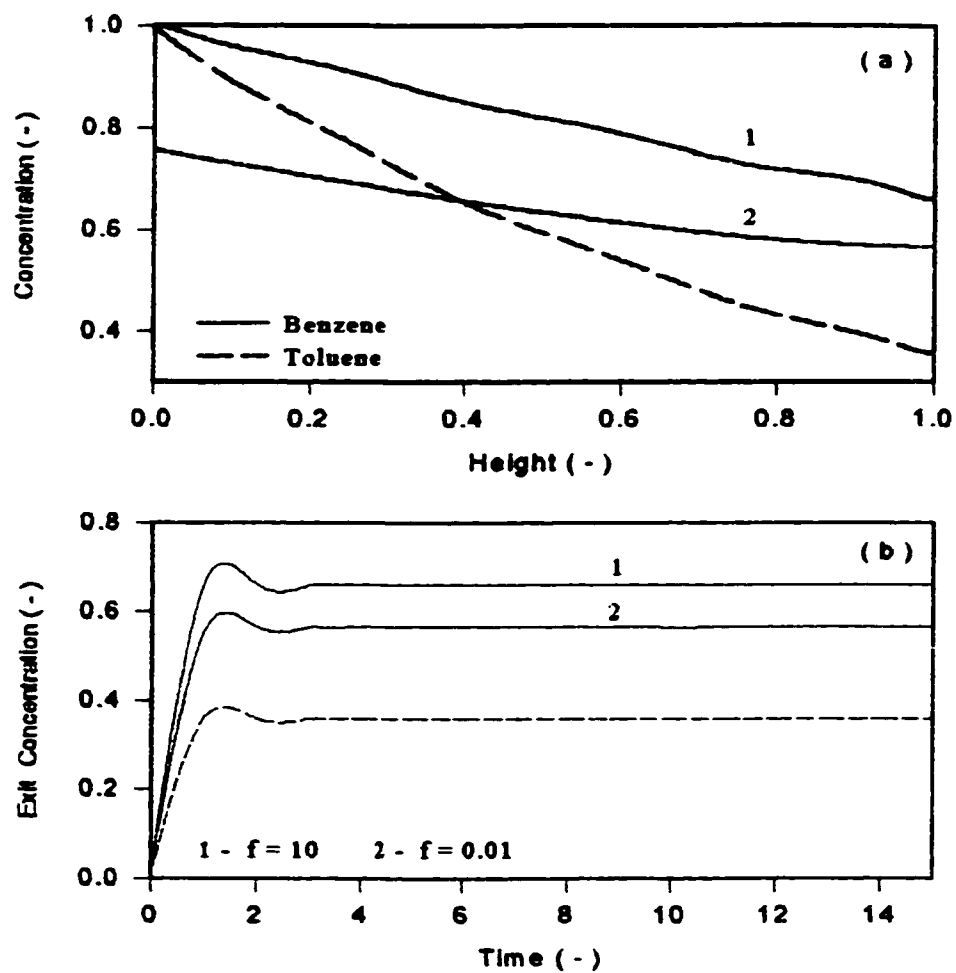


Figure 5.13a & 5.13b: Effect of Pe_B on the transient and column benzene / toluene concentration profiles.

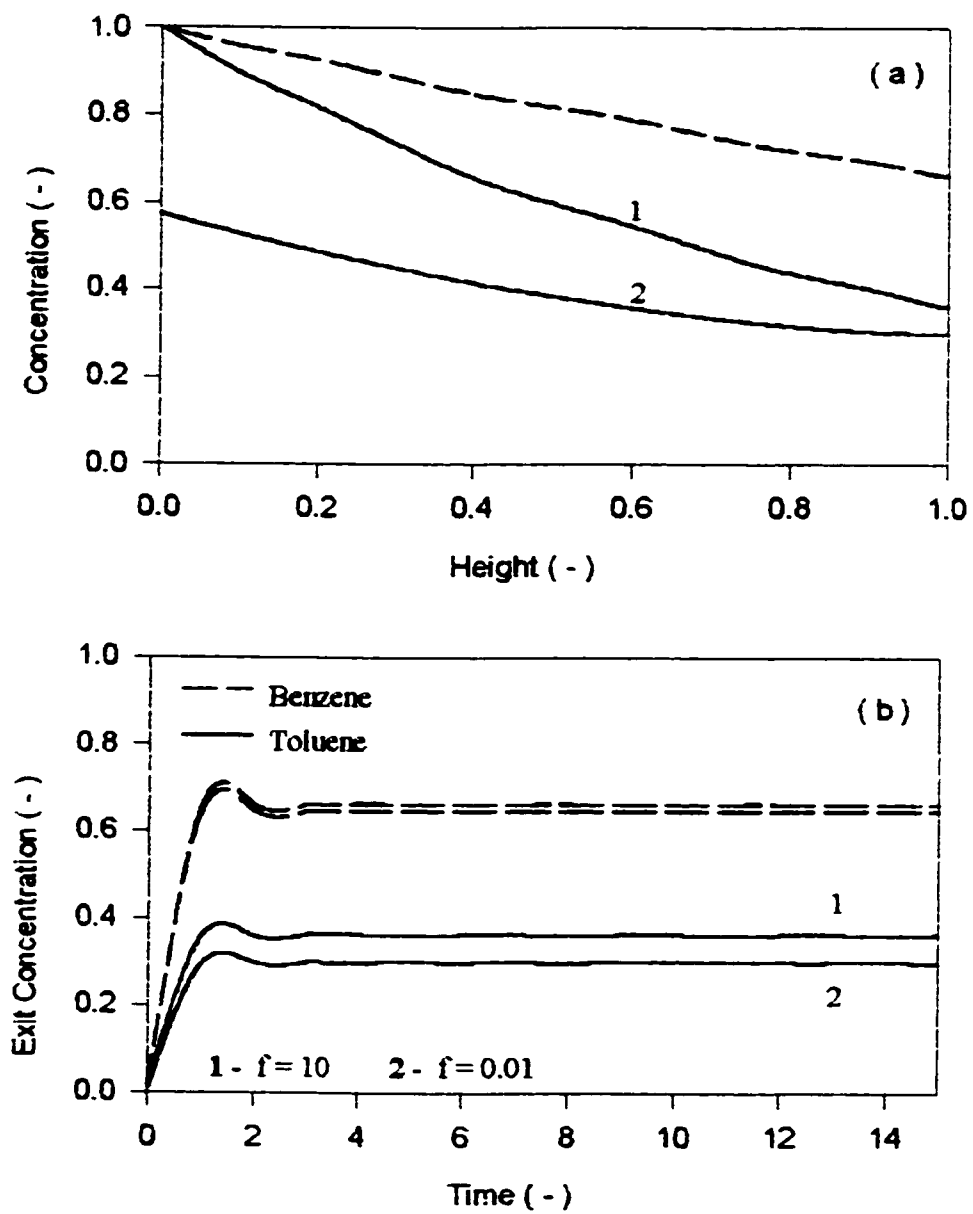


Figure 5.14a & 5.14b: Effect of Pe_T on the transient and column benzene / toluene concentration profiles.

PERTURBATION STUDIES

6.1 INTRODUCTION

Biological reactors are often subjected to variations in environmental conditions. Occasional fluctuations can be expected in the inlet flow rate, concentrations of the emissions from process plants especially if the operation is of batch type (eg., pharmaceutical industry), inlet temperature and pH (in case of acid forming compounds). Therefore, information on dynamic behaviour is needed to define the response of reactors to upsets, to provide data for accurate designing of biofilters and to aid in process control of biofiltration process.

Biofiltration could be applied to the treatment of air streams from batch operations, such as the pharmaceutical industry, only if biofilters can respond effectively to frequent variations in the quantitative and qualitative characteristics of the airstreams. Batch processes utilize different solvents at different time periods (qualitative changes in composition of airstreams); also, the flowrate and concentration of the pollutants may vary with time (quantitative changes).

Abrupt variations in the operation parameters like the flowrate, concentration of pollutants in the inlet stream, pH, temperature etc., are known as shock-loading effects.

Shock loads can be classified based on the nature of change and its magnitude as follows:

Quantitative shock loads involve abrupt variations in the inlet parameters like the inlet flow rate or the inlet concentration of the pollutants, causing a change in the load.

Qualitative shock loads involve changes in the nature of the substrate(s) in the inflow to a process.

Hydraulic shock loads involve changes in the flow rate to the system. If the concentration of the substrate remains constant, the mass rate of inflow of substrate to the system changes under hydraulic shock loading. The hydraulic shock load can also be applied with constant mass rate of substrate fed to the system if a complimentary change in concentration occurs simultaneously.

Temperature & pH shock loads, as the name indicates, they involve changes in the temperature, pH of the system. These may occur either due to changes of temperature and pH of the inlet stream or as a result of the processes taking place in the biofilter, discussed in chapter 1.

In this chapter, we have attempted to study the effects of perturbations in the various inlet parameters like the inlet concentrations, flowrate, temperature in the column and the pH of the system. For the case of inlet concentrations, the following different scenarios have been studied: effect of shock loading to the inlet concentrations of each organic substrate (more than one for mixtures), inlet oxygen concentration, and the inlet concentrations of both the substrates (in case of mixtures). As pointed out before, all

these cases can be commonly encountered in process industries and hence require detailed study.

6.2 ADMINISTRATION OF SHOCK LOADS IN THE MODEL

In the present study, the process variables namely concentration of the substrates, temperature in the biofilm, pH of the system and the inlet gas flow rate are varied in a number of ways. The parameters have been given step input, sinusoidal, triangular and random variations and their effect on the conversion in the column has been studied. The mathematical functions used for effecting these variations for the parameter V in the model are as follows:

Step Input

$$V \Big|_{Z=0^-} = V_{initial}$$

Sinusoidal Variation

$$V \Big|_{Z=0^-} = V_{initial} + A \operatorname{Sin} \left(\frac{\pi (t + CT / 2)}{CT} \right)$$

where, A is the amplitude of the sinusoidal forcing function and CT the cycle time.

Triangular Variation

$$V \Big|_{Z=0^-} = V_{initial} \quad t \leq t_{initial}$$

$$V \Big|_{Z=0^-} = \frac{h_t t}{(t_{half} - t_{initial})} + \frac{1.0 - h_t t}{(t_{half} - t_{initial})} \quad t_{initial} \leq t \leq t_{half}$$

$$V \Big|_{Z=0^-} = \frac{h_t t}{(t_{half} - t_{max})} + \frac{1.0 + h_t - h_t t_{half}}{(t_{half} - t_{max})} \quad t_{half} \leq t \leq t_{max}$$

$$V \Big|_{Z=0^-} = V_{initial} \quad t_{max} \leq t \leq t_{final}$$

where, h_t is the maximum height or amplitude of the triangular forcing function, t_{initial} and t_{max} are the times for the starting and ending the perturbations respectively and t_{half} is the time at which the triangular perturbation reaches the maximum height.

Random Variation

The random values for the inlet variable were calculated by the subroutines from IMSL package.

6.3 PERTURBATION TO THE INLET CONCENTRATIONS

The inlet concentration is one of the most important process parameters that affect the efficiency of a biofilter column. However, in any practical application, the concentration of the effluents seldom remain constant. Large fluctuations in the concentration of the effluents can be expected frequently from a process plant. In addition to changes in the concentration of a particular compound, changes in the composition of the emissions can also be expected. Hence the biofilter should be able to withstand these perturbations in the inlet gas concentrations.

The main effects of an increase in the inlet concentration of the substrate are as follows:

- 1) The concentration gradient in the biofilm is increased thereby causing a flux into the biofilm. This may initially result in increased conversions. But a sustained increase in the inlet concentration may lead to a condition of reaction limitation in the biofilm, thereby causing a drop in the conversion.
- 2) Another phenomenon commonly encountered in biological processes is that of substrate inhibition. Bacteria are susceptible to the action of various chemicals which depending on their nature and concentration either inhibit bacterial growth or kill the bacteria. There are primarily two types of inhibition: Competitive and Non-competitive depending on whether the inhibitor competes with the growth limiting substrate or not.
- 3) The other major problem that arises due to sudden increase in the inlet concentration is that it causes a greater density of microorganisms near the inlet of the biofilter where there is greater concentration gradient, leading to under-utilization of the other

parts of the biofilter. This may result in the decay of microorganisms at other parts of the biofilter especially near the outlet. This may lead to poor operation of the biofilter.

Figures 6.1 and 6.2 compare the model predictions against the recently reported experimental data of Tang et al. (1995). They report shock loading studies with the inlet toluene concentration and gas velocity in biofilters with three types of packing materials: chaff/compost, diatomaceous earth/compost and granular activated carbon/compost. Although the experimental results are interesting, a theoretical model was not presented. In our study, the experimental data of the chaff/compost biofilter were chosen. Since the parameters for chaff/compost packing material were not available, the same parameters as for peat/perlite packing, except for the biolayer surface area, were used to predict the data by the *general* model. The value of the biolayer surface area ($A_S^* \approx 88 \text{ m}^{-1}$), was obtained by fitting the data reported in Figure 6.1. In fitting, an attempt was made to describe all the data points. Notice that there is an abrupt increase in the exit concentration when the inlet concentration is increased to 3.33 g/m^3 from 1.87 g/m^3 . This may be due to desorption of toluene. This part of the data is not well described by the model. Otherwise, with a single fitted parameter value of $88 \text{ m}^2/\text{m}^3$ for A_{ST} , our model is able to predict well the dynamic response of the biofilter to a sudden change in the inlet concentration. This parameter value was unchanged and was used in the model to describe various dynamic response data of Tang et al. (1995) which are shown in Figures 6.2 and 6.13.

Figure 6.2 shows response of the biofilter to shut-down and restart-up conditions. For simulating data, inlet concentration and gas superficial velocity used before shut-down and after restart-up were about 0.89 g/m^3 and 0.67 m/s , respectively. Model predictions show that the biofilter is able to respond to previous steady-state conditions within a day after a six day shut-down period. Thus, both model predictions and experimental data of Tang et al. (1995) show that activity of the biofilter can be restored within one to two days.

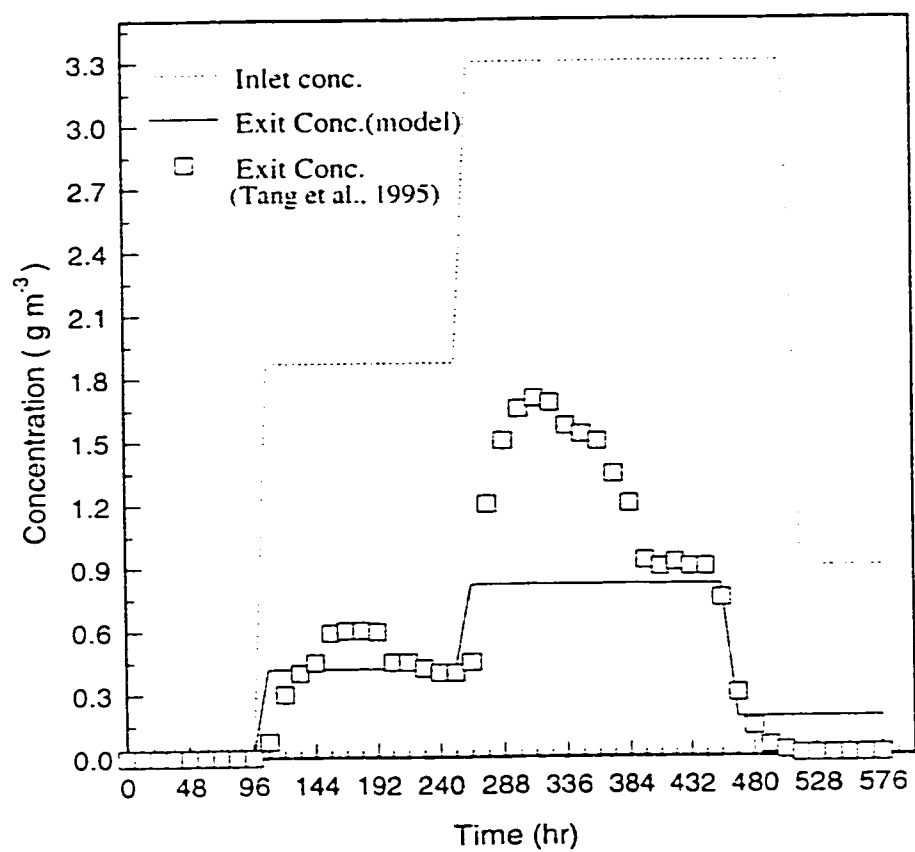


Figure 6.1: Transient response to abrupt change in the *inlet toluene concentration*. Model prediction and Experimental data.

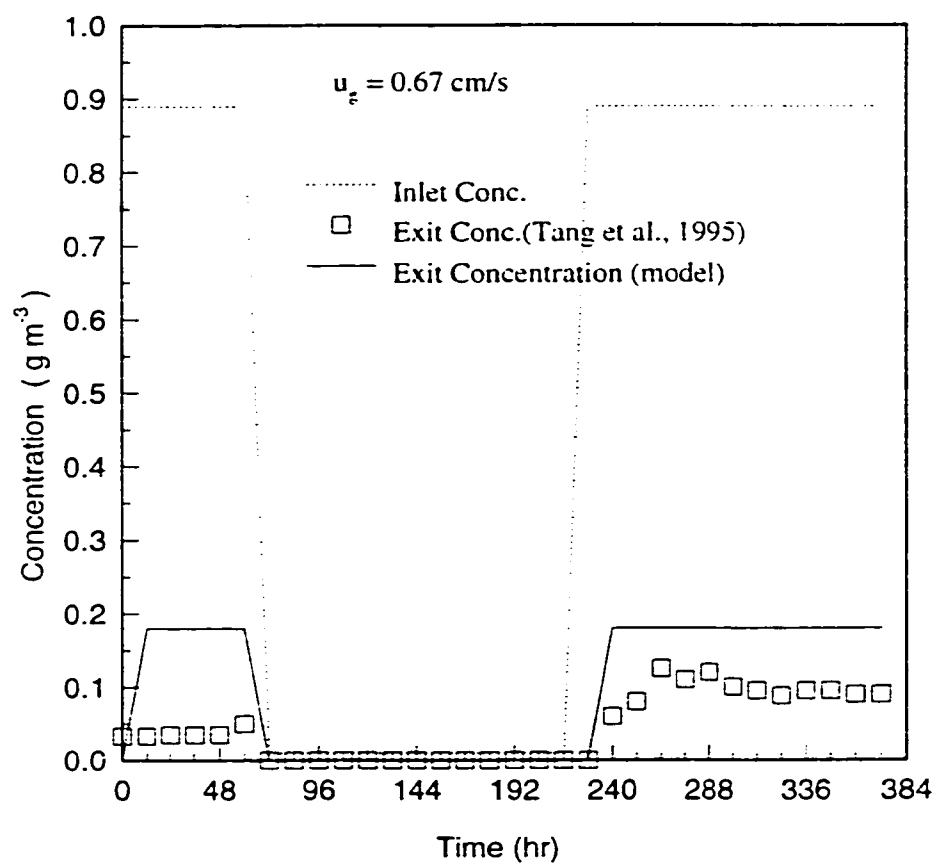


Figure 6.2: Transient response of the exit toluene concentration to *shut down and restart* of the biofilter.

Figure 6.2 shows that the model is able to describe, at least qualitatively, the dynamic response reasonably well considering the fact that the parameters, especially the mass transfer coefficient and isotherm parameters were different. If these parameters were experimentally determined for chaff/compost packing and used in the solution of the model, then the predictions would be much better. Figure 6.3 shows the experimental data (Zarook, 1994) and model predictions of the response to a sudden step change in the operating conditions. Both the concentration of the inlet gas and its flowrate are suddenly changed five days after the start of the experiment. As seen in the figure, the agreement between the data and predictions is good. The dotted line represents the same model predictions in non-dimensional form.

Figures 6.4a, 6.4b and 6.4c show the effects of perturbations, triangular, sinusoidal and random respectively in the inlet toluene concentration to the biofilter on the exit concentration for different inlet conditions. As can be seen in all three cases, there is a small time lag in the response, which is really negligible when converted to real times. Also, after the perturbation is stopped, the time taken to reach steady state is very less. However, the conversion in the biofilter, represented by the exit concentration, is drastically affected by the perturbations in the inlet concentration. The amplitude of the response is nearly doubled when the amplitude of the perturbation is doubled. This can be expected because an increase in the inlet concentration causes a large concentration gradient in the biofilm thereby increasing the diffusion rate in the biofilm. This results in a reaction limitation condition in the biofilm thereby effecting lower conversions. However, as seen from the two cases shown in the graph, this increase in the amplitude of

the exit concentration is reduced by increasing the residence time in the column. Thus, at large residence times, the response of the biofilter is better as also seen from figure 6.6c.

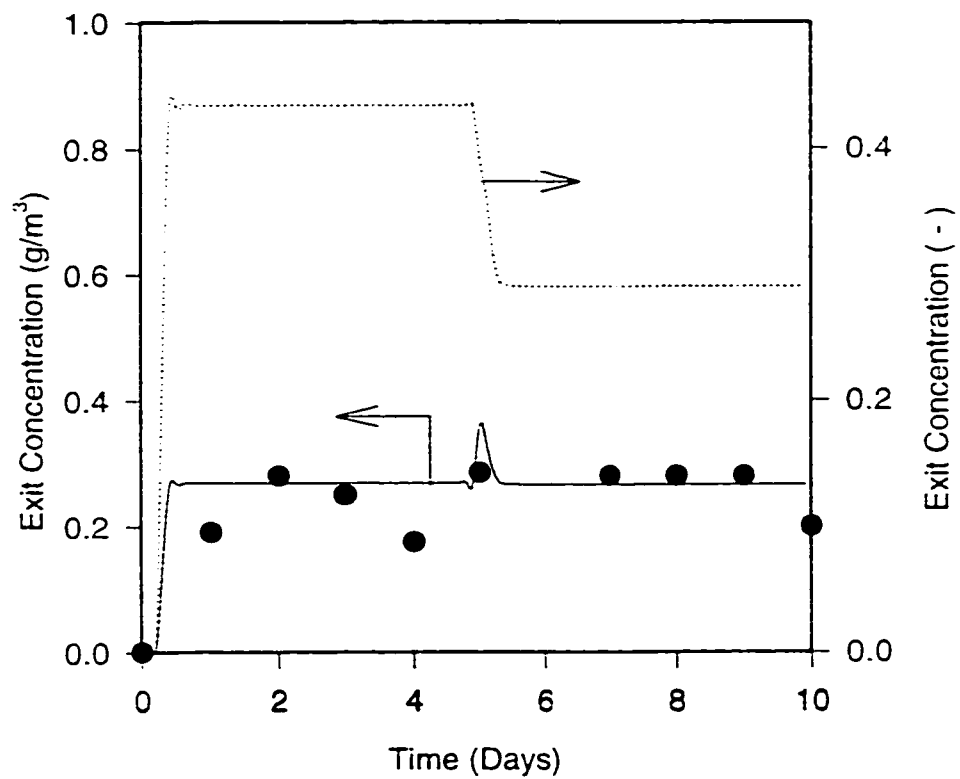


Figure 6.3: Experimental data and model predictions for two consecutive experiments with toluene vapor. Conditions were : $C_{ii}=0.62 \text{ g m}^{-3}$, $\tau=2.7 \text{ min}$. Five days later, the conditions were changed to $C_{ii}=0.92 \text{ g m}^{-3}$, $\tau=4.2 \text{ min}$.

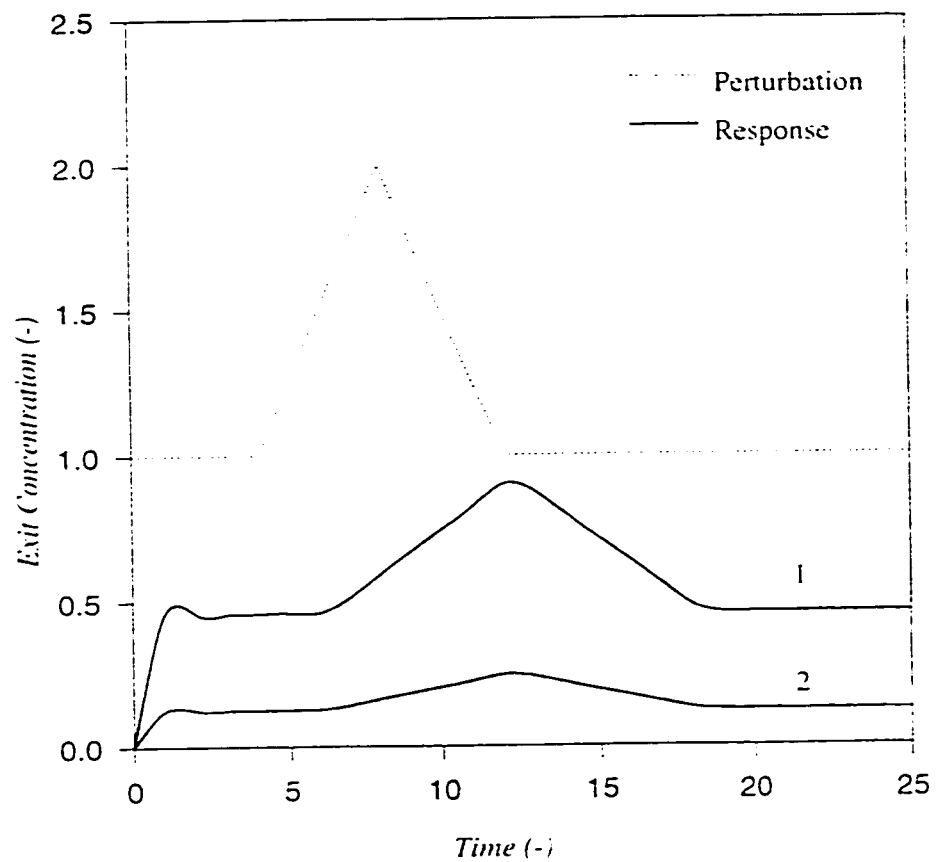


Figure 6.4a: Transient response of the exit toluene concentration to triangular perturbation in the inlet concentration for the two cases studied :

Curve 1: $C_{i1} = 2.7 \text{ g m}^{-3}$: $\tau = 0.62 \text{ min}$

Curve 2: $C_{i2} = 1.65 \text{ g m}^{-3}$: $\tau = 7.7 \text{ min}$

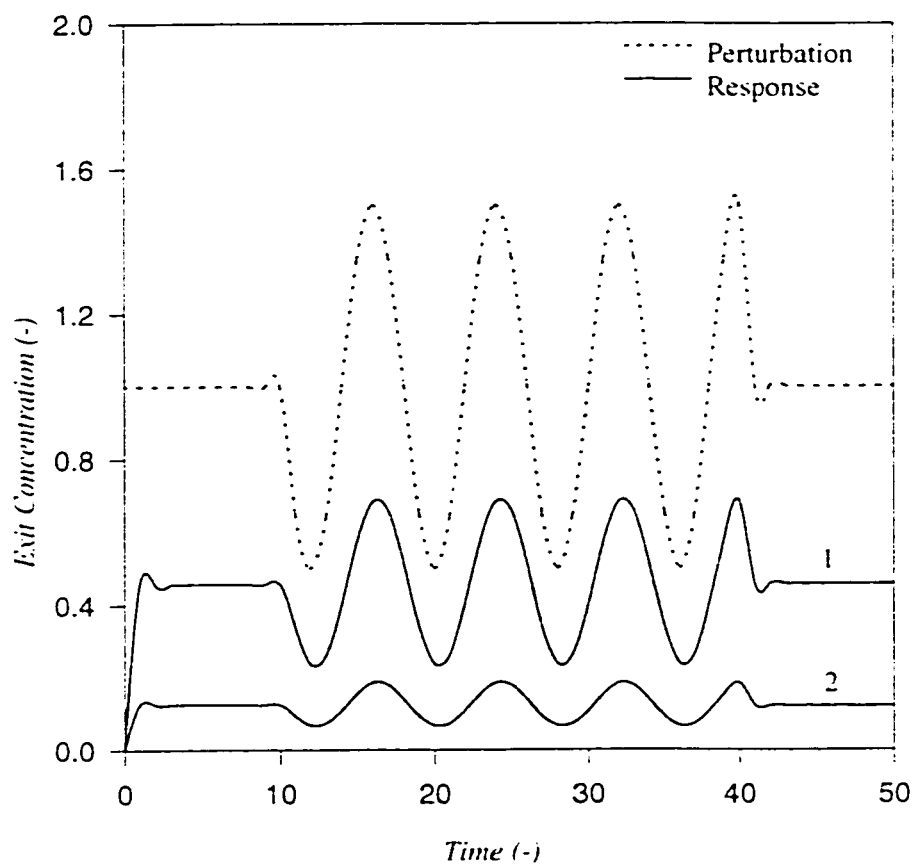


Figure 6.4b: Transient response of the exit toluene concentration to sinusoidal changes in the inlet concentration for the two cases studied

Curve 1: $C_{i1} = 2.7 \text{ g m}^{-3}$: $\tau = 0.62 \text{ min}$

Curve 2: $C_{i2} = 1.65 \text{ g m}^{-3}$: $\tau = 7.7 \text{ min}$

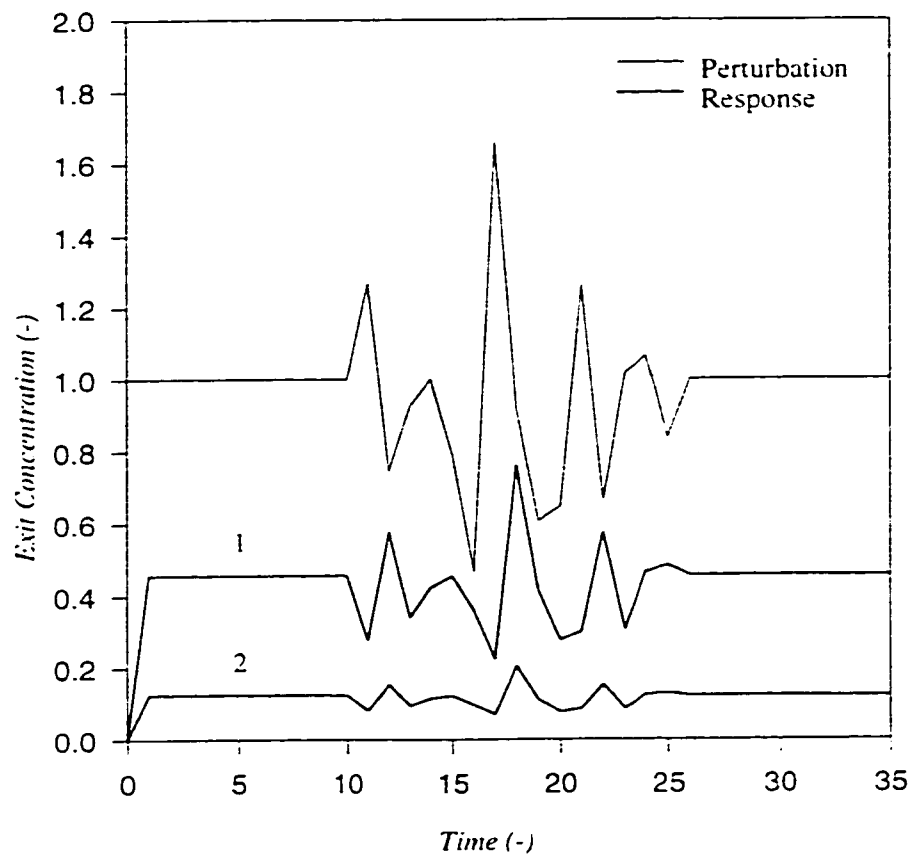


Figure 6.4c: Transient response of the exit toluene concentration to random changes in the inlet concentration for the two cases studied :

Curve 1: $C_{i1}=2.7 \text{ g m}^{-3}$: $\tau = 0.62 \text{ min}$

Curve 2: $C_{i2}=1.65 \text{ g m}^{-3}$: $\tau = 7.7 \text{ min}$

Figures 6.5a and 6.5b show the effect of perturbations, sinusoidal and random respectively, in the inlet toluene concentration, on the exit concentrations of the benzene and toluene mixture. There is a small but observable time lag in the response considering the low residence time of operation and the small perturbation times. As can be seen clearly, an increase in the inlet toluene concentration causes an almost equivalent increase in the concentration of toluene in the exit mixture. This can be expected, because, as explained for single component, an increase in the inlet concentration of the substrate results in greater diffusion in the biofilm resulting in reaction limitation and substrate inhibition in the biofilm. There is also a corresponding small variation in the exit concentration of benzene from the column. This variation is attributed to the interactive kinetics between benzene and toluene. Obviously, increase in the toluene concentration will cause an interference of toluene with the kinetics of benzene degradation. Therefore an increase in the inlet toluene concentration causes a slight increase in the exit benzene concentration.

Figures 6.6a, 6.6b and 6.6c show the effects of different kinds of perturbations in the inlet benzene concentration, on the exit concentration of the mixture. As can be seen, the exit benzene concentration is drastically affected by the perturbations. Also the effect of kinetic interference can be seen in the exit toluene concentration. It is important to note that as compared to Figure 6.5b, Figure 6.6b shows that kinetic interference by benzene has more profound effect on the exit concentration.

Figures 6.7a and 6.7b show the effects of random and sinusoidal perturbations in the inlet gas concentrations of both benzene and toluene. As expected from the previous

discussions, there is a large increase in the exit concentrations of both benzene and toluene with small but observable time lag in the response. The concentration of oxygen was kept constant at a high value, and hence has no change in the exit oxygen concentration as seen. The responses of both benzene and toluene are almost identical.

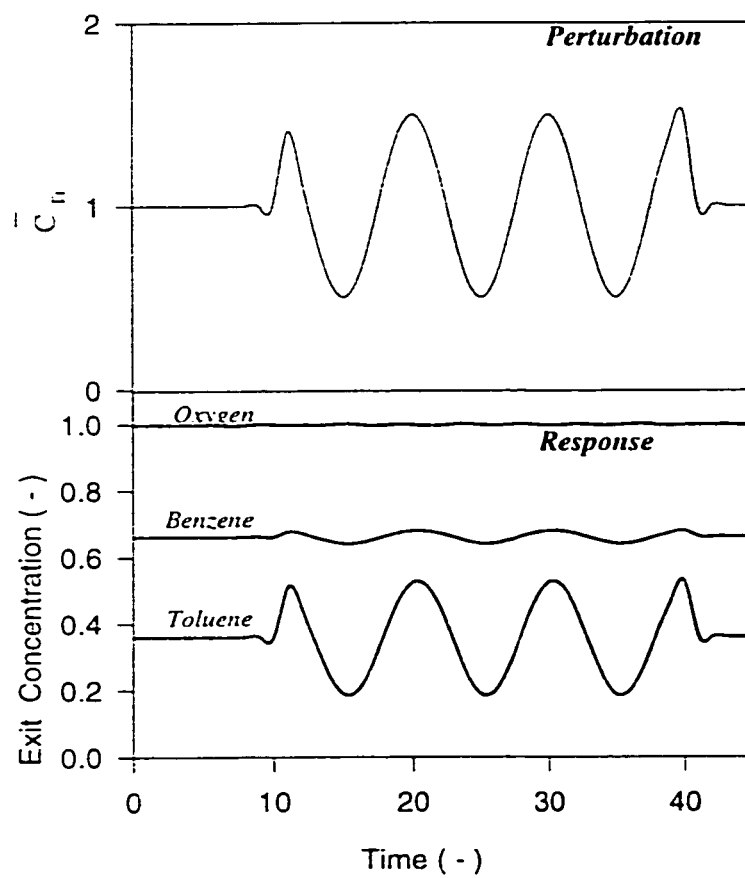


Figure 6.5a: Transient response of the exit concentrations to *sinusoidal* perturbations in the *inlet toluene concentration*.

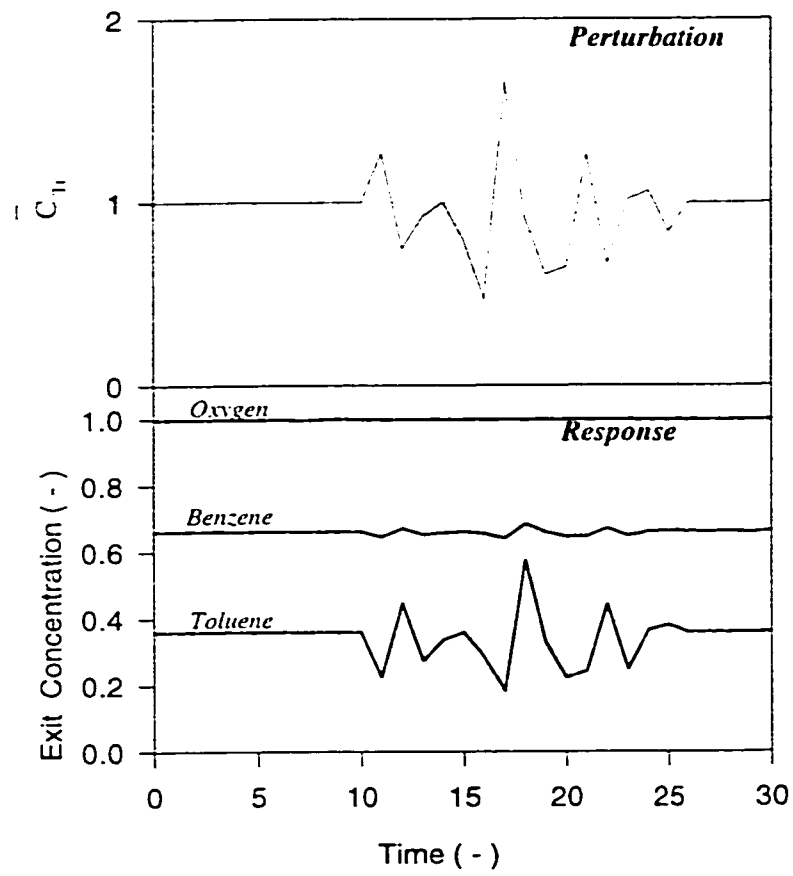


Figure 6.5b: Transient response of the exit concentrations to random perturbations in the inlet toluene concentration.

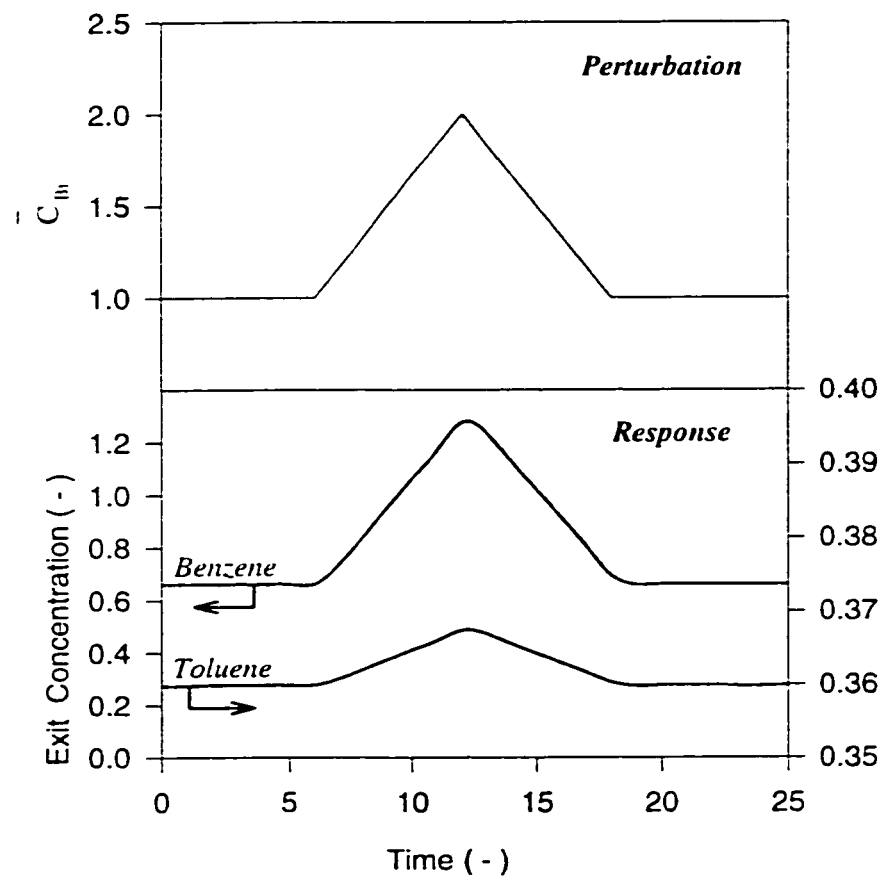


Figure 6.6a: Transient response of the exit concentrations to *triangular* perturbation in the *inlet benzene concentration*.

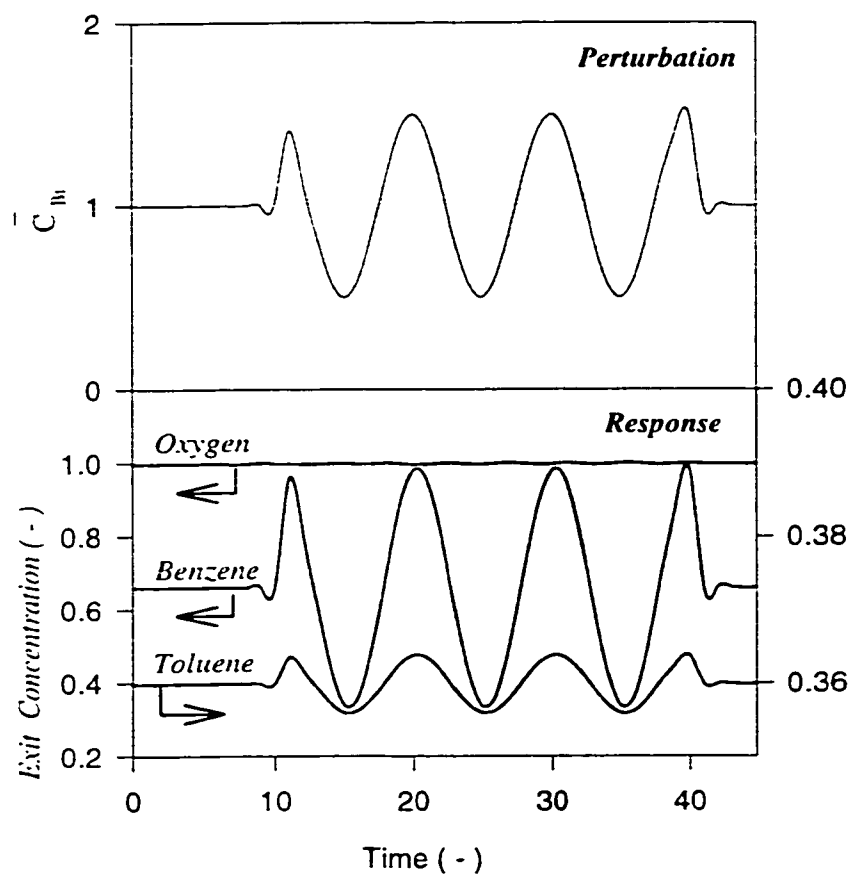


Figure 6.6b: Transient response of the exit concentrations to *sinusoidal* perturbations in the *inlet benzene concentration*.

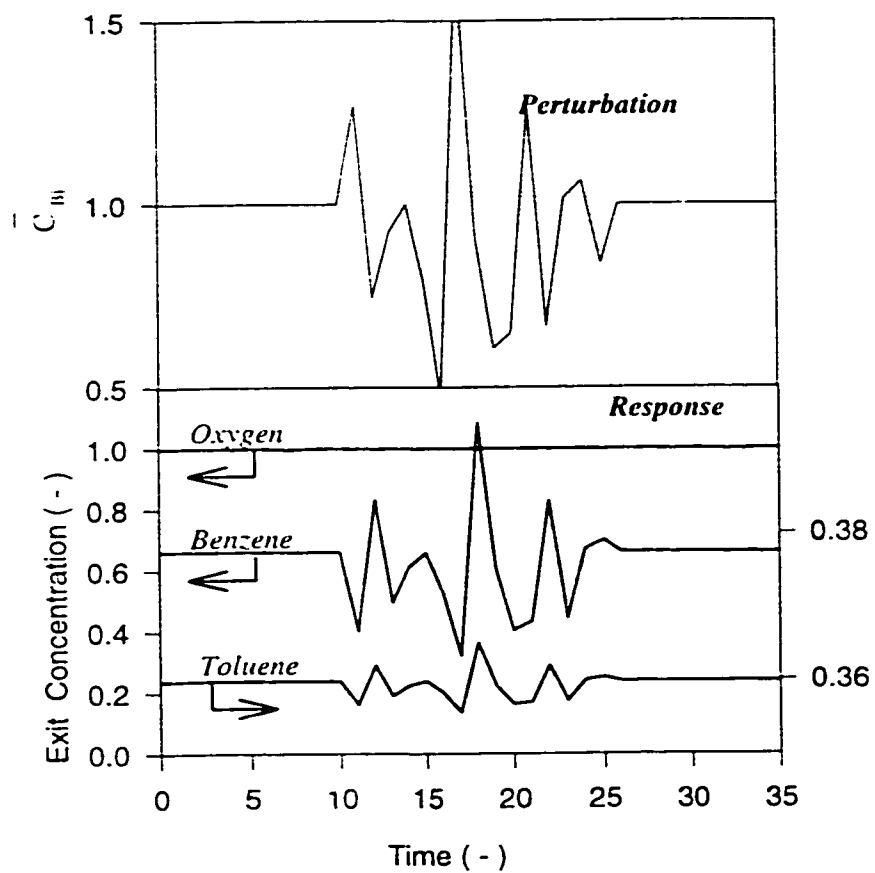


Figure 6.6c: Transient response of the exit concentrations to random perturbations in the inlet benzene concentration.

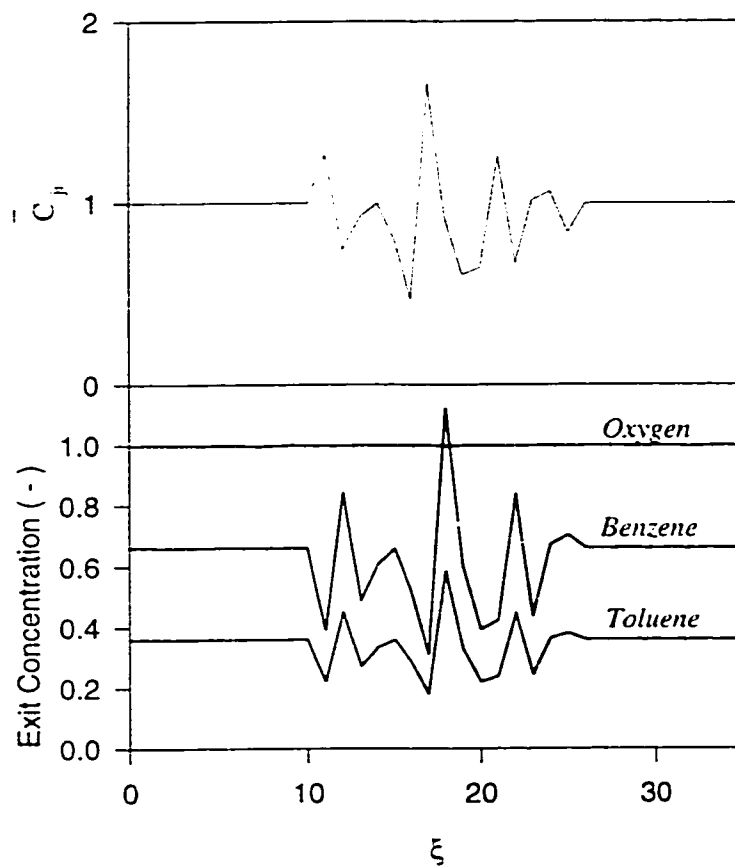


Figure 6.7a: Transient response of the exit concentrations to *random* perturbations in the *inlet* concentration of the mixture.

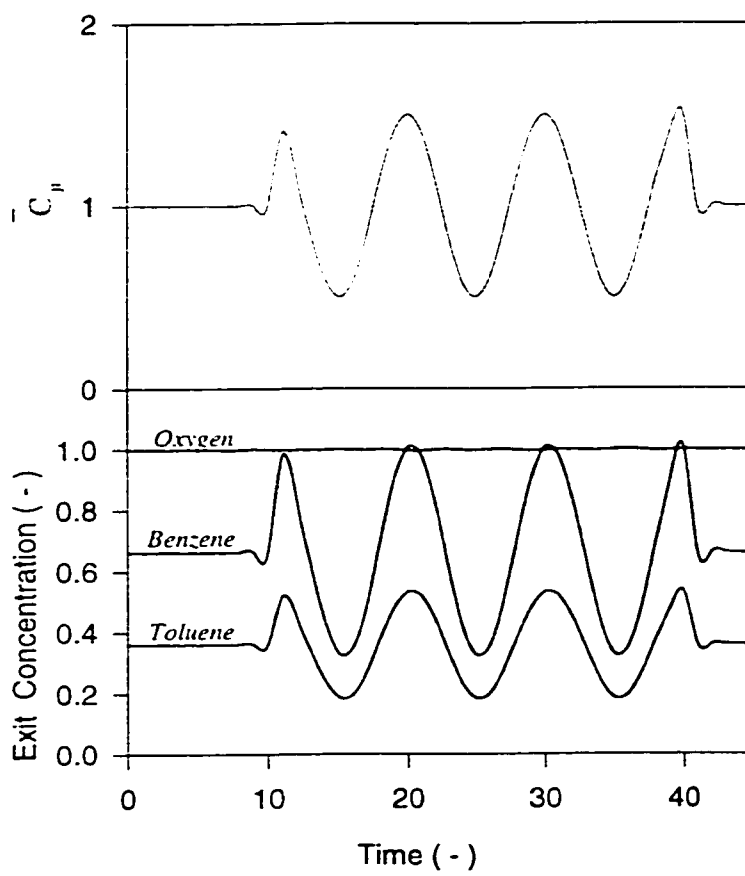


Figure 6.7b: Transient response of the exit concentrations to *sinusoidal* perturbations in the *inlet concentration of the mixture*.

Figures 6.8a, 6.8b and 6.8c show the effects of perturbations in the inlet oxygen concentration. As can be seen, there is almost no effect on the conversion in the column. As explained in Chapters 4 and 5, the change in the inlet concentration of oxygen produces a drastic change in the conversion in the column only at low inlet oxygen concentration values. After a certain value of the inlet oxygen concentration, almost no effect on the removal was observed. This implies that oxygen is still present in sufficient amounts in the column, thereby causing no observable effect on the conversion. However, for higher values of the inlet VOC concentrations, this behavior may change.

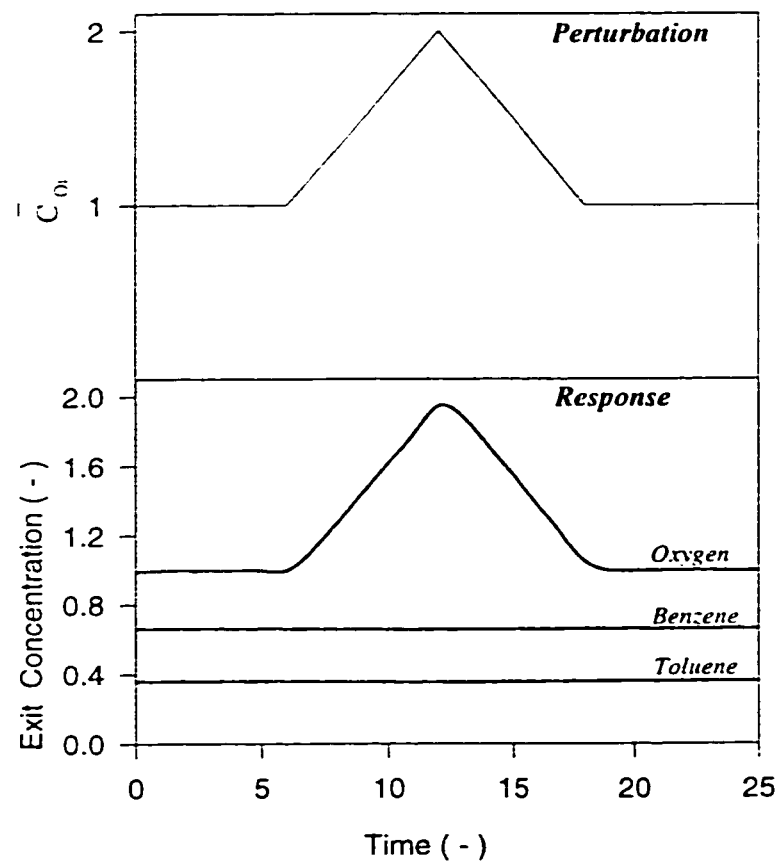


Figure 6.8a: Transient response of the exit concentrations to triangular perturbation in the inlet oxygen concentration

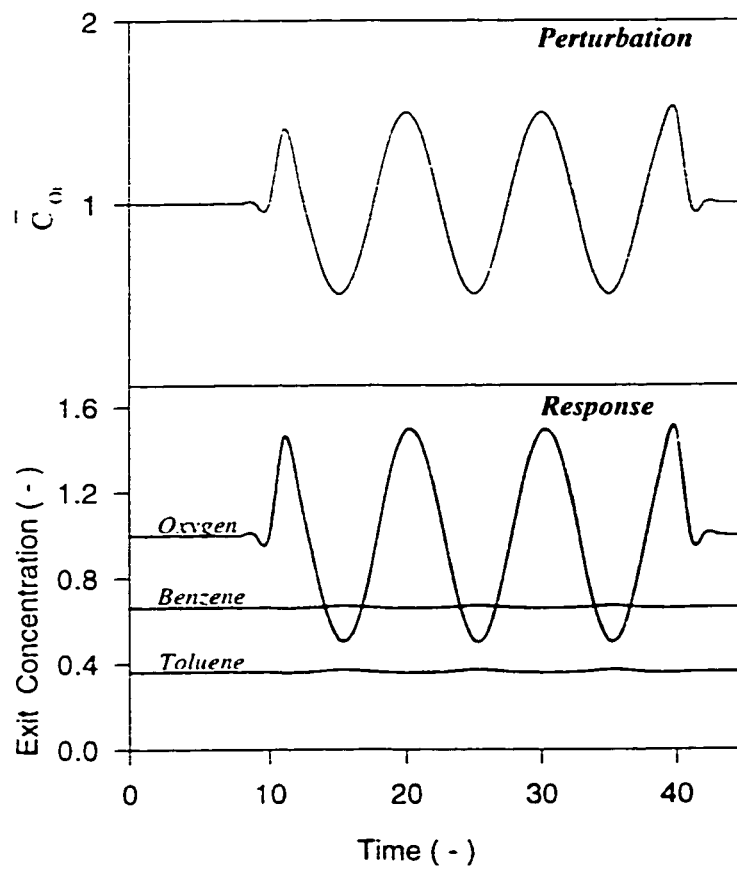


Figure 6.8b: Transient response of the exit concentrations to sinusoidal changes in the inlet oxygen concentration.

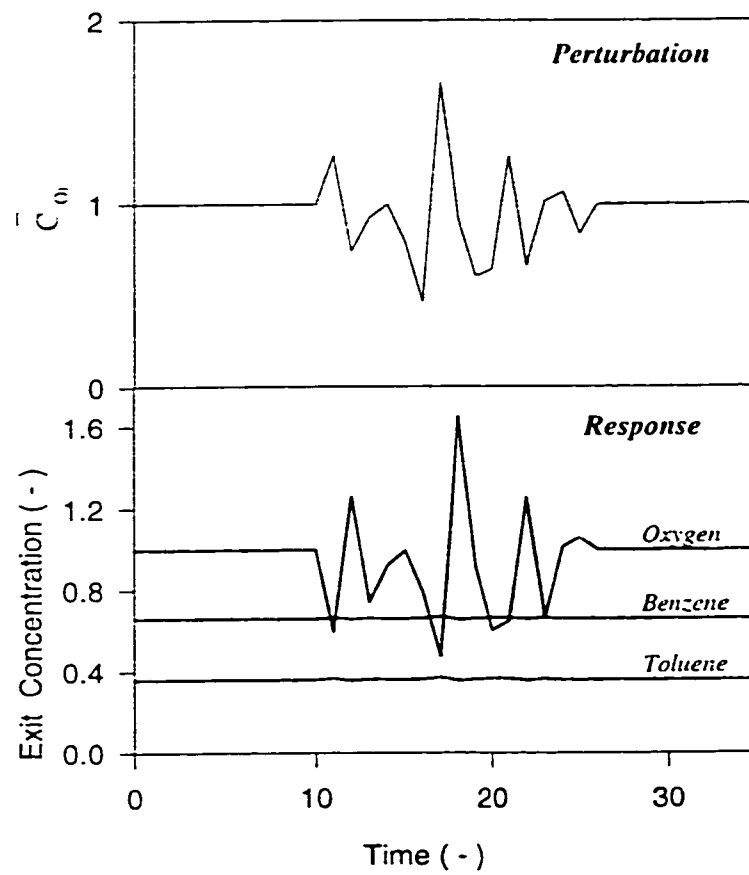


Figure 6.8c: Transient response of the exit concentrations to random perturbations in the inlet oxygen concentration.

6.4 PERTURBATION TO THE TEMPERATURE

Temperature is one of the most important factors affecting both the physiological and biochemical potentials of microbes. The three main temperature ranges used in classification of microbial growth are (i) psychrophilic growth, where the optimum temperature is less than 10 °C (ii) mesophilic growth, where the optimum temperature is between 15 °C to 40 °C and (iii) thermophilic growth, where the optimum temperature is greater than 50 °C. Biofiltration relies predominantly on the activity of mesophilic and, to some extent, thermophilic microorganisms.

An increase in temperature usually enhances the reaction rate, but only within any one of the temperature ranges discussed above. As far as microorganisms are concerned, they exhibit maximum critical temperatures above which growth ceases within 2 or 3 °C. Another important consideration is that operation at high temperatures will shift the population towards thermophilic organisms.

The potential effects of temperature on the biofiltration process include: (i) effect on the maximum specific growth rate of the culture, (ii) effect on the affinity of the bacteria on the growth limiting substrate, (iii) effect on the microbial decay rate, (iv) effect on physical properties like gas solubilities, liquid phase diffusivities and viscosities, equilibrium constants etc., and (v) effect on operational parameters like evaporation of the water from the filter bed.

Optimal temperatures for aerobic compost biofilters have been noted to be between 25 and 40°C, i.e., the mesophilic temperature range (Mueller, 1988). Bohn (1976) suggested that it is critical that biofilter beds do not reach temperatures exceeding 60° C. Thus, for hot streams, it may be necessary to reduce the gas temperature using a heat exchanger upstream of the filter bed.

Figures 6.9a and 6.9b show the effect of triangular and random perturbations in the temperature on the exit toluene concentration for fixed pH and inlet concentration. As can be seen from figure 6.9a for an increase of about 25 C in temperature, the exit concentration drops to nearly zero. The exit concentration passes through a minimum before reaching the steady state condition. The increase in temperature would increase the conversion (or lower the exit concentration), however, this minimum does not correspond to the maximum temperature. The time lag in reaching steady state after the perturbation is also clearly seen. For the case of random perturbations it can be seen that the system responds effectively. It should be noted here that the perturbations to temperature are not given to the inlet gas, rather the effect of perturbations in the biofilm are studied.

Figures 6.10a and 6.10b show the effects of perturbation in the temperature of the system. Because of the Arrhenius type of expression used for temperature, an increase in temperature causes a decrease in the exit concentration.

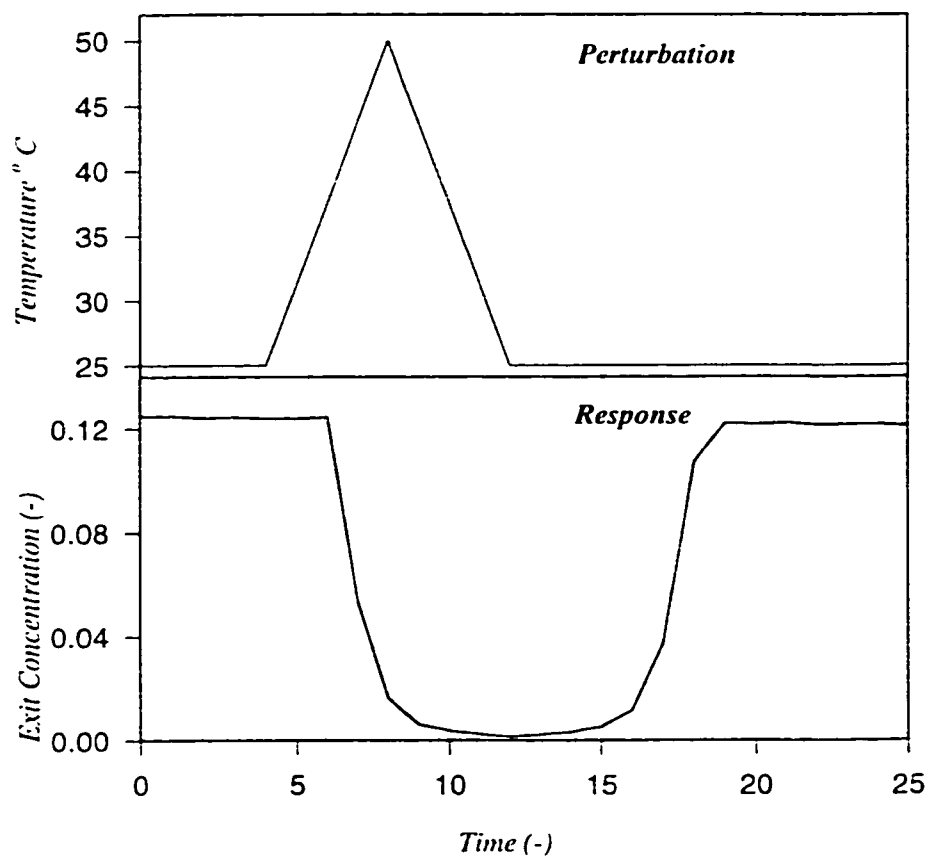


Figure 6.9a: Transient response of the exit toluene concentration to triangular perturbation in the temperature.

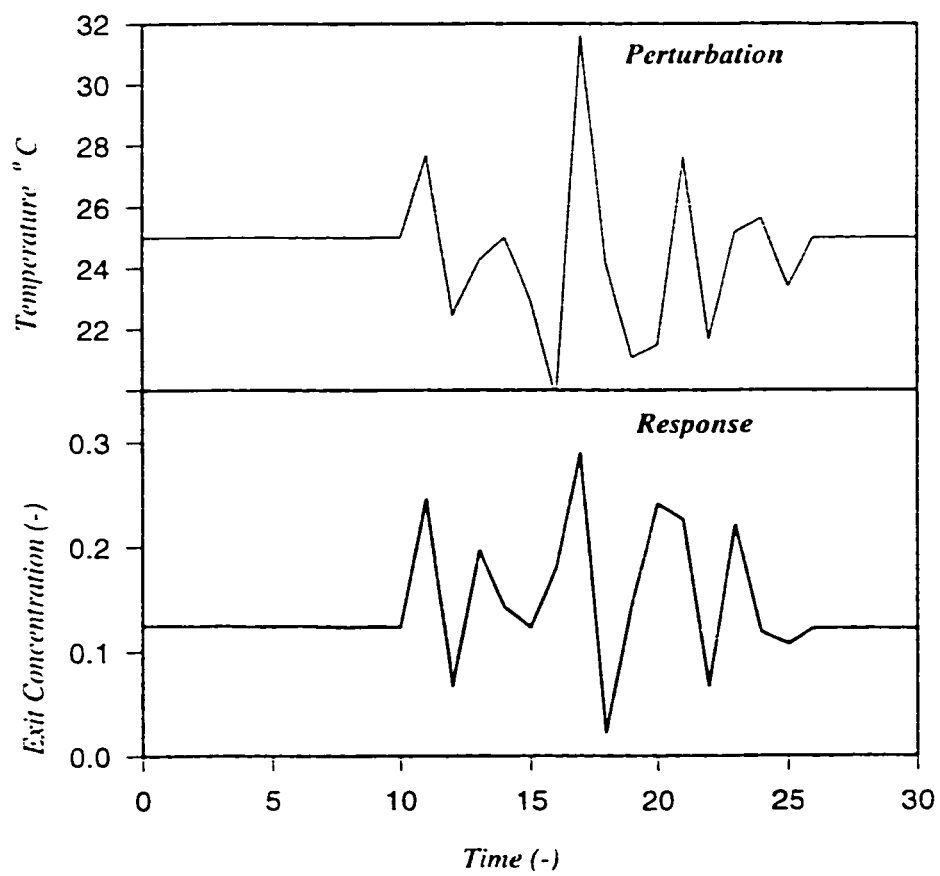


Figure 6.9b: Transient response of the exit toluene concentration to random changes in the temperature of the biofilm.

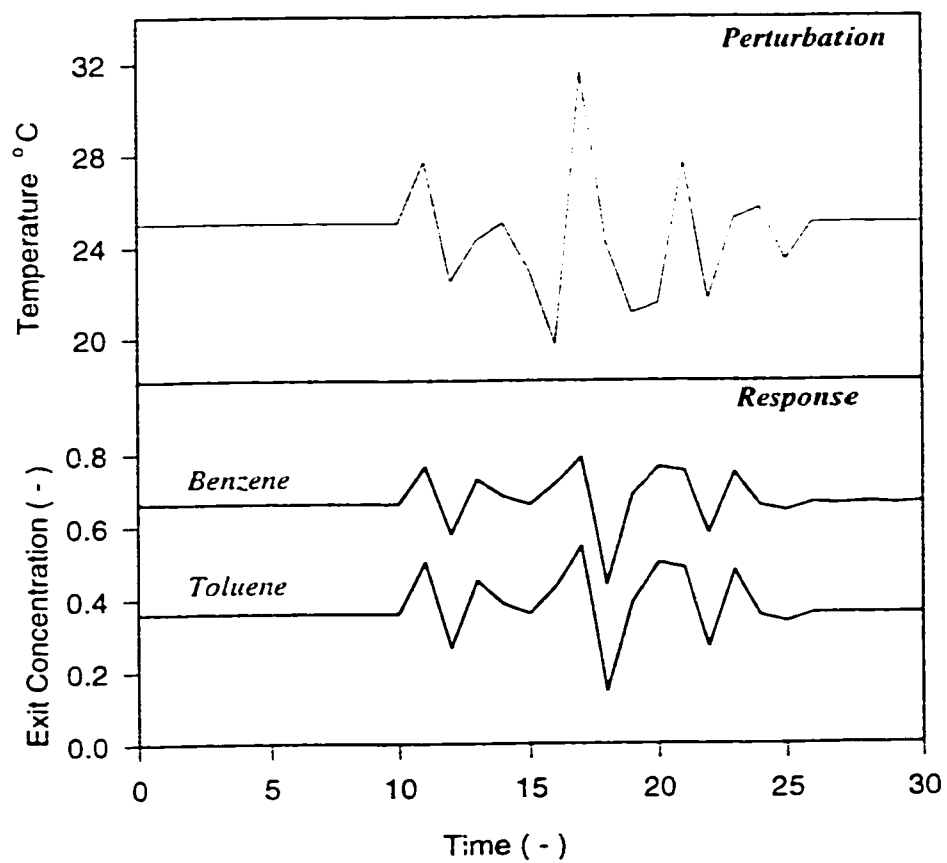


Figure 6.10a: Transient response of the benzene and toluene exit concentrations to random changes in the column temperature.

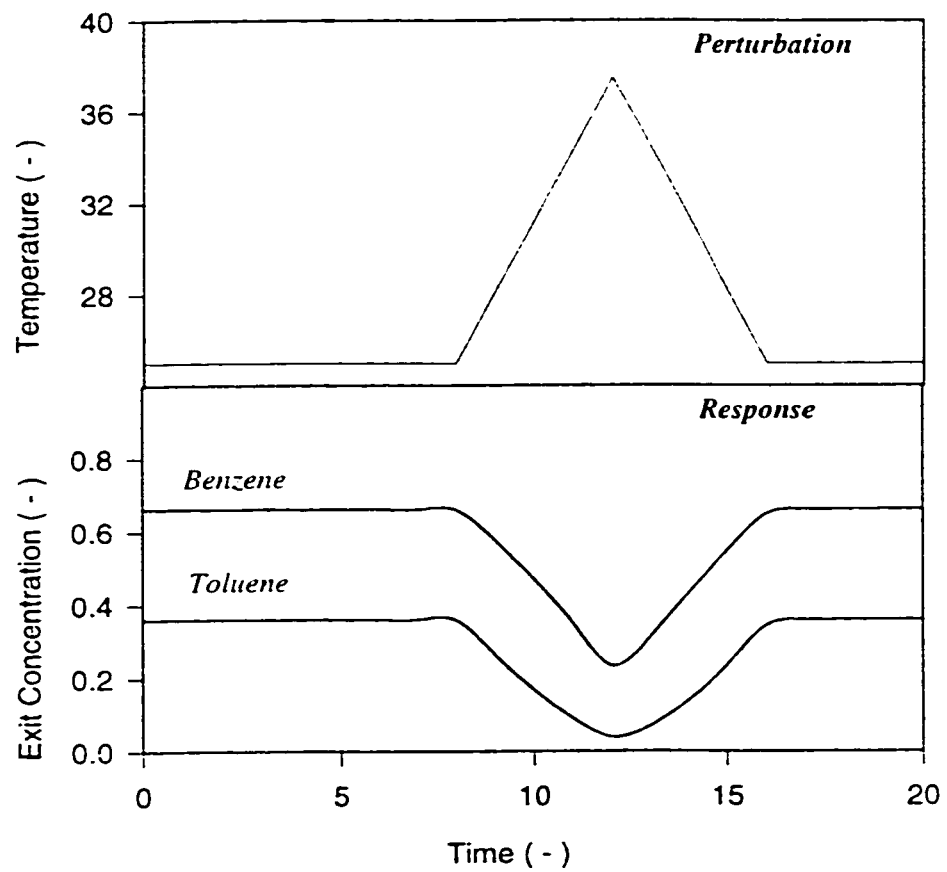


Figure 6.10b: Transient response of the benzene and toluene exit concentrations to triangular change in the column temperature.

6.5 PERTURBATION TO THE pH OF THE SYSTEM

Since most micro-organisms prefer a specific pH range, changes in the pH of the filter material will strongly affect their activity. Mueller (1988) suggested that optimal biofilter performance occurs with a bed pH of 6-8. Leson and Winer (1991) suggested optimal conditions of pH 7-8 for compost biofilters, a range preferred by bacteria and actinomycete. In some cases the biodegradation of air pollutants can generate acidic by-products. The oxidation of sulfur, nitrogen, and chlorine-containing compounds can lead to the formation of acid intermediates which lower bed pH, with a subsequent reduction in VOC removal efficiency. Depending on the type of microorganisms that are present, the resulting drop in the pH can destroy the resident population and reduce, if not eliminate, the filter's degradation capacity. In such cases chemical buffer, such as lime (chalk, marl, oyster shells) are added to buffer the acid production (Ergas et al., 1994; Ottengraf et al., 1983).

Figures 6.11 show the effects of variation of pH on the exit concentration of toluene. In Figure 6.11 a random perturbation is given to the pH of the system which is already operating at a neutral pH of 7 i.e., condition of maximum efficiency. As discussed above, an increase or decrease in the pH leads to lowering the conversion in biological systems. So this explains the Figures 6.11. As also seen, the response is almost synchronized with the perturbation, there is virtually no time lag in the response. This is because, as mentioned earlier, the perturbation

is not given to the inlet , but rather to the conditions in the biofilm. The expression used for the effect of pH is directly related to the kinetic parameters.

Figures 6.12a and 6.12b shows the effect of triangular and random perturbations in pH on the exit benzene and toluene concentrations. It should be noted that the system is already operating at a pH of 7.02 and a triangular increase in the pH is given. As expected there is a drastic decrease in the removal, especially of toluene. The exit concentration of benzene is almost doubled for a pH increase from 7.02 to 11, but the exit concentration of toluene shows a threefold increase.

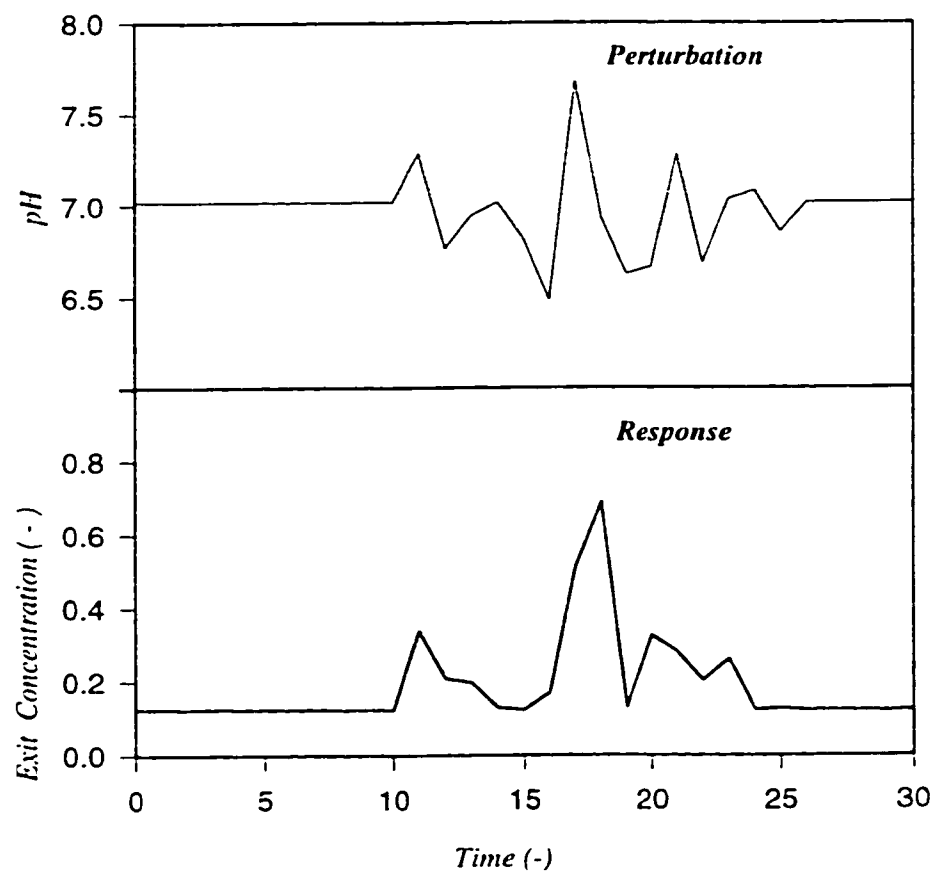


Figure 6.11: Transient response of the exit toluene concentration to random changes in the pH of the system.

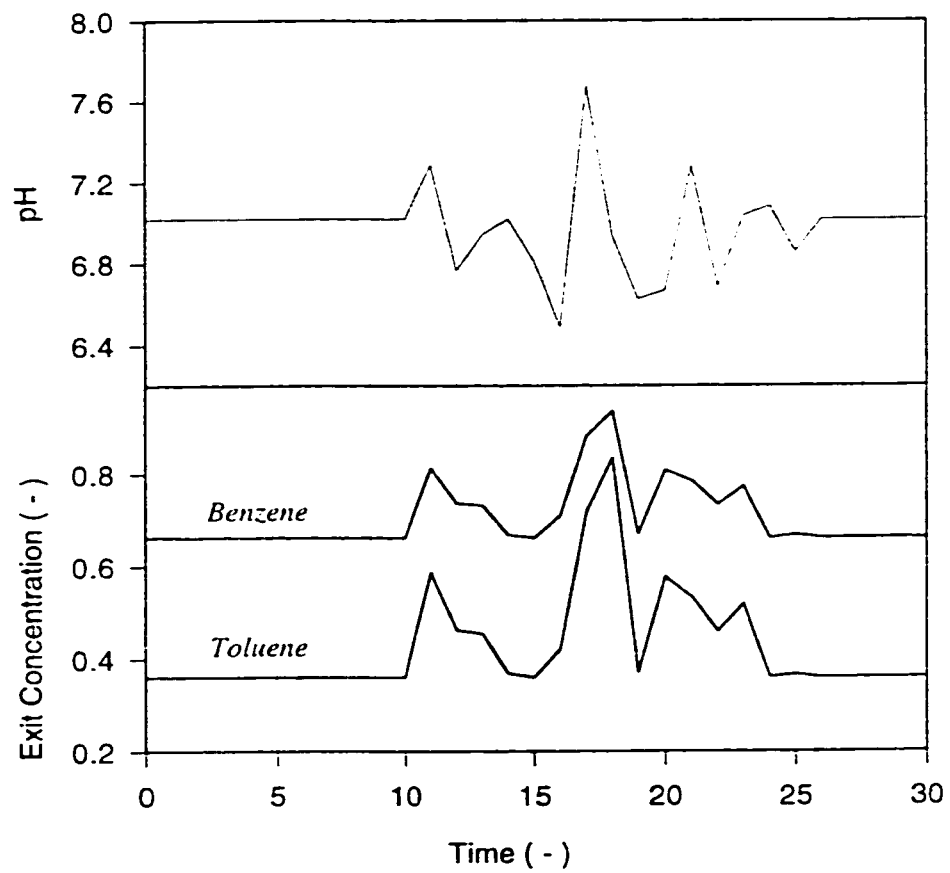


Figure 6.12a: Transient response of the benzene and toluene exit concentrations to random perturbations in the system pH.

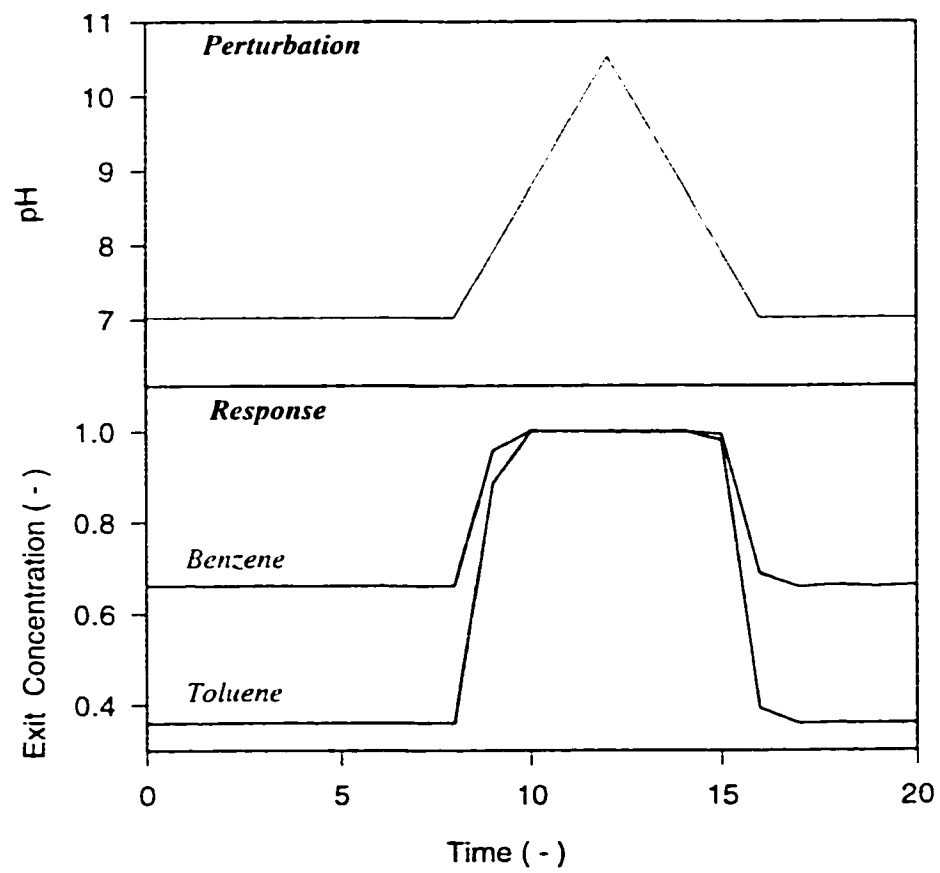


Figure 6.12b: Transient response of the benzene and toluene exit concentrations to triangular change in the system pH.

6.6 PERTURBATION TO THE INLET GAS FLOW RATE

For an existing biofilter, an increase in gas flowrate can have several negative impacts on VOC removal. Large fluctuations in the inlet VOC mass loading can reduce the performance of the biofilter by (1) temporary exceedances of elimination capacity, and /or (2) toxic shock of microorganisms. A sudden but sustained increase in mass loading may require an intermediate acclimation period for microorganisms to 'adapt' to the increased loading. Furthermore, high flowrates results in bed drying and cracking (Bohn, 1976; Barshter et al., 1993).

Figure 6.13 compares the model predictions with the experimental data reported by Tang et al. (1995) for sudden change in the velocity of the inlet gas stream. As explained for Figures 6.1 and 6.2, the data reported is for the packing material compost and the model predictions are based on the data for the packing material peat/perlite mixture. Hence the model prediction is not very accurate. However, the model is able to predict the trend of the exit concentration very well.

Figures 6.14a, 6.14b and 6.14c show the effect of perturbations in the inlet gas flow rate on the toluene exit concentration. As can be seen the exit concentration increases with increase in the inlet flow rate without any observable time lag in the response. The flow rate has a direct impact on the biofiltration of a gas stream. An increase in the flow rate implies a decrease in the residence time of the gas. This results in an increase in the mass transfer resistance in the gas phase further resulting in diffusion limitation in the biofilm. Thus, less substrate is transferred into the biofilm, resulting in lower removal rates.

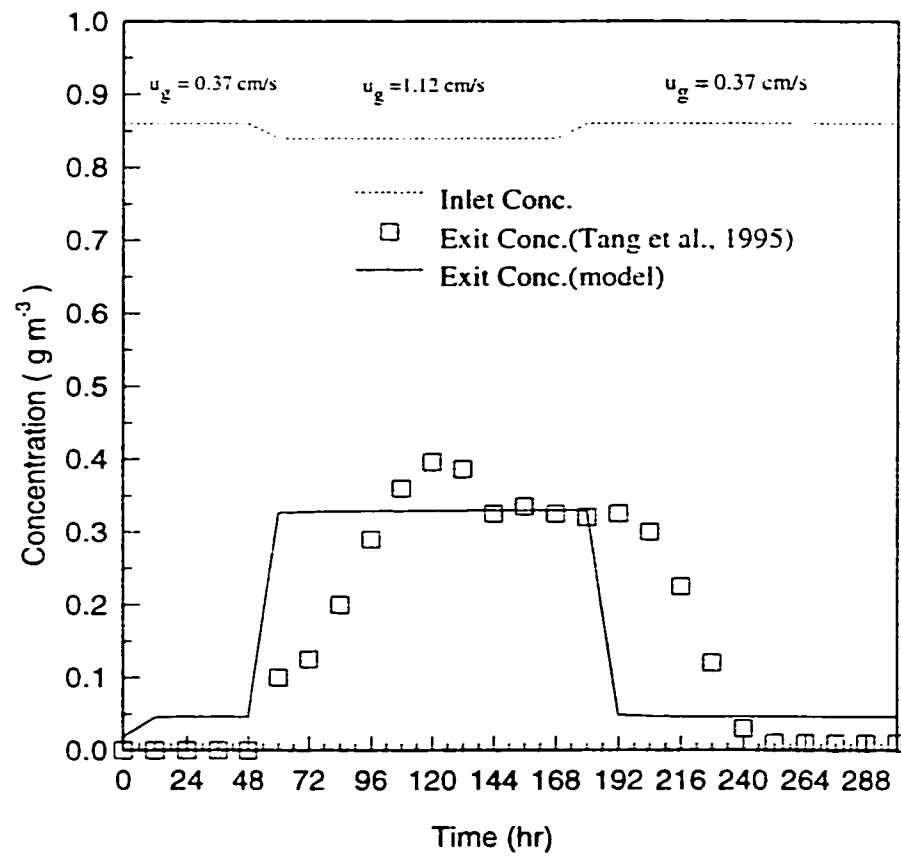


Figure 6.13: Transient response to *abrupt* change in the inlet gas flowrate. Experimental data and Model predictions.

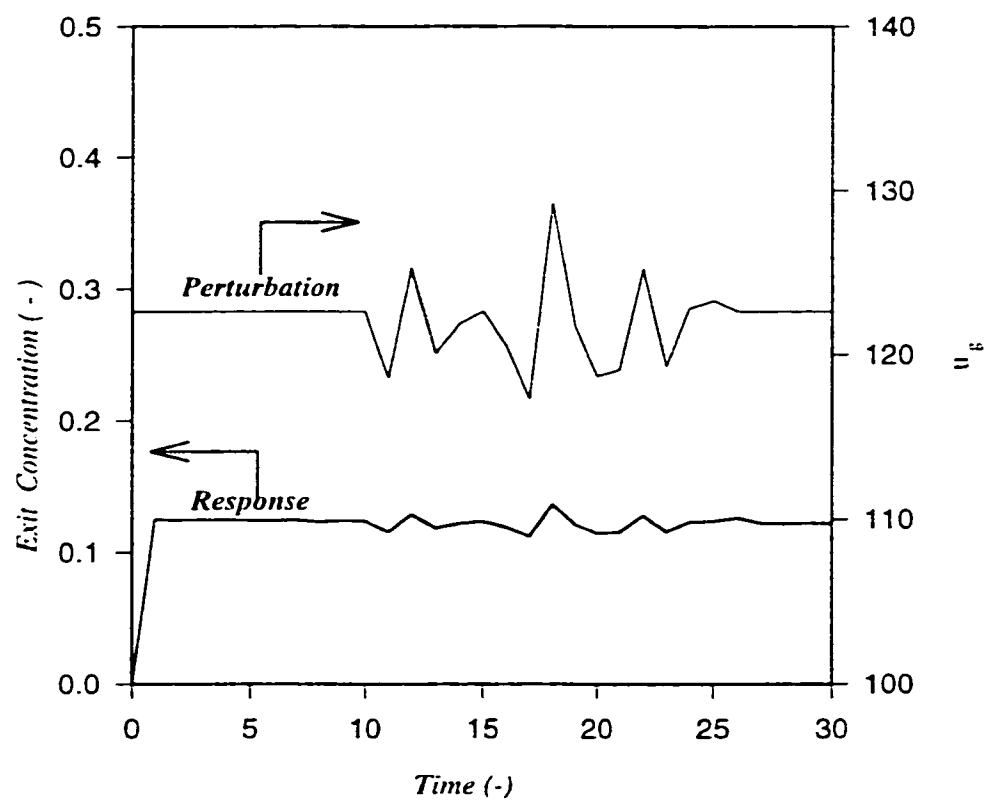


Figure 6.14a: Transient response of the exit toluene concentration to *random* perturbations in the inlet gas flowrate.

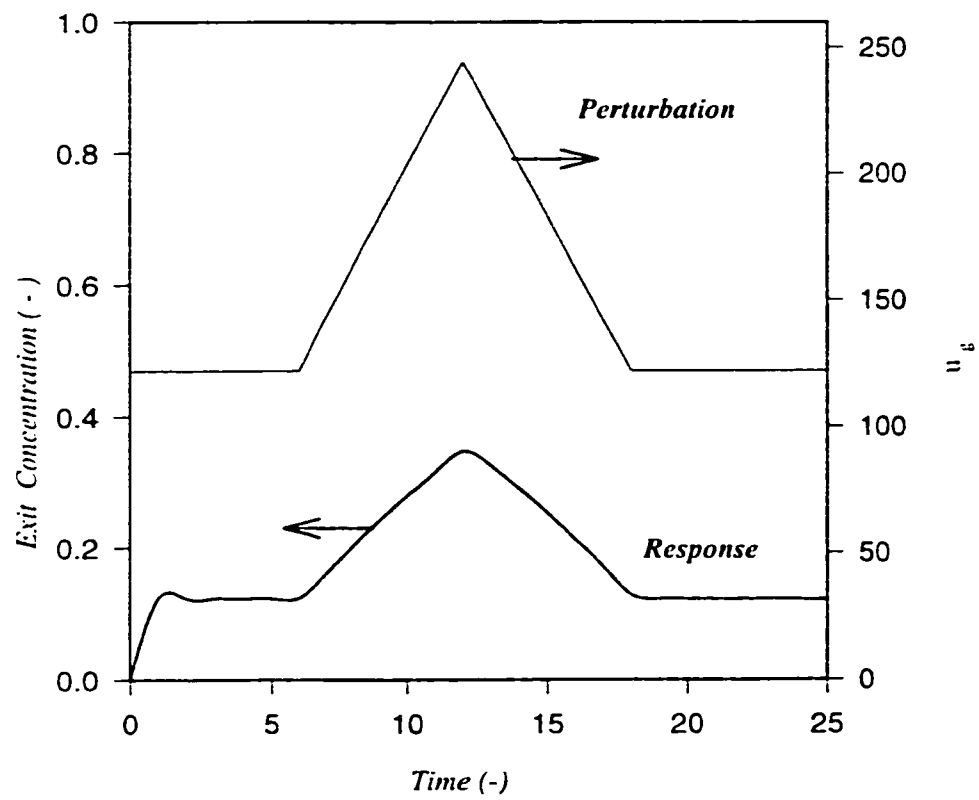


Figure 6.14b: Transient response of the exit toluene concentration to *triangular* perturbations in the inlet gas flowrate.

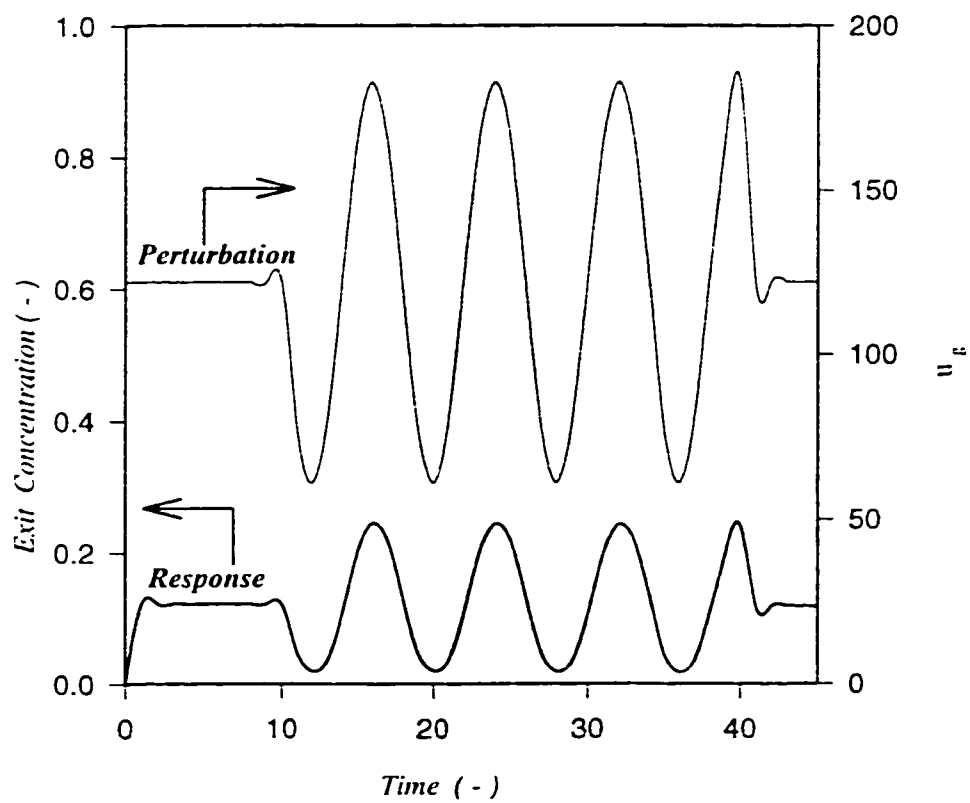


Figure 6.14c: Transient response of the exit toluene concentration to *sinusoidal* perturbations in the inlet gas flowrate.

ASYMPTOTIC STUDY OF THE GENERAL MODEL

In order to verify the generality of our model, asymptotic behavior of the model has been studied. This chapter describes the improvements made in the modeling of the biofiltration process. The general model for the transient biofiltration of mixed VOCs is given below.

$$\frac{\partial S_T}{\partial t} = f(X_V) D_{TW} \frac{\partial^2 S_T}{\partial x^2} - \frac{X_V}{Y_T} \mu_T(S_B, S_T, S_O) \quad (7.1)$$

$$\frac{\partial S_B}{\partial t} = f(X_V) D_{BW} \frac{\partial^2 S_B}{\partial x^2} - \frac{X_V}{Y_B} \mu_B(S_B, S_T, S_O) \quad (7.2)$$

$$\frac{\partial S_O}{\partial t} = f(X_V) D_{OW} \frac{\partial^2 S_O}{\partial x^2} - \frac{X_V}{Y_{OT}} \mu_T(S_B, S_T, S_O) - \frac{X_V}{Y_{OB}} \mu_B(S_B, S_T, S_O) \quad (7.3)$$

$$v \frac{\partial C_T}{\partial t} = D_T v \frac{\partial^2 C_T}{\partial h^2} - u_g \frac{\partial C_T}{\partial h} + f(X_V) D_{TW} \alpha A_s \left(\frac{\partial S_T}{\partial x} \right)_{x=0} - (1 - \alpha) A_s^* k_T (C_T - C_T^*) \quad (7.4)$$

$$v \frac{\partial C_B}{\partial t} = D_B v \frac{\partial^2 C_B}{\partial h^2} - u_g \frac{\partial C_B}{\partial h} + f(X_V) D_{BW} \alpha A_s^* \left(\frac{\partial S_B}{\partial x} \right)_{x=0} - (1-\alpha) A_s^* k_B (C_B - C_B^*) \quad (7.5)$$

$$v \frac{\partial C_O}{\partial t} = D_O v \frac{\partial^2 C_O}{\partial h^2} - u_g \frac{\partial C_O}{\partial h} + f(X_V) D_{OW} \alpha A_s^* \left(\frac{\partial S_O}{\partial x} \right)_{x=0} \quad (7.6)$$

$$(1-v) \rho_P \frac{\partial C_{BP}}{\partial t} = k_B (1-\alpha) A_s^* (C_B - C_B^*) \quad (7.7)$$

$$(1-v) \rho_P \frac{\partial C_{TP}}{\partial t} = k_T (1-\alpha) A_s^* (C_T - C_T^*) \quad (7.8)$$

$$\mu_B(S_B, S_T, S_O) = \frac{\mu_B^* S_B S_O}{(K_B + S_B + K_{BT} S_T)(K_{OB} + S_O)} \quad (7.9)$$

$$\mu_T(S_B, S_T, S_O) = \frac{\mu_T^* S_T S_O}{(K_T + S_T + \frac{S_T^2}{K_{TT}} + K_{TB} S_B)(K_{OT} + S_O)} \quad (7.10)$$

$$C_{TP} = \frac{a_T C_T^*}{1 + b_1 C_T^* + b_2 C_B^*} \quad (7.11)$$

$$C_{BP} = \frac{a_B C_B^*}{1 + b_1 C_T^* + b_2 C_B^*} \quad (7.12)$$

The boundary conditions are as follows:

$$x=0 \quad t > \tau ; h > 0 \quad S_j = \frac{C_j(h)}{m_j} \quad (7.13)$$

$$x=\delta \quad h > 0 ; t > 0 \quad \frac{\partial S_j}{\partial x} = 0 \quad (7.14)$$

$$h=0 \quad t > 0 \quad D_j \frac{\partial C_j}{\partial h} = -u_g (C_j|_{0^-} - C_j|_{0^+})$$

(7.15)

$$h = H \quad t > 0 \quad \frac{\partial C_j}{\partial h} = 0 \quad (7.16)$$

The above set of model equations can be extended to more than two VOCs by including similar equations for each individual component considered. The above model equations can be reduced to the existing models in the literature by applying certain simplifications which are discussed below in this asymptotic study.

7.1 STEADY STATE MODELS

(I) Baltzis and Zarook (1994) model for binary VOC mixtures.

Assumptions:

- Steady State
- Plug flow in the gas phase i.e., no Axial Dispersion or D_B , D_T and $D_O = 0$.

Applying the above simplifying assumptions to equations (7.1 - 7.10), the model equations reduce to the following form :

$$0 = f(X_V) D_{TW} \frac{\partial^2 S_T}{\partial x^2} - \frac{X_V}{Y_T} \mu_T(S_B, S_T, S_O) \quad (7.17)$$

$$0 = f(X_V) D_{BW} \frac{\partial^2 S_B}{\partial x^2} - \frac{X_V}{Y_B} \mu_B(S_B, S_T, S_O) \quad (7.18)$$

$$0 = f(X_V) D_{OW} \frac{\partial^2 S_O}{\partial x^2} - \frac{X_V}{Y_{OT}} \mu_T(S_B, S_T, S_O) - \frac{X_V}{Y_{OB}} \mu_B(S_B, S_T, S_O) \quad (7.19)$$

$$0 = -u_s \frac{\partial C_T}{\partial h} + f(X_V) D_{TW} \alpha A_s^* \left(\frac{\partial S_T}{\partial x} \right)_{x=0} \quad (7.20)$$

$$0 = -u_s \frac{\partial C_B}{\partial h} + f(X_V) D_{BW} \alpha A_s^* \left(\frac{\partial S_B}{\partial x} \right)_{x=0} \quad (7.21)$$

$$0 = -u_s \frac{\partial C_O}{\partial h} + f(X_V) D_{OW} \alpha A_s^* \left(\frac{\partial S_O}{\partial x} \right)_{x=0} \quad (7.22)$$

The assumption of steady state eliminates the terms and equations for the adsorption of the component on the solid surface. This is the steady state model of Baltzis and Zarook (1994) for the biofiltration of VOC mixtures.

(II) Zarook and Baltzis (1994) model for single component

Assumptions:

- Single component $C_{ji} = 0$, where C_{ji} represents the inlet concentration of one of the VOC.
- No kinetic interactions i.e., K_{BT} , $K_{TB} = 0$

Applying the above simplifying assumptions to equations (7.17 - 7.22), the model equations reduce to the following form :

$$0 = f(X_V) D_{jW} \frac{\partial^2 S_j}{\partial x^2} - \frac{X_V}{Y_j} \mu_j(S_j, S_O) \quad (7.23)$$

$$0 = f(X_V) D_{OW} \frac{\partial^2 S_O}{\partial x^2} - \frac{X_V}{Y_{Oj}} \mu_j(S_j, S_O) \quad (7.24)$$

$$0 = -u_s \frac{\partial C_j}{\partial h} + f(X_V) D_{jW} \alpha A_s^* \left(\frac{\partial S_j}{\partial x} \right)_{x=0} \quad (7.25)$$

$$0 = -u_s \frac{\partial C_O}{\partial h} + f(X_V) D_{OW} \alpha A_s^* \left(\frac{\partial S_O}{\partial x} \right)_{x=0} \quad (7.26)$$

This is the model developed by Zarook and Baltzis (1994) for Single component VOC biofiltration.

(III) Ottengraf and Van den Oever (1983)

Assumptions:

- Excess oxygen ; $S_O \gg K_{O_j}$
- Monod Kinetics (reduced to Zero order and First order kinetics under limiting conditions) i.e., $K_{f_j} \rightarrow \infty$. in equations 7.9 & 7.10.

Applying the above simplifying assumptions to equations (7.23 - 7.26), the model equations reduce to the following form :

$$0 = f(X_V) D_{jW} \frac{\partial^2 S_j}{\partial x^2} - \frac{X_V}{Y_j} \mu_j(S_j, S_O) \quad (7.27)$$

$$0 = -u_g \frac{\partial C_j}{\partial h} + f(X_V) D_{jW} \alpha A_s^* \left(\frac{\partial S_j}{\partial x} \right)_{x=0} \quad (7.28)$$

$$\mu_j(S_j) = \frac{\mu_j^* S_j}{(K_j + S_j)} \quad (7.29)$$

$$\text{Case (i) : } S_j \gg K_j \quad \mu_j(S_j) = \frac{\mu_j^* S_j}{(K_j + S_j)} \quad \text{First Order Kinetics}$$

$$\text{Case (i) : } S_j \ll K_j \quad \mu_j(S_j) = \mu_j^* S_j \quad \text{Zero Order Kinetics}$$

This is the steady state biofiltration model developed by Ottengraf and van den Oever (1983).

7.2 TRANSIENT MODELS

(I) General Model for Single Component (Chapter 4)

Assumptions:

- Single Component i.e., $C_{ji} = 0$, where C_{ji} is the concentration of any one of the VOCs.
- Single component kinetics i.e., no kinetic interactions; $K_{BT}, K_{TB} = 0$

Applying the above simplifying assumptions to equations (7.1 - 7.12),

$$\frac{\partial S_j}{\partial t} = f(X_V) D_{jW} \frac{\partial^2 S_j}{\partial x^2} - \frac{X_V}{Y_j} \mu_j(S_j, S_O) \quad (7.30)$$

$$\frac{\partial S_O}{\partial t} = f(X_V) D_{OW} \frac{\partial^2 S_O}{\partial x^2} - \frac{X_V}{Y_O} \mu_j(S_j, S_O) \quad (7.31)$$

$$\begin{aligned} v \frac{\partial C_j}{\partial t} = D_j v \frac{\partial^2 C_j}{\partial h^2} - u_g \frac{\partial C_j}{\partial h} + f(X_V) D_{TW} \alpha A_s^* \left(\frac{\partial S_j}{\partial x} \right)_{x=0} \\ - (1 - \alpha) A_s^* k_j (C_j - C_j^*) \end{aligned} \quad (7.32)$$

$$v \frac{\partial C_O}{\partial t} = D_O v \frac{\partial^2 C_O}{\partial h^2} - u_g \frac{\partial C_O}{\partial h} + f(X_V) D_{OW} \alpha A_s^* \left(\frac{\partial S_O}{\partial x} \right)_{x=0} \quad (7.33)$$

$$(1 - v) \rho_P \frac{\partial C_{jP}}{\partial t} = k_j (1 - \alpha) A_s^* (C_j - C_j^*) \quad (7.34)$$

Monod kinetics (e.g., Benzene)

$$\mu_B(S_B, S_O) = \frac{\mu_B^* S_B S_O}{(K_B + S_B)(K_{OB} + S_O)} \quad (7.35)$$

Andrews kinetics (e.g. Toluene)

$$\mu_T(S_T, S_O) = \frac{\mu_T^* S_T S_O}{(K_T + S_T + \frac{S_T^2}{K_{IT}})(K_{OT} + S_O)} \quad (7.36)$$

7.3 APPROXIMATE MODELS

(I) Approximate Model for Mixtures (Chapter 5)

Assumptions:

- Quasi-steady state in the biofilm.
- Introduce effectiveness factors for the diffusion term in the gas phase equations 7.4, 7.5 & 7.6.

$$\nu \frac{\partial C_T}{\partial t} = D_T \nu \frac{\partial^2 C_T}{\partial h^2} - u_s \frac{\partial C_T}{\partial h} + f(X_V) D_{TW} \alpha A_s^* \left(\frac{\partial S_T}{\partial x} \right)_{x=0} - (1 - \alpha) A_s^* k_T (C_T - C_T^*) \quad (7.37)$$

$$\nu \frac{\partial C_B}{\partial t} = D_B \nu \frac{\partial^2 C_B}{\partial h^2} - u_s \frac{\partial C_B}{\partial h} + f(X_V) D_{BW} \alpha A_s^* \left(\frac{\partial S_B}{\partial x} \right)_{x=0} - (1 - \alpha) A_s^* k_B (C_B - C_B^*) \quad (7.38)$$

$$\nu \frac{\partial C_O}{\partial t} = D_O \nu \frac{\partial^2 C_O}{\partial h^2} - u_s \frac{\partial C_O}{\partial h} + f(X_V) D_{OW} \alpha A_s^* \left(\frac{\partial S_O}{\partial x} \right)_{x=0} \quad (7.39)$$

$$(1 - \nu) \rho_P \frac{\partial C_{BP}}{\partial t} = k_B (1 - \alpha) A_s^* (C_B - C_B^*) \quad (7.40)$$

$$(1 - \nu) \rho_P \frac{\partial C_{TP}}{\partial t} = k_T (1 - \alpha) A_s^* (C_T - C_T^*) \quad (7.41)$$

This is the approximate model for mixtures derived in chapter 6.

(II) Approximate Model for Single Components (Chapter 4)

Assumptions

- Single Component i.e., $C_{ji} = 0$, where C_{ji} is the concentration of any one of the VOCs

- Appropriate adsorption isotherm for the organic substrate. Freundlich isotherm for benzene and toluene obtained by putting $a_j = 0$; $b_1, b_2 = 0$ in eqns 7.11 and 7.12.

Applying the above assumptions to equations 7.37 -7.41 , we get the following set of equations:

$$v \frac{\partial C_j}{\partial t} = D_j v \frac{\partial^2 C_j}{\partial h^2} - u_s \frac{\partial C_j}{\partial h} + \frac{e_j \delta X_v \mu_j \alpha A_s^*}{Y_j} \left(\frac{\partial S_j}{\partial x} \right)_{x=0} - (1-\alpha) A_s^* k_j (C_j - C_j^*) \quad (7.42)$$

$$v \frac{\partial C_o}{\partial t} = D_o v \frac{\partial^2 C_o}{\partial h^2} - u_s \frac{\partial C_o}{\partial h} + \frac{e_j \delta X_v \mu_j \alpha A_s^*}{Y_{oj}} \left(\frac{\partial S_o}{\partial x} \right)_{x=0} \quad (7.43)$$

$$(1-v) \rho_p \frac{\partial C_{jP}}{\partial t} = k_j (1-\alpha) A_s^* (C_j - C_j^*) \quad (7.44)$$

(III) Transient Model (Zarook and Baltzis, 1994)

Assumptions

- No Axial Dispersion in the column i.e., $D_T, D_O = 0$ in equations 7.42 - 7.44.

$$v \frac{\partial C_j}{\partial t} = -u_s \frac{\partial C_j}{\partial h} + \frac{e_j \delta X_v \mu_j \alpha A_s^*}{Y_j} \left(\frac{\partial S_j}{\partial x} \right)_{x=0} - (1-\alpha) A_s^* k_j (C_j - C_j^*) \quad (7.45)$$

$$v \frac{\partial C_o}{\partial t} = -u_s \frac{\partial C_o}{\partial h} + \frac{e_j \delta X_v \mu_j \alpha A_s^*}{Y_{oj}} \left(\frac{\partial S_o}{\partial x} \right)_{x=0} \quad (7.46)$$

$$(1-v) \rho_p \frac{\partial C_{jP}}{\partial t} = k_j (1-\alpha) A_s^* (C_j - C_j^*) \quad (7.47)$$

Thus, it can be seen that our model asymptotically reaches the models of the previous researchers. This is demonstrated in Figure 7.1.

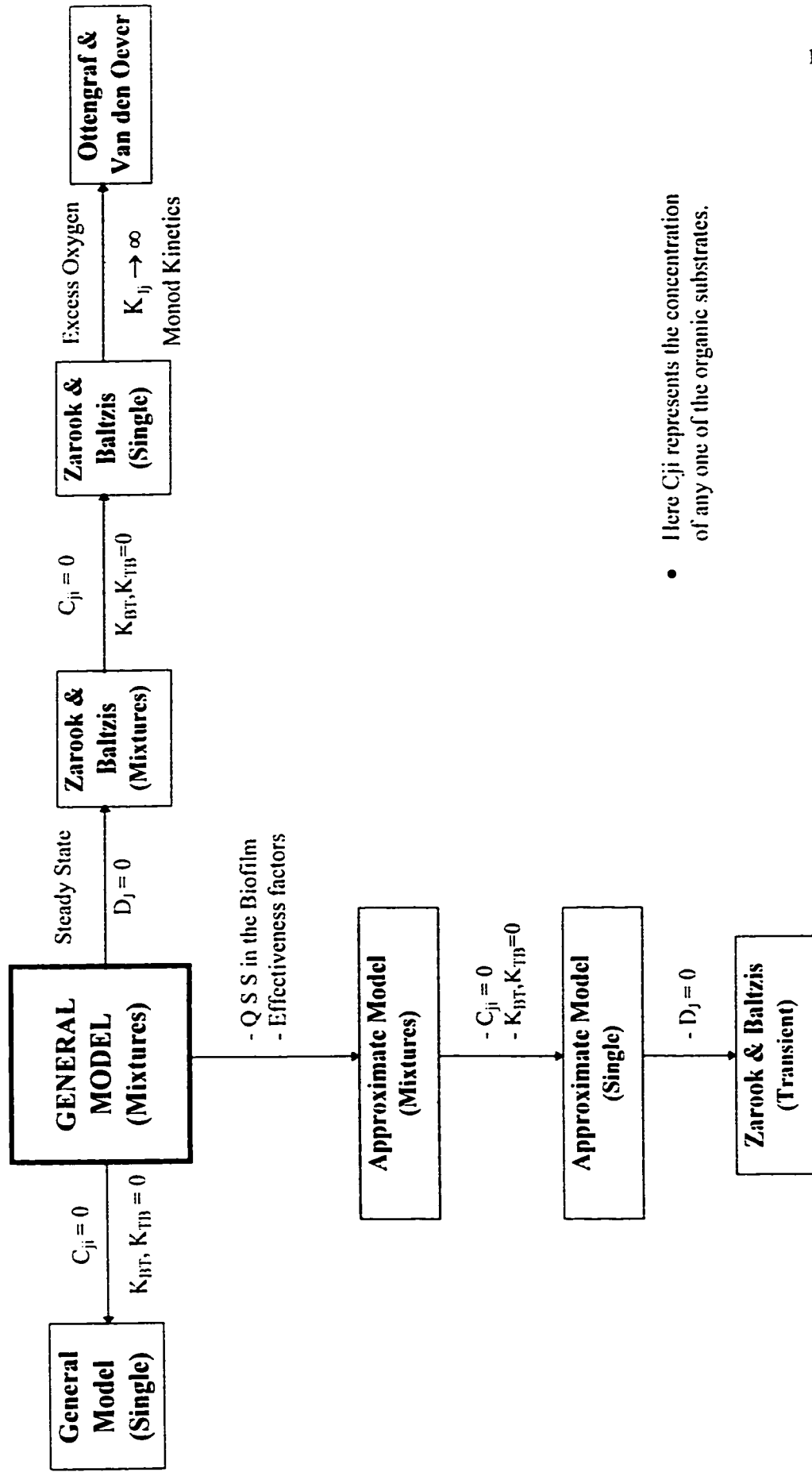


Figure 7.1 : Asymptotic representation of the general model

CONCLUSIONS AND RECOMMENDATIONS

8.1 CONCLUSIONS

Biofiltration is a less expensive and more efficient APC process for treating hazardous VOCs from air streams. A thorough literature review on the modeling of transient biofiltration process shows that theoretical studies are very limited, infact there are only 3 models for the biofiltration of single component VOCs. for the case of VOC Mixtures, there are no transient models available. The existing models are based on a number of restrictive assumptions, hence in the present study a General model which incorporates general mixing phenomena, oxygen limitation aspects, adsorption and general reaction kinetics is developed. For the case of VOC mixtures, kinetic expressions, Monod and Andrews type with kinetic interference between the components are used. Adsorption isotherms are developed and used for describing the process of multicomponent adsorption of the substrates on to the solid surface. Transient models are developed for both single component VOC and binary VOC Mixtures. The model predictions are verified with the experimental results of Zarook (1994) for the biofiltration of benzene and toluene for single component model and benzene - toluene mixtures for mixtures

model. The model can be extended to multi-component VOCs provided the appropriate kinetic and adsorption expressions are known.

The *approximate model* requires correlations for the film thickness and effectiveness factors as in the case of the previous model of Zarook and Baltzis (1994 b) and these correlations are based on the assumption of pseudo-steady-state in the biofilm. Although the *approximate model* is superior to the Plug flow model of Zarook and Baltzis (1994 b) as it includes the mixing phenomena, it is still inferior to the general model. The results show that the predictions by the general model are closer to the actual experimental results.

Studies on oxygen limitation effects show that the assumption of excess oxygen availability is not always true, especially at high inlet gas concentrations. It was found that the inlet oxygen concentration plays an important role in the biofiltration process. It is found to affect the conversion very drastically especially for low relative values. After a certain value of the inlet oxygen concentration, the effects are marginal. Thus, it was found that at low inlet values or high inlet substrate concentrations, oxygen has potential limiting effects on the process.

The relevant dimensionless parameter groups describing the mathematical system were identified and a thorough sensitivity analysis was performed. It is found that the process is very sensitive to some of the model parameters. Hence accurate estimation of these parameters is very important. It is also found that mixing phenomena is very important, thus the plug flow assumption of the previous works is still in question.

The effects of perturbations in the inlet process parameters like the inlet gas concentrations, flowrate, column temperature and pH were studied. The parameters were subjected to different types of perturbations namely triangular, sinusoidal and random. Both the experimental data and model predictions have shown that transient conditions during shut down and restart-up are not very long. Moreover, the theoretical predictions of responses to the perturbations in the operating conditions show that the biofilter is able to withstand extreme conditions commonly encountered in practical applications.

8.2 RECOMMENDATIONS FOR FUTURE WORK

It should be mentioned that this work should be viewed only as a preliminary effort to model the transient biofiltration of mixtures. The model obviously has a few shortcomings and it is very important to recognize these limitations. Hence the following recommendations are made for future studies:

1. The model presented is valid only for a condition when the biofilter is in operation i.e., it does not adequately represent the process during the start-up of a biofilter, during which the biofilm is not fully developed. This becomes a moving boundary problem. This problem has to be studied and incorporated in the present model.
2. Adsorption / desorption processes are of paramount importance and need to be accounted for in detail. In the present model, this phenomenon is incorporated loosely for the uptake of the substrate by the moist packing material. The model should be improved to incorporate the phenomena of substrate diffusion into and out of the solid surface and at the biofilm/solid interface as well.
3. The present model is valid for isothermal conditions. The model should be improved for non-isothermal conditions which are more likely to be encountered in practical applications.
4. A thorough Parameter Sensitivity Analysis shows that some of the model parameters are very sensitive and affect the conversion in the biofilter drastically. Greater care should be taken in measuring these parameters. Hence a thorough work on the Optimization of the biofilter parameters is a must for more efficient results.
5. A thorough experimental study of the RTD in the column needs to be studied.

6. The existence of Multiple Steady States in the process needs to be investigated.
7. The model should be studied to multi-component biofiltration.
8. Since the general model becomes very complex to solve, even with few nodal points, it will be very difficult to use the general model for multi-component biofiltration. Hence the approximate model has to be used in these cases. The approximate model, however, requires correlations for the effectiveness factors and film thickness. Hence a generalized correlation must be developed for these parameters.
9. The assumption of equilibrium at the gas phase - biofilm interface need not be always true. So the model should be improved by considering the mass transfer resistance at the interface.
10. The model could be made more realistic by removing the assumption of constant biofilm density and introducing decay constants in the kinetic expressions.
11. The evolution of carbon dioxide during the biodegradation of the VOCs can also be incorporated in the model.

REFERENCES

- Andrews, J. F., "A Mathematical Model for the Continuous Culture of Microorganisms Utilizing Inhibitory Substrates." *Biotechnol. Bioeng.* 10 (1968): 707-723.
- Baltzis .B. C, and Zarook. S. M, "Biofiltration of VOC Mixtures : Modeling and Pilot Scale Experimental Verification", in Proceedings of the 87th A&WMA Meeting, Paper no. 94-ta260.10P, *Air & Waste Management Association*, Cincinnati, OH, 1994.
- Chang, M. -K., T. C., Voice, and C. S. Criddle, "Kinetics of Competitive Inhibition and Cometabolism in the Biodegradation of Benzene, Toluene, and *p*-Xylene by Two *Pseudomonas* isolates." *Biotechnol. Bioeng.* 41(1993):1057-1065.
- Deshusses, M. A., and I. J. Dunn, "Modeling Experiments on the Kinetics of Mixed-solvent Removal from Waste Gas in a Biofilter", In proceedings of the 6th European Congress on Biotechnology, Florence, June 13-17, 1993.
- Deshusses, M. A., and G. Hamer, "The Removal of Volatile Ketone Mixtures from Air in Biofilters", *Bioprocess Eng.* 9 (1993): 141-146.
- Deshusses, M. A., G. Hamer and I. J. Dunn, 1995, "Behavior of Biofilters for waste air biotreatment I. Dynamic model development", *Environ. Sci. Tech.* 29, 1048.
- Dharmavaram, S., "Biofiltration: A Lean Emissions Abatement Technology," 84th Annual Meeting of the Air & Waste Management Association, Paper No. 91-103.2, Vancouver, BC, June 16-21, 1991.
- Ergas, S. J., E. D. Schroeder, and D. P. Y. Chang, "VOC Emission Control from Wastewater Treatment Facilities Using Biofiltration." 84th Annual Meeting of the Air & Waste Management Association, Paper No. 91-105.4, Vancouver, British Columbia, June 16-21, 1991.
- Ergas, S. J., E. D. Schroeder, and D. P. Y. Chang, "Control of Air Emissions of Dichloromethane, Trichloroethene, and Toluene by Biofiltration." 86th Annual Meeting of the Air & Waste Management Association, Paper No. 93-WA-52B, Denver, CO, June 13-18, 1993.

- Fan, L. -S., K. Fujie, T. -R. Long, and W. -T. Tang, "Characteristics of a Draft Tube Gas-Liquid-Solid Fluidized-Bed Bioreactor with Immobilized Living Cells for Phenol Degradation." *Biotechnol. Bioeng.* 30 (1987): 498-504.
- Fan, L. -S., R. Leyva-Ramos, K. D. Wisecarver, and B. J., Zehner, "Diffusion of Phenol Through a Biofilm Grown on Activated Carbon Particles in a Draft-Tube Three-Phase Fluidized-Bed Bioreactor." *Biotechnol. Bioeng.* 35(1990) : 279-286.
- Harremoes. P. "Biofilm Kinetics", In *WATER POLLUTION MICROBIOLOGY*, Vol.2. Wiley, New York, 1988.
- Hodge. D. and Deviny. J. "Modelling Removal of Air Contaminants by Biofiltration", *J. of Env. Eng.*, 121 (1995) 21.
- Karel, S. F., S. B. Libicki, and C. R. Robertson, "The Immobilization of Whole Cells: Engineering Principles." *Chem. Eng. Sci.* 40 (1985): 1321-1354.
- Leson, G., and A. M. Winer, "Biofiltration: an Innovative Air Pollution Control Technology for VOC Emissions. *J Air & Waste Manage. Assoc.* 41(1991): 1045-1054.
- Monod, J., *Recherches sur la Croissance des Cultures Bacteriennes*, Hermann et Cie, Paris, 1942.
- Oh, Y. -S., *Biofiltration of Solvent Vapors from Air*, Ph.D. Thesis, Rutgers University, New Brunswick, NJ, 1993.
- Ottengraf, S. P. P., "Exhaust Gas Purification." pp. 425-452. In: *Biotechnology*, W. Shonborn (ed.), vol. 8. VCH Verlagsgesellschaft, Weinheim, Germany, 1986.
- Ottengraf, S. P. P., "Biological Systems for Waste Gas Elimination." *Trends Biotechnol.* 5 (1987): 132-136.
- Ottengraf, S. P. P., J. J. P. Meesters, A. H. C. van den Oever, and H. R. Rozema, "Biological Elimination of Volatile Xenobiotic Compounds in Biofilters." *Bioprocess Eng.* 1 (1986): 61-69.

- Ottengraf, S. P. P., and A. H. C. van den Oever, "Kinetics of Organic Compound Removal from Waste Gases with a Biological Filter." *Biotechnol. Bioeng.* 25 (1983): 3089-3102.
- Ottengraf, S. P. P., A. H. C. van Den Oever, and F. J. C. M. Kempenaars, "Waste Gas Purification in a Biological Filter Bed." In: *Innovations in Biotechnology*, Elsevier Science Publications, Amsterdam, 1983.
- Perry, R. H., and Chilton, C. H., *Perry's Chemical Engineers' Handbook*, McGraw-Hill Inc., New York, 1973.
- Potter, T. L., "Fingerprinting Petroleum Products: Unleaded Gasolines." pp. 83-92. In: *Petroleum Contaminated Soils*, Vol. 3, P.T. Kosteki and E.J. Calabrese, (Eds.), Lewis Publishers, Chelsea, MI, 1992.
- Reisch, M. S., "Top 50 Chemicals Production Stagnated Last Year." *Chem. Eng. News* 70 (15)(1992):16-22.
- Rittman, B. E., and McCarty, P. L., "Model of Steady State Biofilm Kinetics", *Biotechnol. Bioeng.*, 22 (1980) 2343.
- Ruthven, D. M., *PRINCIPLES OF ADSORPTION AND ADSORPTION PROCESSES*, John Wiley & Sons, New York, 1994.
- Tang, H., Hwang, S., and Hwang, S., "Dynamics of Toluene Degradation in Biofilters", *Haz. Waste & Haz. Matls.*, 12 (1995) 207.
- Tang, W. -T., K. Wisecarver, and L. -S. Fan, "Dynamics of a Draft Tube Gas-Liquid-Solid Fluidized Bed Bioreactor for Phenol Degradation." *Chem. Eng. Sci.* 42(1987): 2123-2134.
- Tong, C. C., and L. -S. Fan, "Concentration Multiplicity in a Draft Tube Fluidized-Bed Bioreactor Involving Two Limiting Substrates." *Biotechnol. Bioeng.* 31(1988): 24-34.
- Utgikar, V., R. Govind, Y. Shan, S. Safferman, and R. C. Brenner, "Biodegradation of Volatile Organic Chemicals in a Biofilter." pp.233-260. In *Emerging Technologies*

in Hazardous Waste Management II, D.W. Tedder and F. G. Pokland, (Eds.) ACS Symposium Series 468, Washington, DC, 1991.

van Lith, C., S. L. David, and R. Marsh, "Design Criteria for Biofilters." *Trans. IChemE*. 68(1990.): 127-132.

van Lith, C.. "Biofiltration, An Essential Technique in Air Pollution Control." Proceedings of the 8th World Clean Air Congress, pp 393-399, In: *Man and his Ecosystem*, L.J. Brasser and W.C. Mulder (Eds)., Elsevier Publishers B.V., Amsterdam, 1989.

Zarook. S. M, Baltzis. B. C, Oh. Y. S and Bartha. R, "Biofiltration of Methanol Vapor", *Biotechnology and Bioengineering*, 41 (1993) 512-524.

Zarook. S. M, "Engineering Analysis of a Packed-Bed Biofilter for Removal of VOC (Volatile Organic Compound) Emissions", Ph.D. Dissertation, New Jersey Institute of Technology, 1994.

Zarook. S. M, and Baltzis. B. C, "Biological Removal of Hydrophobic Solvent Vapors from Airstreams", pp. 397-404, In *ADVANCES IN BIOPROCESS ENGINEERING*, E. Galindo and O. T. Ramirez, (Eds.), Kluwer Academic Publishers, Dordrecht, The Netherlands, 1994 a.

Zarook. S. M, and Baltzis. B. C, "Biofiltration of Toluene Vapor Under Steady-State and Transient Conditions : Theory and Experimental Results", *Chemical Engineering Science*, 49, (1994 b), 4347.

Zilli, M., A. Converti, A. Lodi, M. Del Borghi, and G. Ferraiolo, "Phenol Removal From Waste Gases with a Biological Filter by *Pseudomonas Putida*." *Biotechnol. Bioeng.* 41 (1993): 693-699.

APPENDIX A

The final model equations are discretized by orthogonal collocation as follows. Here N represents the number of collocation points along the biofilter height for which, A and B are the collocation matrices. The variable I varies from 1 to $N+2$. M represents the number of collocation points along the biofilm depth and AA and BB are the corresponding collocation matrices. The variable I varies from 1 to $N+2$ and L varies from 1 to $M+2$.

APPROXIMATE MODEL

PDE for the VOC in the Gas phase (Equation 5.8)

$$\begin{aligned} \text{CPRIME}(I) = & \frac{1}{\text{Pe}_j} \sum_{k=1}^{N+2} B(I, k) \cdot C(k) - \frac{1}{v} \sum_{k=1}^{N+2} A(I, k) \cdot C(k) \\ & + \beta_1 \frac{C(I) C(I + (N + 2)) \epsilon_T \epsilon_0}{(1 + C(I) \epsilon_T + C(I)^2 \epsilon_T^2 \gamma)(1 + C(I + (N + 2)) \epsilon_0)} \\ & - \chi (C(I) - \psi_j C(I + 2 * (N + 2)))^{\frac{1}{n_j}} \end{aligned} \quad (\text{A-1})$$

$$\text{where. } \beta_1 = \frac{(0.03C(I) + 0.2)(1.5C(I) + 33.4)X_v \alpha A_s^* H \mu_j^*}{Y_j u_g C_{ji} v} \quad (\text{A-2})$$

Boundary Condition 2 for PDE 1 (Equation 5.16 ; J = VOC)

$$C(N + 2) = \frac{-A(N + 2, 1) \left(\sum_{k=1}^{N+2} C(k) A(1, k) + \text{Pe}_T C_T^0 \right) - (\text{Pe}_T - A(1, 1)) \sum_{k=1}^{N+2} C(k) A(N + 2, k)}{A(1, N + 2) A(N + 2, 1) + (\text{Pe}_T - A(1, 1)) A(N + 2, N + 2)} \quad (\text{A-3})$$

Boundary Condition 2 for the above PDE (Equation 5.15 ,J = VOC)

$$C(1) = - \frac{\sum_{k=1}^{N+2} C(k) A(N + 2, k) + C(N + 2) A(N + 2, N + 2)}{A(N + 2, 1)} \quad (\text{A-4})$$

PDE for the Oxygen in the Gas phase (Equation 5.9)

$$\begin{aligned} \text{CPRIME}(I + N + 2) = & \frac{1}{\text{Pe}_O} \sum_{k=1}^{N+2} B(I, k) C(k + (N + 2)) - \frac{1}{v} \sum_{k=1}^{N+2} A(I, k) C(k + (N + 2)) \\ & + \beta_2 \frac{C(I) C(I + (N + 2)) \epsilon_T \epsilon_O}{(1 + C(I + N + 2)) \epsilon_T + C(I + N + 2)^2 \epsilon_T^2 \gamma (1 + C(I + (N + 2))) \epsilon_O} \end{aligned}$$

$$\text{where, } \beta_1 = \frac{(0.03C(I) + 0.2)(15C(I) + 33.4)X_v \alpha A_s^* H \mu_j}{Y_{O_2} u_g C_{O_2} v} \quad (\text{A-5})$$

Boundary Condition 1 for PDE 2 (Equation 5.16 ,J = Oxygen)

$$\text{C}(2(N + 2)) = \frac{-A(N + 2, I) \left(\sum_{K=1}^{N+2} C(K + (N + 2)) A(I, K) + \text{Pe}_O C_O^0 \right) - (\text{Pe}_O - A(I, I)) \sum_{K=1}^{N+2} C(K + (N + 2)) A(N + 2, K)}{A(I, N + 2) A(N + 2, I) + (\text{Pe}_O - A(I, I)) A(N + 2, N + 2)}$$

(A-6)

Boundary Condition 2 for PDE 2 (Equation 5.15 ,J = Oxygen)

$$\text{C}(1 + N + 2) = - \frac{\sum_{K=1}^{N+2} C(K + (N + 2)) A(N + 2, K) + \text{C}(2(N + 2)) A(N + 2, N + 2)}{A(N + 2, I)} \quad (\text{A-7})$$

ODE for the VOC adsorbed on the Solid (Equation 5.10)

$$\text{CPRIME}(I + 3(N + 2)) = \chi (C(I) - \psi_j C(I + 3(N + 2))^{\frac{1}{N}}) \quad (\text{A-8})$$

GENERAL MODEL

PDE for the VOC in the Biofilm (Equation 5.17)

$$\begin{aligned} \text{CPRIME}(I + (2 + L)(N + 2)) &= \phi_1 \sum_{K=1}^{M+2} \text{BB}(L, K) \text{C}(I + (2 + K)(N + 2)) \\ &\quad - \phi_2 \text{g}(\text{C}(I + (2 + L)(N + 2)), \text{C}(I + (M + 4 + L)(N + 2))) \end{aligned} \quad (\text{A-9})$$

Boundary Condition 1 for PDE 1 (Equation 5.22 ,J = VOC)

$$\text{C}(I + 3 * (N + 2)) = \epsilon_T \text{C}(I) \quad (\text{A-10})$$

Boundary Condition 2 for PDE 1 (Equation 5.23 ,J = VOC)

$$\text{C}(I + (M + 4)(N + 2)) = - \frac{\sum_{K=1}^{M+2} \text{AA}(M + 2, K) \text{C}(I + (2 + K)(N + 2))}{\text{AA}(M + 2, M + 2)} \quad (\text{A-11})$$

PDE for the Oxygen in the Biofilm (Equation 5.18)

$$\begin{aligned} \text{CPRIME}(I + (M + 4 + L)(N + 2)) &= \phi_3 \sum_{K=1}^{M+2} \text{BB}(L, K) \text{C}(I + (M + 4 + K)(N + 2)) \\ &\quad - \phi_4 \text{g}(\text{C}(I + (2 + L)(N + 2)), \text{C}(I + (M + 4 + L)(N + 2))) \end{aligned} \quad (\text{A-12})$$

Boundary Condition 1 for PDE 2 (Equation 5.22 ,J = Oxygen)

$$\text{C}(I + (M + 5)(N + 2)) = \epsilon_o \text{C}(I + N + 2) \quad (\text{A-13})$$

Boundary Condition 2 for PDE 2 (Equation 5.23 ,J = Oxygen)

$$\text{C}(I + (2M + 6)(N + 2)) = - \frac{\sum_{K=1}^{M+2} \text{AA}(M + 2, K) \text{C}(I + (M + 4 + K)(N + 2))}{\text{AA}(M + 2, M + 2)} \quad (\text{A-14})$$

PDE 3 for the VOC in the Gas Phase (Equation 5.24)

$$\begin{aligned}
 \text{CPRIME}(I) = & \frac{1}{\text{Pe}_j} \sum_{k=1}^{N+2} B(I, k) \cdot C(k) - \frac{1}{v} \sum_{k=1}^{N+2} A(I, k) \cdot C(k) \\
 & + \beta_3 \sum_{k=1}^{N+2} AA(I, k) \cdot C(I + (k+2)(N+2)) \\
 & - \chi (C(I) - \psi_j C(I + 2(N+2)))^{\frac{1}{N}}
 \end{aligned} \tag{A-15}$$

PDE 4 for the Oxygen in the Gas Phase (Equation 5.25)

$$\begin{aligned}
 \text{CPRIME}(I + N + 2) = & \frac{1}{\text{Pe}_O} \sum_{k=1}^{N+2} B(I, k) \cdot C(k + (N+2)) - \frac{1}{v} \sum_{k=1}^{N+2} A(I, k) \cdot C(k + (N+2)) \\
 & + \beta_4 \sum_{k=1}^{N+2} AA(I, k) \cdot C(I + (M+4+k)(N+2))
 \end{aligned} \tag{A-16}$$

APPENDIX B

$$CTS = \frac{C(I+3(N+2))(1 + \frac{\lambda_{2B} C(I+4(N+2))}{(\lambda_{1B} - \lambda_{2B} C(I+4(N+2)))}}{\lambda_{1T} - \lambda_{2T} C(I+3(N+2)) - \frac{\lambda_{2T} \lambda_{2B} C(I+4(N+2))}{(\lambda_{1B} - \lambda_{2B} C(I+4(N+2)))}} \quad (B-1)$$

$$CBS = \frac{C(I+4(N+2))(1 + \lambda_{2T} CTS)}{\lambda_{1B} - \lambda_{2B} C(I+4(N+2))} \quad (B-2)$$

PDE FOR THE TOLUENE IN THE GAS PHASE (EQUATION 5.12)

$$CPRIME(I) = -\frac{1}{v} \sum_{K=1}^{N+2} A(I,K).C(K) + \frac{1}{Pe_T} \sum_{K=1}^{N+2} B(I,K).C(K) + \beta_{1T} g_T(C(I), C(I+N+2), C(I+2(N+2))) - \chi_T (C(I) - CTS) \quad (B-3)$$

BOUNDARY CONDITION 2 FOR PDE 1 (EQUATION 5.23)

$$C(N+2) = \frac{-A(N+2,1) \left(\sum_{K=1}^{N+1} C(K)A(I,K) + Pe_T C_T^0 \right) - (Pe_T - A(1,1)) \sum_{K=1}^{N+1} C(K)A(N+2,K)}{A(1,N+2)A(N+2,1) + (Pe_T - A(1,1))A(N+2,N+2)} \quad (B-4)$$

BOUNDARY CONDITION 2 FOR PDE 1 (EQUATION 5.24)

$$C(I) = -\frac{\sum_{K=1}^{N+1} C(K)A(N+2,K) + C(N+2)A(N+2,N+2)}{A(N+2,1)} \quad (B-5)$$

PDE FOR THE BENZENE IN THE GAS PHASE (EQUATION 5.13)

$$CPRIME(I+N+2) = -\frac{1}{v} \sum_{K=1}^{N+2} A(I,K).C(I+N+2) + \frac{1}{Pe_B} \sum_{K=1}^{N+2} B(I,K).C(I+N+2) + \beta_{1B} g_B(C(I), C(I+N+2), C(I+2(N+2))) - \chi_B (C(I+N+2) - CBS) \quad (B-6)$$

BOUNDARY CONDITION 2 FOR PDE 2 (EQUATION 5.24)

$$C(2(N+2)) = \frac{-A(N+2,1) \left(\sum_{K=1}^{N+1} C(I+N+2).A(1,K) + Pe_B C_B^0 \right) - (Pe_B - A(1,1)) \sum_{K=1}^{N+1} C(I+N+2).A(N+2,K)}{A(1,N+2)A(N+2,1) + (Pe_B - A(1,1))A(N+2,N+2)}$$

(B-7)

BOUNDARY CONDITION 1 FOR PDE 2 (EQUATION 5.23)

$$C(1+N+2) = - \frac{\sum_{K=1}^{N+1} C(I+N+2).A(N+2,K) + C(2(N+2))A(N+2,N+2)}{A(N+2,1)}$$

(B-8)

PDE FOR THE OXYGEN IN THE GAS PHASE (EQUATION 5.14)

$$\begin{aligned} \text{CPRIME}(I+2(N+2)) = & -\frac{1}{v} \sum_{K=1}^{N+2} A(I,K).C(I+2(N+2)) + \frac{1}{Pe_O} \sum_{K=1}^{N+2} B(I,K).C(I+2(N+2)) + \\ & -\beta_{2T} g_T(C(I), C(I+N+2), C(I+2(N+2))) - \beta_{2B} g_B(C(I), C(I+N+2), C(I+2(N+2))) \end{aligned}$$

(B-9)

BOUNDARY CONDITION 2 FOR PDE 3 (EQUATION 5.24)

$$C(3(N+2)) = \frac{-A(N+2,1) \left(\sum_{K=1}^{N+1} C(I+2(N+2)).A(1,K) + Pe_O C_O^0 \right) - (Pe_O - A(1,1)) \sum_{K=1}^{N+1} C(I+2(N+2)).A(N+2,K)}{A(1,N+2)A(N+2,1) + (Pe_O - A(1,1))A(N+2,N+2)}$$

(B-10)

BOUNDARY CONDITION 1 FOR PDE 3 (EQUATION 5.23)

$$C(1+2(N+2)) = - \frac{\sum_{K=1}^{N+1} C(I+2(N+2)).A(N+2,K) + C(3(N+2))A(N+2,N+2)}{A(N+2,1)}$$

(B-11)

ODE FOR THE TOLUENE IN THE SOLID PHASE (EQUATION 5.15)

$$\text{CPRIME}(I+3(N+2)) = \chi_T (C(I) - \text{CTS})$$

(B-12)

ODE FOR THE BENZENE IN THE SOLID PHASE (EQUATION 5.16)

$$\text{CPRIME}(I+4(N+2)) = \chi_B (CT - \text{CBS})$$

(B-13)

GENERAL MODEL

PDE FOR THE TOLUENE IN THE BIOFILM (EQUATION 5.25)

$$\begin{aligned}
 \text{CPRIME}(I+(4+J)(N+2)) &= \phi_{iT} \sum_{K=1}^{M=2} \text{BB}(J,K) \text{C}(I+(4+K)(N+2)) \\
 &- \eta_{iT} g_3(\text{C}(I+(4+J)(N+2)), \text{C}(I+(J+M+6)(N+2)), \text{C}(I+(J+2M+8)(N+2)))
 \end{aligned}
 \tag{B-14}$$

BOUNDARY CONDITION 1 FOR PDE 1 (EQUATION 5.31)

$$\text{C}(I+5*(N+2)) = \epsilon_T \text{C}(I)
 \tag{B-15}$$

BOUNDARY CONDITION 2 FOR PDE 1 (EQUATION 5.32)

$$\text{C}(I+(M+6)(N+2)) = - \frac{\sum_{K=1}^{M-1} \text{AA}(M+2, K) \text{C}(I+(4+K)(N+2))}{\text{AA}(M+2, M+2)}
 \tag{B-16}$$

PDE FOR BENZENE IN THE BIOFILM (EQUATION 5.26)

$$\begin{aligned}
 \text{CPRIME}(I+(M+6+J)(N+2)) &= \phi_{iB} \sum_{K=1}^{M=2} \text{BB}(J,K) \text{C}(I+(M+6+K)(N+2)) \\
 &- \eta_{iB} g_4(\text{C}(I+(J+4)(N+2)), \text{C}(I+(J+M+6)(N+2)), \text{C}(I+(J+2M+8)(N+2)))
 \end{aligned}
 \tag{B-17}$$

BOUNDARY CONDITION 1 FOR PDE 2 (EQUATION 5.31)

$$\text{C}(I+(M+7)(N+2)) = \epsilon_B \text{C}(I+N+2)
 \tag{B-18}$$

BOUNDARY CONDITION 2 FOR PDE 2 (EQUATION 5.32)

$$\text{C}(I+(2M+8)(N+2)) = - \frac{\sum_{K=1}^{M-1} \text{AA}(M+2, K) \text{C}(I+(M+6+K)(N+2))}{\text{AA}(M+2, M+2)}
 \tag{B-19}$$

PDE FOR THE OXYGEN IN THE BIOFILM (EQUATION 5.27)

$$\begin{aligned}
\text{CPRIME}(I + (2M + 8 + L)(N + 2)) &= \phi_2 \sum_{K=1}^{M+2} \text{BB}(J, K) \text{C}(I + (2M + 8 + K)(N + 2)) \\
&- \eta_{1T} g_3 (\text{C}(I + (J + 4)(N + 2)), \text{C}(I + (J + M + 6)(N + 2)), \text{C}(I + (J + 2M + 8)(N + 2))) \\
&- \eta_{2B} g_4 (\text{C}(I + (J + 4)(N + 2)), \text{C}(I + (J + M + 6)(N + 2)), \text{C}(I + (J + 2M + 8)(N + 2)))
\end{aligned}
\tag{B-20}$$

BOUNDARY CONDITION 1 FOR PDE 3 (EQUATION 5.31)

$$\text{C}(I + (2M + 9)(N + 2)) = \epsilon_0 \text{C}(I + 2(N + 2))
\tag{B-21}$$

BOUNDARY CONDITION 2 FOR PDE 3 (EQUATION 5.32)

$$\text{C}(I + (3M + 10)(N + 2)) = - \frac{\sum_{K=1}^{M+1} \text{AA}(M + 2, K) \text{C}(I + (2M + 8 + K)(N + 2))}{\text{AA}(M + 2, M + 2)}
\tag{B-22}$$

PDE 4 FOR THE TOLUENE IN THE GAS PHASE (EQUATION 5.33)

$$\begin{aligned}
\text{CPRIME}(I) &= \frac{1}{\text{Pe}_T} \sum_{k=1}^{N+2} \text{B}(I, k) \cdot \text{C}(k) - \frac{1}{U} \sum_{k=1}^{N+2} \text{A}(I, k) \cdot \text{C}(k) \\
&+ \beta_{1T} \sum_{k=1}^{M+2} \text{AA}(I, k) \text{C}(I + (k + 4)(N + 2)) - \chi_T (\text{C}(I) - \text{CTS})
\end{aligned}
\tag{B-23}$$

PDE 5 FOR THE BENZENE IN THE GAS PHASE (EQUATION 5.34)

$$\begin{aligned}
\text{CPRIME}(I + N + 2) &= \frac{1}{\text{Pe}_B} \sum_{k=1}^{N+2} \text{B}(I, k) \cdot \text{C}(k + N + 2) - \frac{1}{U} \sum_{k=1}^{N+2} \text{A}(I, k) \cdot \text{C}(k + N + 2) \\
&+ \beta_{3B} \sum_{k=1}^{M+2} \text{AA}(I, k) \text{C}(I + (k + M + 6)(N + 2)) \\
&- \chi_B (\text{C}(I) - \text{CBS})
\end{aligned}
\tag{B-24}$$

PDE 6 FOR THE OXYGEN IN THE GAS PHASE (EQUATION 5.35)

$$\begin{aligned}
 \text{CPRIME}(I + 2(N + 2)) = & \frac{1}{\text{Pe}_O} \sum_{k=1}^{N+2} \text{B}(I, k) \cdot \text{C}(k + 2(N + 2)) - \frac{1}{\nu} \sum_{k=1}^{N+2} \text{A}(I, k) \cdot \text{C}(k + 2(N + 2)) \\
 & + \beta_4 \sum_{k=1}^{N+2} \text{AA}(I, k) \cdot \text{C}(I + (2M + 8 + k)(N + 2))
 \end{aligned}$$

(B-25)

The Boundary conditions for the above 3 PDEs are the same as for the approximate model.

ODE 7 FOR TOLUENE ADSORBED ON THE SOLID (EQUATION 5.36)

$$\text{CPRIME}(I + 3(N + 2)) = \chi_T (C(I) - \text{CTS}) \quad (\text{B-26})$$

ODE 8 FOR BENZENE ADSORBED ON THE SOLID (EQUATION 5.37)

$$\text{CPRIME}(I + 4(N + 2)) = \chi_B (C(I) - \text{CBS}) \quad (\text{B-27})$$

APPENDIX C

```

* .....
* THE APPROXIMATE MODEL FOR SINGLE VOC
* .....

* .....
* Subroutine used : IMSL (DIVPRK)
* No. of ODEs solved : 30 (CAN BE CHANGED BY VARYING N)
* .....

IMPLICIT DOUBLE PRECISION (A-H,O-Z)
PARAMETER (N=8)
PARAMETER (MXPARAM=50,NT=(N+2)*5)

DOUBLE PRECISION Z(N+2),C(NT),A(N+2,N+2),B(N+2,N+2),
PARAM(MXPARAM),CPRIME(NT),SUM(20),KLT,KLB,XT,XOT,
KDT,KDB,ANN,AMUB,AMUT,MB,MT,MO,KMB,KMT,KB,KT,KO,KIT,KBT,KTB

COMMON/A,A,B,V,PEB,PET,PEO,ET,EB,EO,GAMA,SIGMA1,SIGMA2,
BT2,BB2,H,ALPHA,AS,XV,AMUB,AMUT,UG,CBI,YB,CTI,COI,YOB,YOT,YT,
SIT,SIB,B3,B4,ANN,R1,R2,XT,XOT,TEMP,PH,XB,XOB

EXTERNAL DIVPRK,SSET,FCN

CALL INIT2(N,NT,T,C,Z,A,B)

CALL INIT1(TEND,H,ALPHA,AS,XV,V,UG,AMUB,AMUT,
CBI,CTI,COI,YB,YT,YOB,YOT,BB2,BT2,B3,B4,EB,ET,EO,GAMA,
SIGMA1,SIGMA2,PEB,PET,PEO,SIB,SIT,ANN,XT,XOT,XB,XOB)

*-----IMSL Parameters-----
IDO=1
TOL=1.0E-4

CALL SSET(MXPARAM,0.0,PARAM,1)
PARAM(10)=1.0
PARAM(1)=1E-6
PARAM(4)=900000

* .....
* ***** Inlet Concentration Type ( 1 indicates step increase )
* .....

CSIGT=1.0
CSIGO=1.0

DO 10 TEND=1.0,50.0,1.0
CALL DIVPRK(IDO,NT,FCN,T,TEND,TOL,PARAM,C)
WRITE(9,*)T

* .....
* ***** Boundary Conditions for PDE 1
* .....

DO 3510 I=1,2
3510 SUM(I)=0.0
C
DO 3520 K=2,N+1
SUM(1) = SUM(1) + A(N+2,K)*C(K)
3520 SUM(2) = SUM(2) + A(1,K)*C(K)

C(N+2) =(-A(N+2,1)*(SUM(2)+PET*CSIGT)-(PET-A(1,1))*SUM(1))/

```

```

      (A(N+2,1)*A(1,N+2)+(PET-A(1,1))*A(N+2,N+2))
      C(1) =-(SUM(1)+C(N+2)*A(N+2,N+2))/A(N+2,1)
      *
      ***** Boundary Conditions for PDE 2
      *
      DO 3525 I=3,4
3525   SUM(I)=0.0

      DO 3530 K=2,N+1
      SUM(3) = SUM(3) - A(N+2,K)*C(K+N+2)
3530   SUM(4) = SUM(4) - A(1,K)*C(K-N+2)

      C(2*(N+2)) =(-A(N+2,1)*(SUM(4)+PEO*CSIGO)-(PEO-A(1,1))*SUM(3))
      (A(N+2,1)*A(1,N+2)-(PEO-A(1,1))*A(N+2,N+2))

      C(1+N+2) =-(SUM(3)-C(2*(N+2))*A(N+2,N+2))/A(N+2,1)

      **
      ** PRINTING THE RESULTS
      **
      WRITE(6,89) TEND,C(N+2)
89     FORMAT(2(1X,F8.5))
      WRITE(5,99) T,C(N+2)
99     FORMAT(4(2X,F8.4))

      IF (T.LT.9.0) GO TO 10
      WRITE(7,79)T
79     FORMAT(2X,'TIME=',F6.3)
      DO 3 M=1,N+2
3     WRITE(7,98) Z(M),C(M),C(M-(N+2))
98     FORMAT(3(1X,F12.8))

10    CONTINUE

      IDO=3
      CALL DIVPRK(IDO,NT,FCN,T,TEND,TOL,PARAM,C)
9999  END

      .....
      ***** SUBROUTINE FCN
      .....
      SUBROUTINE FCN(NT,T,C,CPRIME)
      IMPLICIT DOUBLE PRECISION (A-H,O-Z)
      PARAMETER (N=8)

C     DOUBLE PRECISION Z(N+2),C(NT),A(N+2,N+2),B(N+2,N+2),
      CPRIME(NT),SUM(20),KLT,KLB,
      KDT,KDB,ANN,AMUB,AMUT,MB,MT,MO,KMB,KMT,KB,KT,KO,KIT,KBT,KTB

      COMMON/A/A,B,V,PEB,PET,PEO,ET,EB,EO,GAMA,SIGMA1,SIGMA2,
      BT2,BB2,H,ALPHA,AS,XV,AMUB,AMUT,UG,CBI,YB,CTI,COI,YOR,YOT,YT,
      SIT,SIB,B3,B4,ANN,R1,R2,XT,XOT,TEMP,PH,XB,XOB

C     TEMP=25.0
      PH=7.2
      CSIGT=1.0
      CSIGO=1.0

```

```

*
***** Boundary Conditions for PDE 1
*
      DO 3510 I=1,2
3510   SUM(I)=0.0

      DO 3520 K=2,N+1
      SUM(1) = SUM(1) + A(N+2,K)*C(K)
3520   SUM(2) = SUM(2) + A(1,K)*C(K)

      C(N+2) = (-A(N+2,1)*(SUM(2)-PET*CSIGT)-(PET-A(1,1))*SUM(1))/
      (A(N+2,1)*A(1,N+2)-(PET-A(1,1))*A(N+2,N+2))

      C(1) = -(SUM(1)+C(N+2)*A(N+2,N+2))/A(N+2,1)

*
***** Boundary Conditions for PDE 1
*
      DO 3525 I=3,4
3525   SUM(I)=0.0

      DO 3530 K=2,N+1
      SUM(3) = SUM(3) + A(N+2,K)*C(K+N+2)
3530   SUM(4) = SUM(4) + A(1,K)*C(K+N+2)

      C(2*(N+2)) = (-A(N+2,1)*(SUM(4)+PEO*CSIGO)-(PEO-A(1,1))*SUM(3))/
      (A(N+2,1)*A(1,N+2)-(PEO-A(1,1))*A(N+2,N+2))

      C(1+N+2) = -(SUM(3)+C(2*(N+2))*A(N+2,N+2))/A(N+2,1)

*
***** PDE 1 FOR VOC (Equation 4.8)
*
      DO 1600 I=2,N+1

      SUM(7)=0.0
      SUM(8)=0.0

      DO 1610 K=1,N+2
      SUM(7) = SUM(7) + B(I,K)*C(K)
1610   SUM(8) = SUM(8) + A(I,K)*C(K)

      G1 = -SUM(8)/V

      G2 = SUM(7)/PET

      G3=(0.03*C(I)*CTI+0.2)*(1.5*C(I)*CTI+33.4)*1.0E-06*XT*
      (C(I)*C(I+(N+2))*ET*EO)/(1.0+C(I)*ET+((C(I)*ET)**2)*GAMA)
      /(1+C(I+(N+2))*EO)

      G4=BT2*(C(I)-SIT*C(I+2*(N+2)))*(1/ANN))

      CPRIME(I) = G1+G2-G3-G4

1600   CONTINUE

*
***** PDE 2 FOR OXYGEN (Equation 4.9)
*

```

```

DO 1640 I=2,N+1

SUM(11)=0.0
SUM(12)=0.0

DO 1650 K=1,N+2
SUM(11) = SUM(11) + B(I,K)*C(K+(N+2))
1650 SUM(12) = SUM(12) + A(I,K)*C(K+(N+2))

H1= -SUM(12)/V

H2= SUM(11)/PEO

H3= (0.03*C(I)*CTI+0.2)*(1.5*C(I)*CTI+33.4)*1.0E-6*XOT*
(C(I)*C(I+(N+2))*ET*EO)/
(1.0+C(I)*ET+((C(I)*ET)**2)*GAMA)/
(1.0+C(I+(N+2))*EO)

CPRIME(I+(N+2))=H1+H2-H3

1640 CONTINUE

*
***** ODE 3 FOR OXYGEN (Equation 4.10)
*
DO 1670 I=1,N+2
1670 CPRIME(I+2*(N+2)) = BT2*(C(I)-SIT*C(I+2*(N+2))**((1/ANN)))

RETURN
END

```

```

.....
***** SUBROUTINE INIT1
.....

```

```

SUBROUTINE INIT2(N,NT,T,C,Z,A,B)
IMPLICIT DOUBLE PRECISION (A-H,O-Z)

```

```

DIMENSION Z(N+2),C(NT),A(N+2,N+2),B(N+2,N+2)

```

```

C-----INITIAL CONCENTRATIONS-----

```

```

T=0
DO 1021 I=1,N+2
1021 READ(1,8) C(I),C(I+N+2),C(I+2*(N+2))
8 FORMAT(3(F11.9,1X))

DO 29 J=1,N+2
29 C(J)=0.001
DO 28 K=N+3,2*(N+2)
28 C(K)=1.0
DO 27 K=(2*(N+2)+1),3*(N+2)
27 C(K)=11.0

```

```

C-----COLLOCATION POINTS,A & B MATRICES-----

```

```

DO 1022 I=1,N+2
1022 READ(2,9) Z(I)
9 FORMAT(11X,F13.11)
C
DO 1023 I=1,N+2
DO 1023 J=1,N+2

```

```

1023 READ(2,*) A(I,J)
C
      DO 1024 I=1,N+2
      DO 1024 J=1,N+2
1024 READ(2,*) B(I,J)
12   FORMAT(11X,F14.11)
      RETURN
      END

```

```

.....
*****          SUBROUTINE INIT2
.....

```

```

SUBROUTINE INIT1(TEND,H,ALPHA,AS,XV,V,UG,AMUB,AMUT,
CBI,CTI,COI,YB,YT,YOB,YOT,BB2,BT2,B3,B4,EB,ET,EO,GAMA,
SIGMA1,SIGMA2,PEB,PET,PEO,SIB,SIT,ANN,XT,XOT,XB,XOB)
IMPLICIT DOUBLE PRECISION (A-H,O-Z)

```

```

C
REAL*8 H,UG,PD,KMB,KMT,KB,KT,KO,KIT,KBT,KTB,AMUB,AMUT,MB,MT,
MO,KDB,KDT,ANN,BB2,BT2,B3,B4,EB,ET,EO,GAMA,SIGMA1,SIGMA2,
PEB,PET,PEO,SIB,SIT

```

```

*
*   Entering Concentration in g/m3 : Res. time in minutes
*

```

```

CBI = 0.120
CTI = 0.62
COI = 275.00
RT=2.7

```

```

*
*   Column Parameters ( units in metres, day )
*

```

```

D=0.100
C VOLUME=0.015291002
VOLUME=0.005150
AREA=3.141592654*(D**2)/4.0
UG= VOLUME*24.0*60.0/AREA/RT
H = VOLUME/AREA
PRINT*,AREA,UG,H

```

```

*
*   Packing Material Properties ( units meters, grams )
*

```

```

DP=4.0E-3
PD = 4.28E+5
V = 0.3

```

```

*
*   Biofilm Properties ( units meters, grams )
*

```

```

AS = 133.3
ALPHA = 0.3
XV = 100000.00

```

```

*
*   Mass Transfer Coefficients ( units meters, grams, day )
*

```

```

KMB = (6.04E-3)*24.0
KMT = (6.04E-3)*24.0

```

```

*
*   Kinetic Properties ( units meters, grams, day )
*

```

```

KB = 12.22
KT = 11.03
KO = 0.26
KIT = 78.94
KBT = 4.50
KTB = 0.20
AMUB = 0.677*24.0
AMUT = 1.504*24.0
YB = 0.708
YT = 0.708
YOB = 0.336
YOT = 0.341
.
.
.  Axial Dispersion Coefficients ( units meters. grams. day )
.
.
GAMA1=0.45+0.55*V
GAMA2=0.5
TERM2=GAMA2*DP*UG/V
DB = 0.02772*24.0*GAMA1+TERM2
DT = 0.02736*24.0*GAMA1+TERM2
DO = 0.06408*24.0*GAMA1+TERM2
.
.
.  Henry's Constant
.
.
MB = 0.23
MT = 0.27
MO = 34.4
.
.
.  Adsorption Isotherm Parameters ( g/g-particle )
.
.
KDB = 2.25E-5
KDT = 2.25E-5
ANN = 1.04
**
**  NON-DIMENSIONAL GROUPS
**
.
.
.  Beta group (without delta and e)
.
.
XT = H*ALPHA*AS*XV*AMUT/V/UG/CTI/YT
XB = H*ALPHA*AS*XV*AMUB/V/UG/CBI/YB
XOT=H*ALPHA*AS*XV*AMUT/V/UG/COI/YOT
XOB=H*ALPHA*AS*XV*AMUB/V/UG/COI/YOB
.
.
.  X Group for Benzene and Toluene (Mass tr. to solid)
.
.
BB2 = (1.0-ALPHA)*AS*KMB*H/V/UG
BT2 = (1.0-ALPHA)*AS*KMT*H/V/UG
.
.
.  Kinetic Groups
.
.
EB = CBI/KB/MB
ET = CTI/KT/MT
EO = COI/KO/MO
GAMA = KT/KIT
SIGMA1 = KT*KBT/KB
SIGMA2 = KB*KTB/KT
.
.
.  Peclet Numbers

```



```
•  
  PEB=UG*H/DB/V  
  PET=UG*H/DT/V  
  PEO=UG*H/DO/V  
•  
•   Adsorption Isotherm Groups  
•  
  SIB = ((V*CBI/(1-V)/PD/KDB)**(1/ANN))/CBI  
  SIT = ((V*CTI/(1-V)/PD/KDT)**(1/ANN))/CTI  
  
C-----ECHO THE INPUT-----  
  WRITE(8,*) H,ALPHA,AS  
  WRITE(8,*) XV,V,UG  
  WRITE(8,*) AMUB,AMUT,ANN  
  WRITE(8,*) CBI,CTI,COI  
  WRITE(8,*) YB,YT,YOB,YOT  
  WRITE(8,*) BB2,BT2  
  WRITE(8,*) B3,B4  
  WRITE(8,*) EB,ET,EO  
  WRITE(8,*) GAMA,SIGMA1,SIGMA2  
  WRITE(8,*) PEB,PET,PEO  
  WRITE(8,*) SIB,SIT  
  
  RETURN  
  END
```

APPENDIX D

```

* .....
* THE GENERAL MODEL FOR SINGLE VOC
* .....

```

```

* .....
* Subroutine used : IMSL (DIVPRK)
* No. of ODEs solved : 150 (CAN BE CHANGED BY VARYING N)
* .....

```

```

IMPLICIT DOUBLE PRECISION (A-H,O-Z)
PARAMETER (N=8,M=4)
PARAMETER (MXPARM=50,NT=(N+2)*(2*M+7))

```

```

DOUBLE PRECISION Z(N+2),C(NT),A(N+2,N+2),B(N+2,N+2),
PARAM(MXPARM),CPRIME(NT),SUM(20),AA(M+2,M+2),ANN,
BB(M+2,M+2),X(M-2)

```

```

COMMON/A,A,B,AA,BB,PET,PEO,ET,EO,V,GAMA,BETA1,BETA2,
SIT,ANN,BETA5,PHI1,PHI2,PHI5,PHI6

```

```

EXTERNAL DIVPRK,SSET,FCN

```

```

CALL INIT(N,M,NT,T,C,Z,A,B,X,AA,BB,PET,PEO,ET,EO,
V,GAMA,BETA1,BETA2,SIT,ANN,BETA5,PHI1,PHI2,PHI5,PHI6)

```

```

C-----IMSL PARAMETERS-----

```

```

CALL SSET(MXPARM,0.0,PARAM,1)
IDO=1
TOL=1.0E-2
PARAM(10)=1.0
PARAM(1)=1E-6
PARAM(4)=900000

```

```

* .....
* Inlet Concentration Type (1 implies Step Change)
* .....

```

```

CSIGT=1.0
CSIGO=1.0

```

```

DO 10 TEND=1.0,15.0,1.0
WRITE(9,*)TEND
CALL DIVPRK(IDO,NT,FCN,T,TEND,TOL,PARAM,C)

```

```

* .....
* Boundary Conditions for PDE 3 (Eqn. 4.15, 4.16)
* .....

```

```

DO 3510 I=1,2
3510 SUM(I)=0.0

```

```

C
DO 3520 K=2,N+1
SUM(1) = SUM(1) + A(N+2,K)*C(K)
3520 SUM(2) = SUM(2) + A(1,K)*C(K)

```

```

C(N+2) = (-A(N+2,1)*(SUM(2)+PET*CSIGT)-(PET-A(1,1))*SUM(1))/
(A(N+2,1)*A(1,N+2)+(PET-A(1,1))*A(N+2,N+2))

```

```

C(1) = -(SUM(1)+C(N+2)*A(N+2,N+2))/A(N+2,1)

```

```

* .....
* Boundary Conditions for PDE 4 (Eqn. 4.15, 4.16)
* .....

```

```

DO 3525 I=3,4
3525 SUM(I)=0.0

```

```

DO 3530 K=2,N+1
SUM(3) = SUM(3) + A(N+2,K)*C(K+N+2)
3530 SUM(4) = SUM(4) + A(1,K)*C(K+N+2)

C(2*(N+2)) = (-A(N+2,1)*(SUM(4)+PEO*CSIGO)-(PEO-A(1,1))*SUM(3))/
(A(N+2,1)*A(1,N+2)+(PEO-A(1,1))*A(N+2,N+2))

C(1+N+2) = -(SUM(3)+C(2*(N+2))*A(N+2,N+2))/A(N+2,1)

*
***** Boundary Condition 1 for PDEs 1 & 2 (Eqn. 4.22)
*
DO 3535 I=1,N+2
C(1-3*(N+2))=ET*C(I)
C(1+(M+5)*(N+2))=EO*C(1-N+2)
3535 CONTINUE

***** Boundary Condition 2 for PDEs 1 & 2 (Eqn. 4.23)
*
DO 3545 I=1,N+2
SUM(5)=0.0
SUM(6)=0.0
DO 3550 K=1,M+1
SUM(5) = SUM(5) + AA(M+2,K)*C(I+(2+K)*(N+2))
3550 SUM(6) = SUM(6) + AA(M+2,K)*C(I+(M+4+K)*(N+2))

C(1+(M+4)*(N+2)) = -SUM(5)/AA(M+2,M+2)
3545 C(1+(2*M+6)*(N+2)) = -SUM(6)/AA(M+2,M+2)

**
** PRINTING THE RESULTS
**
WRITE(6,99) TEND,CSIGT,C(N+2)
99 FORMAT(3(1X,F12.8))

WRITE(10,*)TEND
DO 92 J=1,M+2
WRITE(10,91)X(J),C((J+3)*(N+2)),C((J+9)*(N+2))
91 FORMAT(3(2X,F12.8))
92 CONTINUE

IF(TEND.LE.14.0) GOTO 10
DO 98 I=1,N+2
WRITE(8,102)Z(I),C(I),C(I+N+2)
102 FORMAT(3(2X,F12.8))
C WRITE(7,101)Z(I),I
C 101 FORMAT(/,3X,'HEIGHT =',F10.6,2X,'COLL. POINT =',I2)
DO 98 J=1,M+2
WRITE(7,100) X(J),C(I+(2+J)*(N+2)),C(I+(M+4+J)*(N+2))
100 FORMAT(3(2X,F12.8))
98 CONTINUE

10 CONTINUE

IDO=3
CALL DIVPRK(IDO,NT,FCN,T,TEND,TOL,PARAM,C)
9999 END

```

```

*****
***** SUBROUTINE FCN
*****
SUBROUTINE FCN(NT,T,C,CPRIME)
IMPLICIT DOUBLE PRECISION (A-H,O-Z)

```

```

PARAMETER (N=8,M=4)
C
DOUBLE PRECISION Z(N+2),C(NT),A(N+2,N+2),B(N+2,N+2),
CPRIME(NT),SUM(20),AA(M+2,M+2),ANN,
BB(M+2,M+2),X(M+2)

COMMON/A,A,B,AA,BB,PET,PEO,ET,EO,V,GAMA,BETA1,BETA2,
SIT,ANN,BETA5,PHI1,PHI2,PHI5,PHI6
C
CTI=1.65
CSIGT=1.0
CSIGO=1.0
TINIT=4.0
TMAX=12.0
THALF=(TINIT + TMAX)/2.0
CMAX=0.5
.
***** Boundary Conditions for PDE 3 (Eqn. 4.15, 4.16)
.
DO 3510 I=1,2
3510  SUM(I)=0.0

DO 3520 K=2,N+1
SUM(1) = SUM(1) + A(N+2,K)*C(K)
3520  SUM(2) = SUM(2) + A(1,K)*C(K)

C(N+2) = (-A(N+2,1)*(SUM(2)+PET*CSIGT)-(PET-A(1,1))*SUM(1))/
(A(N+2,1)*A(1,N+2)+(PET-A(1,1))*A(N+2,N+2))

C(1) = -(SUM(1)+C(N+2)*A(N+2,N+2))/A(N+2,1)
.
***** Boundary Conditions for PDE 4 (Eqn. 4.15, 4.16)
.
DO 3525 I=3,4
3525  SUM(I)=0.0

DO 3530 K=2,N+1
SUM(3) = SUM(3) + A(N+2,K)*C(K+N+2)
3530  SUM(4) = SUM(4) + A(1,K)*C(K+N-2)

C(2*(N+2)) = (-A(N+2,1)*(SUM(4)+PEO*CSIGO)-(PEO-A(1,1))*SUM(3))/
(A(N+2,1)*A(1,N+2)+(PEO-A(1,1))*A(N+2,N+2))

C(1+N+2) = -(SUM(3)+C(2*(N+2))*A(N+2,N+2))/A(N+2,1)
.
***** Boundary Condition 1 for PDEs 1 & 2 (Eqn. 4.22)
.
DO 3535 I=1,N+2
C(1-3*(N+2))=ET*C(I)
C(1+(M+5)*(N+2))=EO*C(1+N+2)
3535  CONTINUE
.
***** Boundary Condition 2 for PDEs 1 & 2 (Eqn. 4.23)
.
DO 3545 I=1,N+2

SUM(5)=0.0
SUM(6)=0.0

DO 3550 K=1,M+1
SUM(5) = SUM(5) + AA(M+2,K)*C(1+(2+K)*(N+2))
3550  SUM(6) = SUM(6) + AA(M+2,K)*C(1+(M+4+K)*(N+2))

C(1+(M+4)*(N+2)) = -SUM(5)/AA(M+2,M+2)

```

3545 $C(I+(2*M+6)*(N+2)) = -SUM(6)/AA(M+2,M+2)$

..... PDE 3 FOR THE VOC IN THE COLUMN (Eqn.4.23)

```

DO 1600 I=2,N+1
SUM(7)=0.0
SUM(8)=0.0
SUM(9)=0.0

DO 1610 K=1,N+2
SUM(7) = SUM(7) + B(I,K)*C(K)
1610 SUM(8) = SUM(8) + A(I,K)*C(K)

DO 1615 J=1,M+2
1615 SUM(9) = SUM(9) + AA(I,J)*C(I+(J+2)*(N+2))

G1 = -SUM(8)/V
G2 = SUM(7)/PET
G3 = BETA1*SUM(9)/40.0E-6
G4 = BETA2*(C(I)-SIT*C(I+2*(N+2)))*(1/ANN))

CPRIME(I) = G1+G2+G3-G4
1600 CONTINUE

```

..... PDE 4 FOR OXYGEN IN THE COLUMN (Eqn. 4.24)

```

DO 1640 I=2,N+1
SUM(11)=0.0
SUM(12)=0.0
SUM(13)=0.0

DO 1650 K=1,N+2
SUM(11) = SUM(11) + B(I,K)*C(K+N+2)
1650 SUM(12) = SUM(12) + A(I,K)*C(K+N+2)

DO 1655 J=1,M+2
1655 SUM(13) = SUM(13) + AA(I,J)*C(I+(N+2)*(M+4+J))

G1 = -SUM(12)/V
G2 = SUM(13)/PEO
G3 = BETA5*SUM(13)/(40.0E-6)
CPRIME(I+N+2) = G1+G2+G3

1640 CONTINUE

```

..... ODE 5 FOR THE VOC IN THE PARTICLE (Eqn. 4.10)

```

DO 1660 I=1,N+2
1660 CPRIME(I+2*(N+2)) = BETA2*(C(I)-SIT*(C(I+2*(N+2)))*(1/ANN)))

```

..... PDE 1 FOR THE VOC IN THE BIOFILM (Eqn. 4.17)

```

DO 1670 I = 1,N+2

DO 1675 J = 2,M+1
SUM(14)= 0.0

DO 1680 K = 1,M+2
1680 SUM(14) = SUM(14) + BB(J,K)*C(I+(2+K)*(N+2))

```

```

      G1 = PHI1*SUM(I4)/(40.0E-6)**2.0
      G2 = PHI2*C(I+(2+J)*(N+2))*C(I+(M+4+J)*(N+2))/
      (1.0+C(I+(2+J)*(N+2))+C(I+(2+J)*(N+2))**2)*GAMA/
      (1.0 + C(I+(M+4+J)*(N+2)))
      CPRIME(I+(2+J)*(N+2)) = G1-G2
1675  CONTINUE
1670  CONTINUE
.
***** PDE 2 FOR THE OXYGEN IN THE BIOFILM (Eqn. 4.18)
.
      DO 1685 I = 1,N+2

      DO 1690 J = 2,M+1
      SUM(15)= 0.0

      DO 1695 K = 1,M+2
1695  SUM(15) = SUM(15) + BB(J,K)*C(I-(M-4+K)*(N+2))

      G1 = PHI5*SUM(15)/(40.0E-6)**2.0
      G2 = PHI6*C(I+(2+J)*(N+2))*C(I+(M+4+J)*(N+2))/
      (1.0+C(I-(2+J)*(N+2))+C(I+(2+J)*(N+2))**2)*GAMA/
      (1.0 + C(I+(M+4+J)*(N+2)))
      CPRIME(I+(M+4+J)*(N+2)) = G1-G2
1690  CONTINUE
1685  CONTINUE

      RETURN
      END

*****
*****          SUBROUTINE INIT
*****
SUBROUTINE INIT(N,M,NT,T,C,Z,A,B,X,AA,BB,PET,PEO,ET,EO,
V,GAMA,BETA1,BETA2,SIT,ANN,BETA5,PHI1,PHI2,PHI5,PHI6)
IMPLICIT DOUBLE PRECISION (A-H,O-Z)

REAL*8 H,U,G,PD,KMB,KMT,KB,KT,KO,KIT,KBT,KTB,AMUB,AMUT,MB,MT,
MO,KDB,KDT,ANN,BB2,BT2,B3,B4,EB,ET,EO,GAMA,SIGMA1,SIGMA2,
PEB,PET,PEO,SIB,SIT,FXV,DTW,DBW,DOW,BETA1,BETA2,BETA3,BETA4,
BETA5,PHI1,PHI2,PHI3,PHI4,PHI5,PHI6

DIMENSION Z(N+2),C(NT),A(N+2,N+2),B(N+2,N+2),X(M+2),
AA(M+2,M+2),BB(M+2,M+2)

C-----INITIAL CONCENTRATIONS-----
      T=0
      DO 1021 I=1,N+2
1021  READ(1.8) C(I),C(I+N+2),C(I+2*(N+2))
      8   FORMAT(3(F11.9,1X))

      DO 29 J=1,N+2
      C(J)=0.1
      C(J+3*(N+2))=ET*C(J)
      C(J+N+2)=1.0
29     C(J+(5+M)*(N+2))=EO*C(J+N+2)
      DO 30 I=1,N+2
      DO 30 J=2,M+2
      C(I+(2+J)*(N+2))=0.4
30     C(I+(4+M+J)*(N+2))=18.0

C-----COLLOCATION POINTS,A & B MATRICES-----
      DO 1022 I=1,N+2
1022  READ(2.9) Z(I)

```

```

9      FORMAT(11X,F13.11)
C
      DO 1023 I=1,N+2
      DO 1023 J=1,N+2
1023   READ(2,*) A(I,J)
C
      DO 1024 I=1,N+2
      DO 1024 J=1,N+2
1024   READ(2,*) B(I,J)

C-----COLLOCATION POINTS,AA & BB MATRICES-----
      DO 1025 I=1,M+2
1025   READ(3,19) X(I)
19     FORMAT(11X,F13.11)
C
      DO 1026 I=1,M+2
      DO 1026 J=1,M+2
1026   READ(3,*) AA(I,J)
C
      DO 1027 I=1,M+2
      DO 1027 J=1,M+2
1027   READ(3,*) BB(I,J)

.
.
.      Inlet Concentrations and Residence Time (units: g, m, min)
.
      CBI = 0.367
      CTI = 1.65
      COI = 275.0
      RT=7.7
.
.
.      Column Parameters
.
      D=0.100
      VOLUME=0.00515
      AREA=3.141592654*(D**2)/4.0
      UG= VOLUME*24.0*60.0/AREA/RT
      H = VOLUME/AREA
      PRINT*,AREA,UG,H
.
.
.      Biofilm Parameters
.
      AS = 133.3
      AL.PHA = 0.3
      XV = 100000.00
.
.
.      Particle Parameters
.
      PD = 4.28E+5
      DP=4.0E-3
      V = 0.3
.
.
.      Diffusion Coefficient in water ( m. day)
.
      DOW = (2.41E-9)*3600.0*24.0
      DTW = (1.03E-9)*3600.0*24.0
      DBW = (1.04E-9)*3600.0*24.0
      FXV = 0.195
.
.
.      Kinetic Parameters
.
      KB = 12.22
      KT = 11.03
      KO = 0.26

```

KIT = 78.94
 KBT = 4.50
 KTB = 0.20
 AMUB = 0.677*24.0
 AMUT = 1.504*24.0
 YB = 0.708
 YT = 0.708
 YOB = 0.336
 YOT = 0.341

*
 * Axial Dispersion Coefficients (m. day)
 *

GAMA1=0.45-0.55*V
 GAMA2=0.5
 TERM2=GAMA2*DP*UG/V
 DB = 0.02772*24.0*GAMA1+TERM2
 DT = 0.02736*24.0*GAMA1+TERM2
 DO = 0.06408*24.0*GAMA1+TERM2
 PRINT*.DP,GAMA2,TERM2,DT

*
 * Henry's Constant
 *

MB = 0.23
 MT = 0.27
 MO = 34.4

*
 * Adsorption Isotherm Parameters
 *

KDB = 2.25E-5
 KDT = 2.25E-5
 ANN = 1.04

*
 * Mass Transfer Coefficients for the solid (m. day)
 *

KMB = (6.04E-3)*24.0
 KMT = (6.04E-3)*24.0

..
 NON-DIMENSIONAL GROUPS
 ..

*
 * Betas for PDE 3 - Toluene
 *

BETA1 = DTW*FXV*ALPHA*AS*KT*H/CTI/V/UG
 BETA2 = (1-ALPHA)*AS*KMT*H/V/UG

*
 * Betas for PDE 3 - Benzene
 *

BETA3 = DBW*FXV*ALPHA*AS*KB*H/CBI/V/UG
 BETA4 = (1-ALPHA)*AS*KMB*H/V/UG

*
 * Beta for PDE 4
 *

BETA5 = DOW*FXV*ALPHA*AS*KO*H/COI/V/UG

*
 * Kinetic Groups
 *

EB = CBI/KB/MB
 ET = CTI/KT/MT
 EO = COI/KO/MO
 GAMA = KT/KIT
 SIGMA1 = KT*KBT/KB
 SIGMA2 = KB*KTB/KT


```

.
.   Pecllet Numbers
.
PEB=UG*H/DB/V
PET=UG*H/DT/V
PEO=UG*H/DO/V
.
.   Adsorption Isotherm Coefficients
.
SIB = ((V*CBI/(1-V)/PD/KDB)**(1/ANN))/CBI
SIT = ((V*CTI/(1-V)/PD/KDT)**(1/ANN))/CTI
.
.   Biofilm Groups for PDE 1 for Toluene and Benzene
.
PHI1 = FXV*DTW*H/UG
PHI2 = AMUT*XV*H/KT/YT/UG
PHI3 = FXV*DBW*H/UG
PHI4 = AMUB*XV*H/KB/YB/UG
.
.   Biofilm Groups for PDE 2
.
PHI5 = FXV*DOW*H/UG
PHI6 = AMUT*XV*H/YOT/KO/UG
PHI7 = AMUB*XV*H/YOB/KO/UG

```

```

C-----ECHO-----
WRITE(8,*) PET,PEO
WRITE(8,*) ET,EO
WRITE(8,*) V,GAMA
WRITE(8,*) BETA1,BETA2
WRITE(8,*) SIT,ANN
WRITE(8,*) BETA5
WRITE(8,*) PHI1,PHI2
WRITE(8,*) PHI5,PHI6

RETURN
END

```

APPENDIX E

```

.....
* THE APPROXIMATE MODEL FOR BINARY VOC MIXTURES
.....

.....
* Subroutine used : IMSL (DIVPRK)
* No. of ODEs solved : 50 (CAN BE CHANGED BY VARYING N)
.....

IMPLICIT DOUBLE PRECISION (A-H,O-Z)
PARAMETER (N=8)
PARAMETER (MXPARM=50,NT=(N+2)*5)

DOUBLE PRECISION Z(N+2),C(NT),A(N+2,N+2),B(N+2,N+2),
PARAM(MXPARM),CPRIME(NT),SUM(20),KLT,KLB,KDT,KDB,
ANN,AMUB,AMUT,MB,MT,MO,KMB,KMT,KB,KT,KO,KIT,KBT,KTB

COMMON A/A,B,H,ALPHA,AS,XV,V,UG,AMUB,AMUT,ANN,CBI,CTI,COI,
YB,YT,YOB,YOT,BB2,BT2,B3,B4,EB,ET,EO,GAMA,SIGMA1,SIGMA2,
PEB,PET,PEO,SIB,SIT,PEB1,PET1,PEO1,F,XB,XT,XOB,XOT,R1,R2,
T1,T2,T3,T4

CALL INIT(N,NT,T,C,Z,A,B,H,ALPHA,AS,XV,V,UG,AMUB,AMUT,
ANN,CBI,CTI,COI,YB,YT,YOB,YOT,BB2,BT2,EB,ET,EO,GAMA,
SIGMA1,SIGMA2,PEB,PET,PEO,XB,XT,XOB,XOT,T1,T2,T3,T4)

C-----PARAMETERS FOR IMSL-----
CSIGT=1.0
CSIGB=1.0
CSIGO=1.0

IDO=1
TOL=1E-2
CALL SSET(MXPARM,0.0,PARAM,1)
PARAM(10)=1.0
PARAM(1)=1E-6
PARAM(4)=2000000

DO 10 TEND=1.0,45.0,1.0
WRITE(*,*)TEND,CSIGB,CSIGT
CALL DIVPRK(IDO,NT,FCN,T,TEND,TOL,PARAM,C)

C-----B C FOR PDE 1-----
DO 3510 I=1,2
3510 SUM(I)=0.0

DO 3520 K=2,N+1
SUM(1) = SUM(1) + A(N+2,K)*C(K)
3520 SUM(2) = SUM(2) + A(1,K)*C(K)

C(N+2) =(-A(N+2,1)*(SUM(2)+PEB*CSIGB)-(PEB-A(1,1))*SUM(1))/
(A(N+2,1)*A(1,N+2)+(PEB-A(1,1))*A(N+2,N+2))

C(1) =-(SUM(1)+C(N+2)*A(N+2,N+2))/A(N+2,1)

C-----B C FOR PDE 2-----
DO 3525 I=3,4

```

```

3525  SUM(I)=0.0

      DO 3530 K=2,N+1
      SUM(3) = SUM(3) + A(N+2,K)*C(K+N+2)
3530  SUM(4) = SUM(4) + A(1,K)*C(K+N+2)

      C(2*(N+2)) =(-A(N+2,1)*(SUM(4)+PET*CSIGT)-(PET-A(1,1))*SUM(3))/
      (A(N+2,1)*A(1,N+2)+(PET-A(1,1))*A(N+2,N+2))

      C(1+N+2) =-(SUM(3)+C(2*(N+2))*A(N+2,N+2))/A(N+2,1)

C-----BC FOR PDE 3-----
      DO 3535 I=5,6
3535  SUM(I)=0.0

      DO 3540 K=2,N+1
      SUM(5) = SUM(5) + A(N+2,K)*C(K+2*(N+2))
3540  SUM(6) = SUM(6) + A(1,K)*C(K+2*(N+2))

      C(3*(N+2)) =(-A(N+2,1)*(SUM(6)+PEO*CSIGO)-(PEO-A(1,1))*SUM(5))/
      (A(N+2,1)*A(1,N+2)+(PEO-A(1,1))*A(N+2,N+2))

      C(1+2*(N+2)) =-(SUM(5)+C(3*(N+2))*A(N+2,N+2))/A(N+2,1)

C-----PRINT THE OUTPUT-----
      WRITE(6,91)TEND,C(N+2),C(2*(N+2)),C(3*(N+2)),CSIGT
91    FORMAT(1X,F6.3,4(2X,F9.5))

10    CONTINUE

      IDO=3
      CALL DIVPRK(IDO,NT,FCN,T,TEND,TOL,PARAM,C)
9999  END

* .....
* ***** SUBROUTINE FCN *****
* .....
SUBROUTINE FCN(NT,T,C,CPRIME)
IMPLICIT DOUBLE PRECISION (A-H,O-Z)
PARAMETER (N=8)

C
DOUBLE PRECISION Z(N+2),C(NT),A(N+2,N+2),B(N+2,N+2),
CPRIME(NT),SUM(20),KLT,KLB,KDT,KDB,
ANN,AMUB,AMUT,MB,MT,MO,KMB,KMT,KB,KT,KO,KIT,KBT,KT,
REAL R(5)

COMMON/A/A,B,H,ALPHA,AS,XV,V,UG,AMUB,AMUT,ANN,CBI,CTI,COI,
YB,YT,YOB,YOT,BB2,BT2,B3,B4,EB,ET,EO,GAMA,SIGMA1,SIGMA2,
PEB,PET,PEO,SIB,SIT,PEB1,PET1,PEO1,F,XB,XT,XOB,XOT,R1,R2,
T1,T2,T3,T4

C
CSIGT=1.0
CSIGB=1.0
CSIGO=1.0

C-----B C FOR PDE 1-----
      DO 3510 I=1,2
3510  SUM(I)=0.0

      DO 3520 K=2,N+1

```

```

SUM(1) = SUM(1) + A(N+2,K)*C(K)
3520 SUM(2) = SUM(2) + A(1,K)*C(K)

C(N+2) = (-A(N+2,1)*(SUM(2)+PEB*CSIGB)-(PEB-A(1,1))*SUM(1))/
(A(N+2,1)*A(1,N+2)+(PEB-A(1,1))*A(N+2,N+2))

C(1) = -(SUM(1)+C(N+2)*A(N+2,N+2))/A(N+2,1)

```

C-----**BC FOR PDE 2**-----

```

DO 3525 I=3,4
3525 SUM(I)=0.0

DO 3530 K=2,N+1
SUM(3) = SUM(3) + A(N+2,K)*C(K+N+2)
3530 SUM(4) = SUM(4) + A(1,K)*C(K+N+2)

C(2*(N+2)) = (-A(N+2,1)*(SUM(4)+PET*CSIGT)-(PET-A(1,1))*SUM(3))/
(A(N+2,1)*A(1,N+2)-(PET-A(1,1))*A(N+2,N+2))

C(1+N+2) = -(SUM(3)+C(2*(N+2))*A(N+2,N+2))/A(N+2,1)

```

C-----**BC FOR PDE 3**-----

```

DO 3535 I=5,6
3535 SUM(I)=0.0

DO 3540 K=2,N+1
SUM(5) = SUM(5) + A(N+2,K)*C(K+2*(N+2))
3540 SUM(6) = SUM(6) + A(1,K)*C(K+2*(N+2))

C(3*(N+2)) = (-A(N+2,1)*(SUM(6)+PEO*CSIGO)-(PEO-A(1,1))*SUM(5))/
(A(N+2,1)*A(1,N+2)+(PEO-A(1,1))*A(N+2,N+2))

C(1+2*(N+2)) = -(SUM(5)+C(3*(N+2))*A(N+2,N+2))/A(N+2,1)

```

C-----**RESOLVING PDE 1**-----

```

DO 1600 I=2,N+1
SUM(7)=0.0
SUM(8)=0.0

DO 1610 K=1,N+2
SUM(7) = SUM(7) + B(I,K)*C(K)
1610 SUM(8) = SUM(8) + A(I,K)*C(K)

G1 = -SUM(8)/V + SUM(7)/PEB
G2 = -(0.03*C(1)-0.2)*(1.5*CT1+32.0)*1.0E-06*XB*
(C(1)*C(1+2*(N+2))*EB*EO)/(1.0+C(1)*EB+C(1+N+2)*ET*SIGMA1)
/(1.0+C(1+2*(N+2))*EO)

CTS = C(1+4*(N+2))*(1.0+T3*C(1+3*(N+2)))/
(T4-T3*C(1+3*(N+2)))/
((T1-T2*C(1+4*(N+2))-T2*T3*C(1+3*(N+2)))/(T4-T3*C(1+3*(N+2))))

G3 = -BB2*(C(1)-C(1+3*(N+2))*(1.0+T2*CTS)/(T4-T3*C(1+3*(N+2))))

1600 CPRIME(I)=G1+C2+G3
CONTINUE

```

C-----**RESOLVING PDE 2**-----

```
DO 1620 I=2,N+1
```

```

SUM(9)=0.0
SUM(10)=0.0

DO 1630 K=1,N+2
SUM(9) = SUM(9) + B(I,K)*C(K+N+2)
1630 SUM(10) = SUM(10) + A(I,K)*C(K+N+2)

H1 = -SUM(10)/V + SUM(9)/PET
H2 = -(0.03*C(I+N+2)+0.2)*(1.5*CTI+32.0)*1.0E-06*XT*
(C(I+N+2)*C(I+2*(N+2))*ET*EO)/
(1.0+C(I+N+2)*ET+(C(I-N+2)*ET)**2*GAMA+SIGMA2*EB*C(I)/
(1.0-C(I+2*(N+2))*EO)

CTS=C(I-4*(N+2))*(1.0+T3*C(I+3*(N+2))/
(T4-T3*C(I+3*(N+2))))/
(T1-T2*C(I+4*(N+2))-T2*T3*C(I-3*(N+2)))/(T4-T3*C(I+3*(N+2)))

H3 = -BT2*(C(I+N+2)-CTS)

CPRIME(I-N+2)=H1+H2-H3
1620 CONTINUE

```

C-----RESOLVING PDE 3-----

```

DO 1640 I=2,N+1
SUM(11)=0.0
SUM(12)=0.0

DO 1650 K=1,N+2
SUM(11) = SUM(11) + B(I,K)*C(K+2*(N+2))
1650 SUM(12) = SUM(12) + A(I,K)*C(K+2*(N+2))

CPRIME(I-2*(N+2)) = -SUM(12)/V + SUM(11)/PEO-
(0.03*C(I+(N+2))+0.2)*(1.5*CTI+32.0)*1.0E-6*XOT*
(C(I+N+2)*C(I-2*(N+2))*ET*EO)/
(1.0+C(I+N+2)*ET+(C(I+N+2)*ET)**2*GAMA+SIGMA2*EB*C(I)/
(1.0+C(I+2*(N+2))*EO)-
(0.03*C(I)+0.2)*(1.5*CTI+32.0)*1.0E-6*XOB*
(C(I)*C(I+2*(N+2))*EB*EO)/
(1.0+C(I)*EB+C(I+N+2)*ET*SIGMA1)/
(1.0-C(I+2*(N+2))*EO)
C
1640 CONTINUE

```

C-----RESOLVING EQN 4-----

```

DO 1660 I=1,N+2

CTS=C(I+4*(N+2))*(1.0+T3*C(I+3*(N+2))/
(T4-T3*C(I+3*(N+2))))/
(T1-T2*C(I+4*(N+2))-T2*T3*C(I-3*(N+2)))/(T4-T3*C(I+3*(N+2)))

1660 CPRIME(I+3*(N+2))=BB2*(C(I)-C(I+3*(N+2)))*(1.0+T2*CTS)
/(T4-T3*C(I+3*(N+2)))

```

C-----RESOLVING EQN 5-----

```

DO 1670 I=1,N+2
CTS=C(I-4*(N+2))*(1.0+T3*C(I+3*(N+2))/
(T4-T3*C(I+3*(N+2))))/
(T1-T2*C(I+4*(N+2))-T2*T3*C(I+3*(N+2)))/(T4-T3*C(I+3*(N+2)))

1670 CPRIME(I+4*(N+2))=BT2*(C(I)-CTS)

```

RETURN
END

```

* .....
* ***** SUBROUTINE INIT *****
* .....

SUBROUTINE INIT(N,NT,T,C,Z,A,B,H,ALPHA,AS,XV,V,UG,AMUB,AMUT,
ANN,CBI,CTI,COI,YB,YT,YOB,YOT,BB2,BT2,EB,ET,EO,GAMA,
SIGMA1,SIGMA2,PEB,PET,PEO,XB,XT,XOB,XOT,T1,T2,T3,T4)

IMPLICIT DOUBLE PRECISION (A-H,O-Z)
DIMENSION Z(N+2),C(NT),A(N+2,N+2),B(N+2,N+2)
REAL*8 H,UG,PD,KMB,KMT,KB,KT,KO,KIT,KBT,KTB,MUB,MUT,MB,MT,
MO,KDB,KDT,ANN,BB2,BT2,B3,B4,EB,ET,EO,GAMA,SIGMA1,SIGMA2,
PEB,PET,PEO,SIB,SIT

OPEN(1,FILE='CAUSER\ANSARI\ANSARI\ANSI1.DAT',STATUS='OLD')
OPEN(2,FILE='CAUSER\ANSARI\ANSARI\ANSI2.DAT',STATUS='OLD')

```

C-----INITIAL CONCENTRATIONS-----

```

T=0
DO 1021 I=1,N+2
1021 READ(1,8) C(I),C(I+N+2),C(I+2*(N+2)),C(I+3*(N+2)),C(I+4*(N+2))
8 FORMAT(5(F11.9,1X))

DO 29 I=1,N+2
C(I)=0.01
29 C(I+N+2)=0.01

```

C-----COLLOCATION POINTS,A & B MATRICES-----

```

DO 1022 I=1,N+2
1022 READ(2,9) Z(I)
9 FORMAT(11X,F13.11)
C
DO 1023 I=1,N+2
DO 1023 J=1,N+2
1023 READ(2,*) A(I,J)
C
DO 1024 I=1,N+2
DO 1024 J=1,N+2
1024 READ(2,*) B(I,J)

```

C-----INLET CONCENTRATION-----

```

C UNITS = G,M,MIN
CBI = 0.367
CTI = 0.225
COI = 275.00
RT=3.1

```

C-----BIOFILM PARAMETERS-----

```

C UNITS = M,DAYS
AS = 133.3
ALPHA = 0.3
XV = 100000.00

```

C-----COLUMN PARAMETERS-----

```

C UNITS = M,DAYS
D=0.152

```

C VOLUME=0.015291002
 C VOLUME=0.005097
 FLOW=0.60
 V = 0.3
 AREA=3.141592654*(D**2)/4.0
 UG= VOLUME*24.0*60.0/AREA/RT
 H = VOLUME/AREA

C-----PARTICLE PARAMETERS-----

C UNITS = G.M
 PD = 4.28E+5
 DP=4.0E-3

C-----KINETIC PARAMETERS-----

YB = 0.708
 YT = 0.708
 YOB = 0.336
 YOT = 0.341
 KB = 12.22
 KT = 11.03
 KO = 0.26
 KIT = 78.94
 KBT = 4.50
 KTB = 0.20
 AMUB = 0.677*24.0
 AMUT = 1.504*24.0

C-----MASS TRANSFER COEFFICIENTS-M/HR-----

KMB = (6.04E-10)*24.0
 KMT = (6.04E-10)*24.0

C-----DISPERSION COEFFICIENTS-IN M²/H-----

GAMA1=0.45+0.55*V
 GAMA2=0.5
 TERM2=GAMA2*DP*UG/V
 DB = 0.02772*24.0*GAMA1+TERM2
 DT = 0.02736*24.0*GAMA1+TERM2
 DO = 0.06408*24.0*GAMA1+TERM2

C-----HENRY'S CONSTANT-----

MB = 0.23
 MT = 0.27
 MO = 34.4

C-----ADSORPTION ISOTHERM PARAMETERS-----

KDB = 2.25E-5
 KDT = 2.25E-5
 ANN = 1.04

*****NON-DIMENSIONAL PARAMETERS*****

C-----NITA-----
 BB2 = (1.0-ALPHA)*AS*KMB*H/V/UG
 BT2 = (1.0-ALPHA)*AS*KMT*H/V/UG

C-----EPSILON, GAMA, SIGMA-----

EB = CBI/KB/MB
 ET = CTI/KT/MT
 EO = COI/KO/MO

GAMA = KT/KIT
 SIGMA1 = KT*KBT/KB
 SIGMA2 = KB*KTB/KT

C-----PECLET NUMBERS-----

PEB=UG*H/DB
 PET=UG*H/DT
 PEO=UG*H/DO

C-----BETA-----

XB=H*ALPHA*AS*XV*AMUB/V/UG/CBI/YB
 XT=H*ALPHA*AS*XV*AMUT/V/UG/CTI/YT
 XOB=H*ALPHA*AS*XV*AMUB/V/UG/COI/YOB
 XOT=H*ALPHA*AS*XV*AMUT/V/UG/COI/YOT

C-----PHI-----

PHI1=XB*1E-6*EB*EO
 PHI2=ET*SIGMA1
 PHI3=ET*EO*XT*1E-6
 PHI4=GAMA*(ET**2)
 PHI5=EB*SIGMA2
 PHI6=XOB*(1E-6)*EB*EO
 PHI7=XOT*(1E-6)*ET*EO

C-----EXTENDED LANGMUIR ISOTHERM-----

A1=2.34E-5
 A2=8.38E-6
 B1=0.02
 B2=0.01356
 T1=A1*PD*(1.0-V)/V
 T2=B1*CTI
 T3=B2*CBI
 T4=A2*PD*(1.0-V)/V

C-----ECHO-----

WRITE(10,*) H,ALPHA,AS
 WRITE(10,*) XV,V,UG
 WRITE(10,*) AMUB,AMUT,ANN
 WRITE(10,*) CBI,CTI,COI
 WRITE(10,*) YB,YT,YOB,YOT
 WRITE(10,*) BB2,BT2
 WRITE(10,*) B3,B4
 WRITE(10,*) EB,ET,EO
 WRITE(10,*) GAMA,SIGMA1,SIGMA2
 WRITE(10,*) PEB,PET,PEO
 WRITE(10,*) SIB,SIT

RETURN
 END

APPENDIX F

```

.....
* THE GENERAL MODEL FOR BINARY VOC MIXTURES
.....

.....
* Subroutine used : IMSL (DIVPAG)
* No. of ODEs solved : 230 (CAN BE CHANGED BY VARYING M & N)
.....

IMPLICIT DOUBLE PRECISION (A-H,O-Z)
PARAMETER (N=8,M=4)
PARAMETER (MXPARAM=50,NT=(N+2)*(3*M+11))

DOUBLE PRECISION Z(N+2),C(NT),A(N+2,N+2),B(N+2,N+2),
PARAM(MXPARAM),CPRIME(NT),SUM(30),AA(M+2,M+2),ANN,
BB(M+2,M+2),X(M+2),AK(1,1)

COMMON/A,A,B,AA,BB,PET,PEB,PEO,ET,EB,EO,V,GAMA,BETA1,BETA2,
BETA3,BETA4,SIT,SIB,ANN,BETA5,PHI1,PHI2,PHI3,PHI4,PHI5,PHI6,
SIGMA1,SIGMA2,PHI7

EXTERNAL DIVPAG,SSET,FCN,FCNJ

CALL INIT(N,M,NT,T,C,Z,A,B,X,AA,BB,PET,PEB,PEO,ET,EB,
EO,V,GAMA,SIGMA1,SIGMA2,BETA1,BETA2,BETA3,BETA4,SIT,SIB,ANN,
BETA5,PHI1,PHI2,PHI3,PHI4,PHI5,PHI6,PHI7)

C-----IMSL PARAMETERS -----
IDO=1
TOL=1.0E-2
CALL SSET(MXPARAM,0.0,PARAM,1)
PARAM(10)=1.0
PARAM(1)=1.0E-8
PARAM(4)=900000

DO 10 TEND=0.10 ,15.0,0.10
CALL DIVPAG(IDO,NT,FCN,FCNJ,AK,T,TEND,TOL,PARAM,C)
WRITE(6,*)TEND

C-----B C FOR PDE 1 -----
DO 1510 K=1,2
1510 SUM(K)=0.0

DO 1520 K=2,N+1
SUM(1) = SUM(1) + A(N+2,K)*C(K)
1520 SUM(2) = SUM(2) + A(1,K)*C(K)

C(N+2) =(-A(N+2,1)*(SUM(2)+PET)-(PET-A(1,1))*SUM(1))/
(A(N+2,1)*A(1,N+2)+(PET-A(1,1))*A(N+2,N+2))

C(1) =-(SUM(1)+C(N+2)*A(N+2,N+2))/A(N+2,1)

```

```

C-----B C FOR PDE 2 -----
      DO 1525 J=3,4
1525  SUM(J)=0.0

      DO 1530 K=2,N+1
      SUM(3) = SUM(3) + A(N+2,K)*C(K+N+2)
1530  SUM(4) = SUM(4) + A(1,K)*C(K+N+2)

      C(2*(N+2)) = (-A(N+2,1)*(SUM(4)+PEB)-(PEB-A(1,1))*SUM(3))/
      (A(N+2,1)*A(1,N+2)+(PEB-A(1,1))*A(N+2,N+2))

      C(1+N+2) = -(SUM(3)+C(2*(N+2))*A(N+2,N+2))/A(N+2,1)

```

```

C-----B C FOR PDE 3 -----
      DO 1535 J=5,6
1535  SUM(J)=0.0

      DO 1540 K=2,N+1
      SUM(5) = SUM(5) + A(N+2,K)*C(K+2*(N+2))
1540  SUM(6) = SUM(6) + A(1,K)*C(K+2*(N+2))

      C(3*(N+2)) = (-A(N+2,1)*(SUM(6)+PEO)-(PEO-A(1,1))*SUM(5))/
      (A(N+2,1)*A(1,N+2)+(PEO-A(1,1))*A(N+2,N+2))

      C(1+2*(N+2)) = -(SUM(5)-C(3*(N+2))*A(N+2,N+2))/A(N+2,1)

```

```

C-----BC1 FOR PDES 4 & 5-----
      DO 1545 J=1,N+2
      C(J+5*(N+2))=ET*C(J)
      C(J+(M+7)*(N+2))=EB*C(J+N+2)
      C(J+(2*M+9)*(N+2))=EO*C(J+2*(N+2))
1545  CONTINUE

```

```

C-----BC2 FOR PDES 4 & 5-----
      DO 1550 J=1,N+2
      SUM(7)=0.0
      SUM(8)=0.0
      SUM(9)=0.0
      DO 1555 K=1,M+1
      SUM(7) = SUM(7) + AA(M+2,K)*C(J+(4+K)*(N+2))
      SUM(8) = SUM(8) + AA(M+2,K)*C(J+(M+6+K)*(N+2))
1555  SUM(9) = SUM(9) + AA(M+2,K)*C(J+(2*M+8+K)*(N+2))

      C(J+(M+6)*(N+2)) = -SUM(7)/AA(M+2,M+2)
      C(J+(2*M+8)*(N+2)) = -SUM(8)/AA(M+2,M+2)
1550  C(J+(3*M+10)*(N+2)) = -SUM(9)/AA(M+2,M+2)

```

```

C-----
C      P R I N T I N G
      WRITE(16,99) T,C(N+2),C(2*(N+2)),C(3*(N+2))
99    FORMAT(4(1X,F12.8))

```

```

IF(TEND.LE.14.0) GOTO 10

DO 98 I=1,N+2
WRITE(18,102)Z(I),C(I),C(I+N+2),C(I+2*(N+2)),C(I+3*(N+2))
102  FORMAT(5(2X,F12.8))
WRITE(17,101)Z(I),I
101  FORMAT(/,3X,'HEIGHT =',F10.6,2X,'COLL. POINT =',I2)
DO 98 J=1,M+2
WRITE(17,100) X(J),C(I+(4+J)*(N+2)),C(I+(M+6+J)*(N+2)),
C(I+(J+2*M+8)*(N+2))
100  FORMAT(4(2X,F12.8))
98   CONTINUE

10   CONTINUE

IDO=3
CALL DIVPAG(IDO,NT,FCN,FCNJ,AK,T,TEND,TOL,PARAM,C)
STOP
END

*****
*****          SUBROUTINE FCN
*****
SUBROUTINE FCN(NT,T,C,CPRIME)
IMPLICIT DOUBLE PRECISION (A-H,O-Z)
PARAMETER (N=8,M=4)
C
DOUBLE PRECISION Z(N+2),C(NT),A(N+2,N+2),B(N+2,N+2),
CPRIME(NT),SUM(30),AA(M+2,M+2),ANN,
BB(M+2,M+2),X(M+2)

COMMON/A/A,B,AA,BB,PET,PEB,PEO,ET,EB,EO,V,GAMA,BETA1,BETA2,
BETA3,BETA4,SIT,SIB,ANN,BETA5,PHI1,PHI2,PHI3,PHI4,PHI5,PHI6,
SIGMA1,SIGMA2,PHI7

CBI=0.367
CTI=0.225

V=0.3
PD=4.28E+5
A1=2.34E-5
A2=8.38E-6
B1=0.02
B2=0.01356
T1=A1*PD*(1.0-V)/V
T2=B1*CTI
T3=B2*CBI
T4=A2*PD*(1.0-V)/V

C-----B C FOR PDE 1 -----
DO 3510 I=10,11
3510  SUM(I)=0.0

DO 3520 K=2,N+1

```

```

SUM(10) = SUM(10) + A(N+2,K)*C(K)
3520 SUM(11) = SUM(11) + A(1,K)*C(K)

C(N+2) = (-A(N+2,1)*(SUM(11)+PET)-(PET-A(1,1))*SUM(10))/
(A(N+2,1)*A(1,N+2)+(PET-A(1,1))*A(N+2,N+2))

C(1) = -(SUM(10)+C(N+2)*A(N+2,N+2))/A(N+2,1)

C-----B C FOR PDE 2 -----
DO 3525 I=12,13
3525 SUM(I)=0.0

DO 3530 K=2,N+1
SUM(12) = SUM(12) + A(N+2,K)*C(K+N+2)
3530 SUM(13) = SUM(13) - A(1,K)*C(K+N+2)

C(2*(N+2)) = (-A(N+2,1)*(SUM(13)+PEB)-(PEB-A(1,1))*SUM(12))/
(A(N+2,1)*A(1,N+2)+(PEB-A(1,1))*A(N+2,N+2))

C(1-N+2) = -(SUM(12)+C(2*(N+2))*A(N+2,N+2))/A(N+2,1)

C-----B C FOR PDE 3 -----
DO 3526 I=13,14
3526 SUM(I)=0.0

DO 3531 K=2,N+1
SUM(13) = SUM(13) + A(N+2,K)*C(K+2*(N+2))
3531 SUM(14) = SUM(14) + A(1,K)*C(K+2*(N+2))

C(3*(N+2)) = (-A(N+2,1)*(SUM(14)+PEO)-(PEO-A(1,1))*SUM(13))/
(A(N+2,1)*A(1,N+2)+(PEO-A(1,1))*A(N+2,N+2))

C(1+2*(N+2)) = -(SUM(13)+C(3*(N+2))*A(N+2,N+2))/A(N+2,1)

C-----BC1 FOR PDES 4 & 5-----
DO 3535 I=1,N+2
C(I+5*(N+2))=ET*C(I)
C(I+(M+7)*(N+2))=EB*C(I+N+2)
C(I+(2*M+9)*(N+2))=EO*C(I+2*(N+2))
3535 CONTINUE

C-----BC2 FOR PDES 4 & 5-----

DO 3545 I=1,N+2

SUM(15)=0.0
SUM(16)=0.0
SUM(17)=0.0

DO 3550 K=1,M+1
SUM(15) = SUM(15) + AA(M+2,K)*C(I+(4+K)*(N+2))
SUM(16) = SUM(16) + AA(M+2,K)*C(I+(M+6+K)*(N+2))
3550 SUM(17) = SUM(17) + AA(M+2,K)*C(I+(2*M+8+K)*(N+2))

```

$C(I+(M+6)*(N+2)) = -SUM(15)/AA(M+2,M+2)$
 $C(I+(2*M+8)*(N+2)) = -SUM(16)/AA(M+2,M+2)$
 3545 $C(I+(3*M+10)*(N+2)) = -SUM(17)/AA(M+2,M+2)$

C-----RESOLVING PDE 1-----

```

DO 1600 I=2,N+1
SUM(18)=0.0
SUM(19)=0.0
SUM(20)=0.0

DO 1610 K=1,N+2
SUM(18) = SUM(18) + B(I,K)*C(K)
1610 SUM(19) = SUM(19) + A(I,K)*C(K)

DO 1615 J=1,M+2
1615 SUM(20) = SUM(20) + AA(I,J)*C(I+(J+4)*(N+2))

G1 = -SUM(19)/V
G2 = SUM(18)/PET
C G3 = BETA1*SUM(20)/(1.5*C(I)*CTI+33.4)/1.0E-6
G3 = BETA1*SUM(20)/40.0E-6

CTS=C(I+3*(N+2))*(1.0+T3*C(I+4*(N+2)))/
(T4-T3*C(I+4*(N+2)))
(T1-T2*C(I+3*(N+2))-T2*T3*C(I+4*(N+2)))/(T4-T3*C(I+4*(N+2)))

G4 = BETA2*(C(I)-CTS)

CPRIME(I) = G1+G2+G3-G4
C WRITE(9,*)G1,G2,G3,G4,CPRIME(I)
1600 CONTINUE

```

C-----RESOLVING PDE 2-----

```

DO 1601 I=2,N+1
SUM(21)=0.0
SUM(22)=0.0
SUM(23)=0.0

DO 1611 K=1,N+2
SUM(21) = SUM(21) + B(I,K)*C(K+N+2)
1611 SUM(22) = SUM(22) + A(I,K)*C(K+N+2)

DO 1616 J=1,M+2
1616 SUM(23) = SUM(23) + AA(I,J)*C(I+(J+M+6)*(N+2))

G1 = -SUM(22)/V
G2 = SUM(21)/PET
C G3 = BETA3*SUM(23)/(1.5*C(I)*CTI+33.4)/1.0E-6
G3 = BETA3*SUM(23)/40.0E-6

```

```

CTS=C(I+3*(N+2))*(1.0+T3*C(I+4*(N+2))/  

(T4-T3*C(I+4*(N+2))))/  

(T1-T2*C(I+3*(N+2))-T2*T3*C(I+4*(N+2)))/(T4-T3*C(I+4*(N+2))))  

G4=BETA4*(C(I+N+2)-C(I+4*(N+2)))*(1.0+T2*CTS/  

(T4-T3*C(I+4*(N+2))))  

CPRIME(I+N+2) = G1+G2+G3-G4  

C WRITE(9,*)G1,G2,G3,G4,CPRIME(I+N+2)  

1601 CONTINUE  

C-----RESOLVING PDE 3 -----  

DO 1640 I=2,N+1  

SUM(24)=0.0  

SUM(25)=0.0  

SUM(26)=0.0  

DO 1650 K=1,N+2  

SUM(24) = SUM(24) + B(I,K)*C(K+2*(N+2))  

1650 SUM(25) = SUM(25) + A(I,K)*C(K+2*(N+2))  

DO 1655 J=1,M+2  

1655 SUM(26) = SUM(26) + AA(I,J)*C(I+(N+2)*(2*M+8+J))  

G1 = -SUM(25)/V  

G2 = SUM(24)/PEO  

C G3 = BETA5*SUM(26)/(1.5*C(I)*CTI+33.4)/1.0E-6  

G3 = BETA5*SUM(26)/40.0E-6  

CPRIME(I+2*(N+2)) = G1 + G2 + G3  

C WRITE(9,*) G1,G2,G3,CPRIME(I+2*(N+2))  

1640 CONTINUE  

C-----RESOLVING EQN 4 -----  

DO 1660 I=1,N+2  

C1660 CPRIME(I+3*(N+2)) = BETA2*(C(I)-SIT*C(I+3*(N+2)))*(1.0/ANN)  

CTS=C(I+3*(N+2))*(1.0+T3*C(I+4*(N+2))/  

(T4-T3*C(I+4*(N+2))))/  

(T1-T2*C(I+3*(N+2))-T2*T3*C(I+4*(N+2)))/(T4-T3*C(I+4*(N+2))))  

1660 CPRIME(I+3*(N+2)) = BETA2*(C(I)-CTS)  

C-----RESOLVING EQN 5 -----  

DO 1661 I=1,N+2  

CTS=C(I+3*(N+2))*(1.0+T3*C(I+4*(N+2))/  

(T4-T3*C(I+4*(N+2))))/  

(T1-T2*C(I+3*(N+2))-T2*T3*C(I+4*(N+2)))/(T4-T3*C(I+4*(N+2))))  

G=C(I+4*(N+2))*(1.0+T2*CTS)/(T4-T3*C(I+4*(N+2)))  

1661 CPRIME(I+4*(N+2))=BETA4*(C(I+N+2)-G)

```

C-----RESOLVING PDE 6-----

```

DO 1670 I = 1,N+2

DO 1675 J = 2,M+1
SUM(27)= 0.0

DO 1680 K = 1,M+2
1680 SUM(27) = SUM(27) + BB(J,K)*C(I+(4+K)*(N+2))

C    G1 = PH11*SUM(27)/((1.5*C(I)*CTI+33.4)*1.0E-6)**2
    G1 = PH11*SUM(27)/(40.0E-6)**2

    G2 = PH12*C(I+(4+J)*(N+2))*C(I+(J+2*M+8)*(N+2))/
    (1.0-C(I+(4+J)*(N+2))-C(I+(4+J)*(N+2))**2.0)*GAMA+
    SIGMA2*C(I+(J+M+6)*(N+2))/
    (1.0 + C(I+(J+2*M+8)*(N+2)))
    CPRIME(I+(4+J)*(N+2)) = G1-G2
1675 CONTINUE
1670 CONTINUE

```

C-----RESOLVING PDE 7-----

```

DO 1671 I = 1,N+2

DO 1676 J = 2,M+1
SUM(28)= 0.0

DO 1681 K = 1,M+2
1681 SUM(28) = SUM(28) + BB(J,K)*C(I+(M+6+K)*(N+2))

C    G1 = PH13*SUM(28)/((1.5*C(I)*CTI+33.4)*1.0E-6)**2
    G1 = PH13*SUM(28)/(40.0E-6)**2

    G2 = PH14*C(I+(M+6+J)*(N+2))*C(I+(J+2*M+8)*(N+2))/
    (1.0+C(I+(M+6+J)*(N+2))+SIGMA1*C(I+(J+4)*(N+2)))/
    (1.0 + C(I+(J+2*M+8)*(N+2)))
    CPRIME(I+(M+6+J)*(N+2)) = G1-G2
C    WRITE(9,*)G1,G2,CPRIME(I+(M+6+J)*(N+2))
1676 CONTINUE
1671 CONTINUE

```

C-----RESOLVING PDE 8-----

```

DO 1685 I = 1,N+2

DO 1690 J = 2,M+1
SUM(29)= 0.0

DO 1695 K = 1,M+2
1695 SUM(29) = SUM(29) + BB(J,K)*C(I+(2*M+8+K)*(N+2))

C    G1 = PH15*SUM(29)/((1.5*C(I)*CTI+33.4)*1.0E-6)**2
    G1 = PH15*SUM(29)/(40.0E-6)**2

    G2 = PH16*C(I+(4+J)*(N+2))*C(I+(J+2*M+8)*(N+2))/
    (1.0+C(I+(4+J)*(N+2))+((C(I+(4+J)*(N+2))**2)*GAMA+

```

```

      SIGMA2*C(I+(J+M+6)*(N+2)))/
      (1.0 + C(I+(J+2*M+8)*(N+2)))
      G3 = PHI7*C(I+(M+6+J)*(N+2))*C(I+(J+2*M+8)*(N+2))/
      (1.0+C(I+(M+6+J)*(N+2))+SIGMA1*C(I+(J+4)*(N+2)))/
      (1.0 + C(I+(J+2*M+8)*(N+2)))
      CPRIME(I+(2*M+8+J)*(N+2)) = G1-G2-G3
C     WRITE(9,*)G1,G2,G3
1690  CONTINUE
1685  CONTINUE

      RETURN
      END

.....
*****          SUBROUTINE INIT          *****
.....
      SUBROUTINE INIT(N,M,NT,T,C,Z,A,B,X,AA,BB,PET,PEB,PEO,ET,EB,
      EO,V,GAMA,SIGMA1,SIGMA2,BETA1,BETA2,BETA3,BETA4,SIT,SIB,ANN,
      BETA5,PHI1,PHI2,PHI3,PHI4,PHI5,PHI6)

      IMPLICIT DOUBLE PRECISION (A-H,O-Z)

      REAL*8 H,UG,PD,KMB,KMT,KB,KT,KO,KIT,KBT,KTB,AMUB,AMUT,MB,MT,
      MO,KDB,KDT,ANN,BB2,BT2,B3,B4,EB,ET,EO,GAMA,SIGMA1,SIGMA2,
      PEB,PET,PEO,SIB,SIT,FXV,DTW,DBW,DOW,BETA1,BETA2,BETA3,BETA4,
      BETA5,PHI1,PHI2,PHI3,PHI4,PHI5,PHI6

      DIMENSION Z(N+2),C(NT),A(N+2,N+2),B(N+2,N+2),X(M+2),
      AA(M+2,M+2),BB(M+2,M+2)
      OPEN(1,FILE='C:\USER\ANSAR\ANSAR2\DATA1.DAT',STATUS='OLD')
      OPEN(2,FILE='C:\USER\ANSAR\ANSAR2\DATA2.DAT',STATUS='OLD')
      OPEN(3,FILE='C:\USER\ANSAR\ANSAR2\DATA3.DAT',STATUS='OLD')
C-----INITIAL CONCENTRATIONS-----
      T=0
      DO 29 J=1,N+2
      C(J)=0.1
      C(J+5*(N+2))=ET*C(J)
      C(J+N+2)=0.1
      C(J+(7+M)*(N+2))=EB*C(J+N+2)
      C(J+2*(N+2))=1.0
29    C(J+(9+2*M)*(N+2))=EO*C(J+2*(N+2))
      DO 30 I=1,N+2
      DO 30 J=2,M+2
      C(I+(4+J)*(N+2))=0.4
      C(I+(6+M+J)*(N+2))=0.4
30    C(I+(8+2*M+J)*(N+2))=20.0

C-----COLLOCATION POINTS,A & B MATRICES-----
      DO 1022 I=1,N+2
1022  READ(2,9) Z(I)
      9   FORMAT(11X,F13.11)
C
      DO 1023 I=1,N+2
      DO 1023 J=1,N+2

```



```

1023 READ(2,*) A(I,J)
C
      DO 1024 I=1,N+2
      DO 1024 J=1,N+2
1024 READ(2,*) B(I,J)
C 12  FORMAT(11X,F14.11)

C-----COLLOCATION POINTS,AA & BB MATRICES-----
      DO 1025 I=1,M+2
1025 READ(3,19) X(I)
19   FORMAT(11X,F13.11)
C
      DO 1026 I=1,M+2
      DO 1026 J=1,M+2
1026 READ(3,*) AA(I,J)
C
      DO 1027 I=1,M+2
      DO 1027 J=1,M+2
1027 READ(3,*) BB(I,J)
C 12  FORMAT(11X,F14.11)

      D=0.152
C     VOLUME=0.005097
      VOLUME=0.015291002
      FLOW=0.60
      RT=1.5

C-----ENTERING CONCENTRATION-----
C-----UNITS == G/M"3
      CBI = 0.367
      CTI = 0.225
      COI = 275.00

      AS = 133.3
C     AS = 40.0
      ALPHA = 0.3
      V = 0.3
      DP=4.0E-3
C
C-----COLUMN PARAMETERS-----AREA,VELOCITY,HEIGHT-----
C-----UNITS == M"3, 1/M, M"3/DAY
      AREA=3.141592654*(D**2)/4.0
      UG= VOLUME*24.0*60.0/AREA/RT
      H = VOLUME/AREA
C     PRINT*,AREA,UG,H

C-----PARTICLE DENSITY,FILM THICKNESS,DENSITY-----
C-----UNITS == G/M"3, G/M"3
      PD = 4.28E+5
      XV = 100000.00

C-----DIFFUSION COEFFICIENT IN WATER
      DOW = (2.41E-9)*3600.0*24.0

```

DTW = (1.03E-9)*3600.0*24.0
 DBW = (1.04E-9)*3600.0*24.0
 FXV = 0.195

C-----YIELD COEFFICIENTS-----

YB = 0.708
 YT = 0.708
 YOB = 0.336
 YOT = 0.341

C-----MASS TRANSFER COEFFICIENTS-M/HR-----

KMB = (6.04E-3)*24.0
 KMT = (6.04E-3)*24.0

C-----DEGRADATION RATE PARAMETERS--G/M³--1/HR---

KB = 12.22
 KT = 11.03
 KO = 0.26
 KIT = 78.94
 KBT = 4.50
 KTB = 0.20
 AMUB = 0.677*24.0
 AMUT = 1.504*24.0

C-----DISPERSION COEFFICIENTS-IN M²/H-----

GAMA1=0.45+0.55*V
 GAMA2=0.5
 TERM2=GAMA2*DP*UG/V
 DB = 0.02772*24.0*GAMA1+TERM2
 DT = 0.02736*24.0*GAMA1+TERM2
 DO = 0.06408*24.0*GAMA1+TERM2

C PRINT*,DP,GAMA2,TERM2,DT

C-----HENRY'S CONSTANT-----

MB = 0.23
 MT = 0.27
 MO = 34.4

C-----ADSORPTION ISOTHERM PARAMETERS---G/G-PARTICLE--

KDB = 2.25E-5
 KDT = 2.25E-5
 ANN = 1.04

C-----NON-DIMENSIONAL PARAMETERS-----

C PDE 1 == BETA1 & 2 FOR TOLUENE-IN THE MAIN PROGRAM

BETA1 = DTW*FXV*ALPHA*AS*KT*H/CTI/V/UG
 BETA2 = (1.0-ALPHA)*AS*KMT*H/V/UG

C PDE 2 == BETA3 & 4 FOR BENZENE-IN THE MAIN PROGRAM

BETA3 = DBW*FXV*ALPHA*AS*KB*H/CBI/V/UG
 BETA4 = (1.0-ALPHA)*AS*KMB*H/V/UG

```

C PDE 3 == BETA FOR OXYGEN IN THE GAS PHASE
  BETA5 = DOW*FXV*ALPHA*AS*KO*H/COI/V/UG

C EPSILON, GAMA, SIGMA1&2 == USED IN FUNCTION G
  EB = CBI/KB/MB
  ET = CTI/KT/MT
  EO = COI/KO/MO

  GAMA = KT/KIT
  SIGMA1 = KT*KBT/KB
  SIGMA2 = KB*KTB/KT

C PECLLET NUMBERS == PDES 1,2,3
  PEB=UG*H/DB/V
  PET=UG*H/DT/V
  PEO=UG*H/DO/V
C PRINT*.PET,PEO

C---ADSORPTION ISOTHERM COEFFICIENT -----
  SIB = ((V*CBI/(1-V)/PD/KDB)**(1/ANN))/CBI
  SIT = ((V*CTI/(1-V)/PD/KDT)**(1/ANN))/CTI
C
  PHI1 = FXV*DTW*H/UG
  PHI2 = AMUT*XV*H/KT/YT/UG
  PHI3= FXV*DBW*H/UG
  PHI4= AMUB*XV*H/KB/YB/UG
  PHI5= FXV*DOW*H/UG
  PHI6= AMUT*XV*H/YOT/KO/UG
  PHI7= AMUB*XV*H/YOB/KO/UG

C-----DIMENSIONLESS PARAMETERS -----
C WRITE(9,*) PET,PEB,PEO
C WRITE(9,*) ET,EB,EO
C WRITE(9,*) V,GAMA
C WRITE(9,*) SIGMA1,SIGMA2
C WRITE(9,*) BETA1,BETA2
C WRITE(9,*) BETA3,BETA4
C WRITE(9,*) SIT,SIB,ANN
C WRITE(9,*) BETA5
C WRITE(9,*) PHI1,PHI2
C WRITE(9,*) PHI3,PHI4
C WRITE(9,*) PHI5,PHI6
C WRITE(9,*) PHI7
  RETURN
  END

  SUBROUTINE FCNJ(NT,Z,C,DUMMY)
  DOUBLE PRECISION C(NT),DUMMY(NT,NT)
  RETURN
  END

```